JOINT SYMPOSIUM ON OIL SHALE, TAR SANDS, AND RELATED MATERIAL
PRESENTED BEFORE THE DIVISION OF PETROLEUM CHEMISTRY, INC.
AND THE DIVISION OF WATER, AIR, AND WASTE CHEMISTRY
AMERICAN CHEMICAL SOCIETY
SAN FRANCISCO MEETING, April 2-5, 1968

GREAT CANADIAN OIL SANDS EXPERIENCE IN THE COMMERCIAL PROCESSING OF ATHABASCA TAR SANDS

By

G. F. Andrews and H. M. Lewis
Great Canadian Oil Sands, Limited,
Fort McMurray, Alberta, Canada

and

E. W. Dobson
Sun Oil Company, Marcus Hook, Pennsylvania

INTRODUCTION

The Great Canadian Oil Sands plant for recovery and upgrading of bitumen from Athabasca Tar Sands officially opened on September 30, 1967. This opening ceremony represented the climax of many years of experimentation, design, construction, and start-up effort that at its peak utilized the services of 2500 people. Some key dates leading up to the event were:

1953 - Great Canadian Oil Sands Limited organized.

1960 - Initial attempt to obtain permission to develop the Athabasca tar sands. Action deferred (1) by the Alberta Oil and Gas Conservation Board until 1962.

1962 - Approval granted (2) by the Oil and Gas Conservation Board for a plant to recover 31,500 barrels per day of synthetic crude.

1963 - Detailed engineering work underway. Construction and operation of an experimental plant 20 miles north of Fort McMurray, Alberta on the west bank of the Athabasca River.

1964 - Approval granted (3) for an increase in the design capacity of the plant to 45,000 barrels per day. Began construction work on the commercial plant.

1965 - Completed road and bridge connecting the plant site with Fort McMurray. Completed work in the experimental plant.

1966 - Engineering work completed. Construction effort reached its peak.

1967 - Completed construction. Plant start-up. Official opening ceremony.

Some of the design and development problems encountered have been the subject of recent papers. For example:

1. Discussions of problems encountered in the development of the hot water process as utilized by G.C.O.S., including a description of the test plant (4,5).
2. A discussion of the overall commercial plant flow sheet, material and energy balances, and scale-up problems (5).
3. A geological description of the area to be mined by G.C.O.S., with emphasis on the unusual geological exploration problems encountered and how they were overcome (6).
4. A discussion of the properties and processing characteristics of synthetic crude oil produced from Athabasca bitumen in a pilot scale simulation of the G.C.O.S. plant (7).

We wish to build on the background developed in these papers and discuss the commercial plant performance, but first let us take a brief look at the plant itself. Figure 1 shows the plant location in Northeastern Alberta, 20 miles north of Fort McMurray and 270 miles north of Edmonton. Toronto is 1700 miles to the southeast, Salt Lake City 1100 miles directly south, and Seattle 800 miles to the southwest.

Figure 2 is an aerial view of the project. The tar sand mining area is in the background, facilities for extracting bitumen from the tar sand are to the left rear, and process units for upgrading bitumen to synthetic crude are in the center.

Figures 3 through 7 show a series of plant scenes in the same order as the plant operating

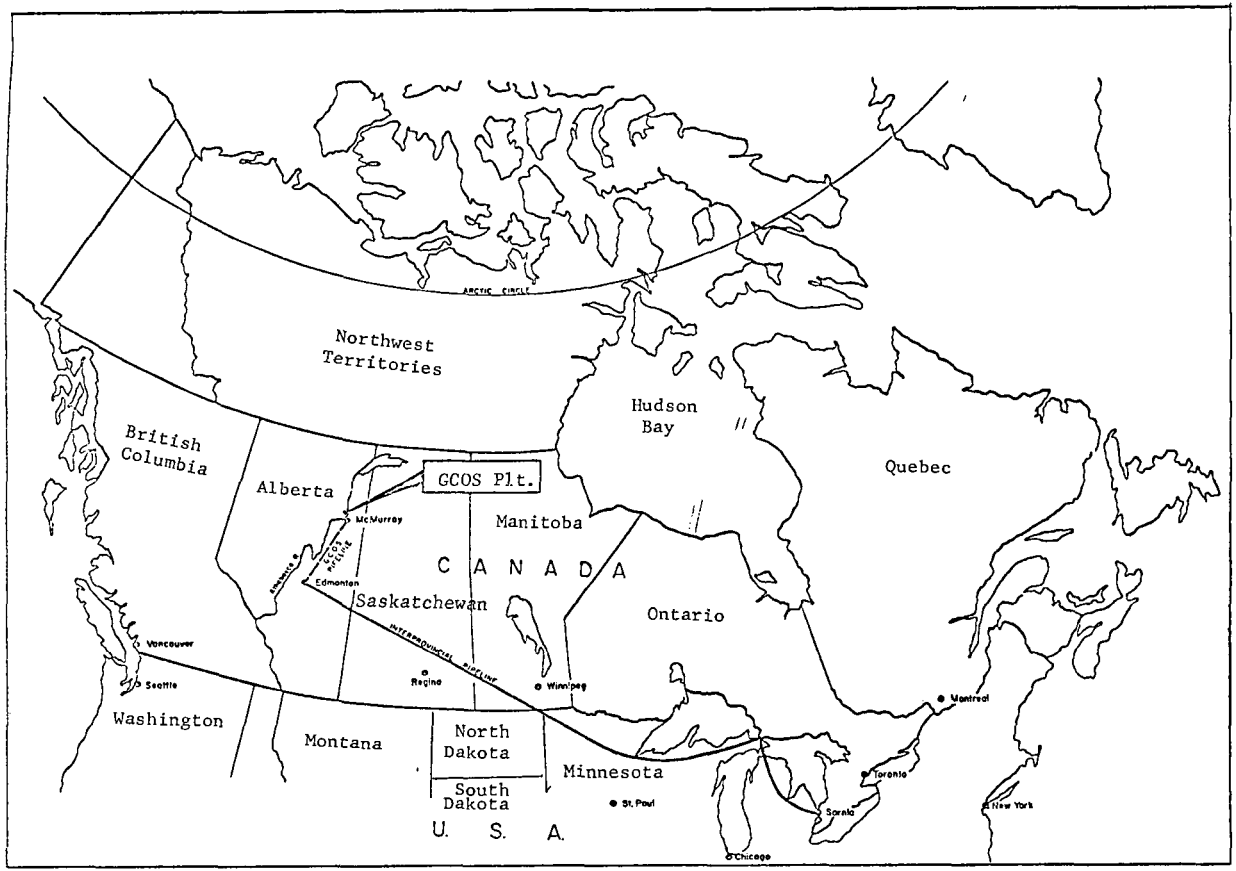

FIGURE 1

MAP SHOWING GEOGRAPHICAL LOCATION OF GREAT CANADIAN OIL SANDS PLANT SITE

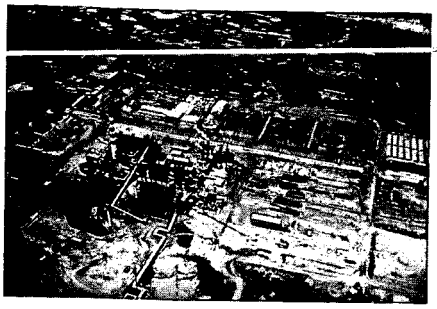

FIGURE 2

AERIAL VIEW OF THE G.C.O.S. PLANT

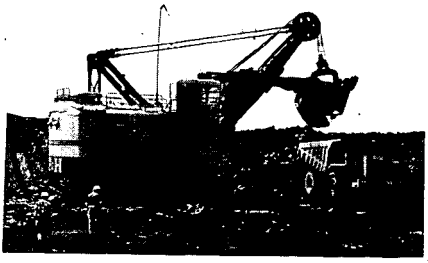

FIGURE 3

OVERBURDEN REMOVAL

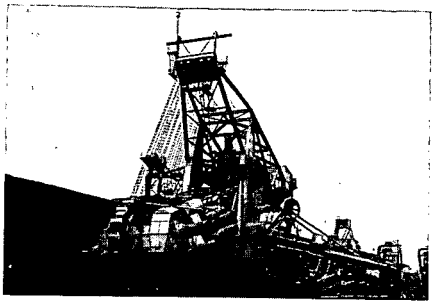

FIGURE 4

BUCKETWHEEL EXCAVATOR

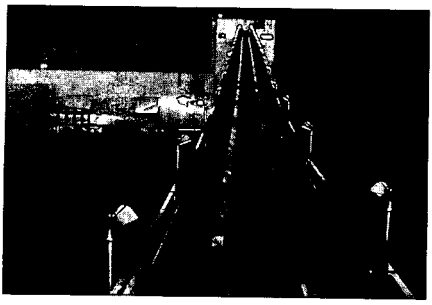

FIGURE 5

FEED CONVEYOR

FIGURE 6

EXTRACTION PLANT

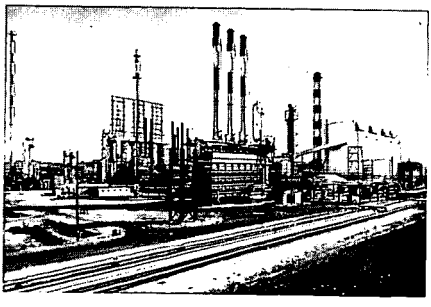

FIGURE 7

BITUMEN PROCESSING AREA AND POWERHOUSE

(Sulfur plant on left, cokers in left center, hydrorefining units in center, hydrogen plant in right center, and powerhouse on the far right)

sequence. First the overburden layer is removed (Figure 3) to expose the ore body. Bucket-wheel excavators (Figure 4) mine the tar sand and transfer it to a series of belt conveyors (Figure 5). These conveyors discharge at the extraction plant (Figure 6) where bitumen is separated in a two stage extraction. Bitumen is then upgraded to synthetic crude oil by coking and hydrorefining (Figure 7).

Some essential auxiliary steps in the plant complex are:

1. Disposal of the sand tailings from the extraction plant operation.
2. Hydrogen production.
3. Sulfur recovery.
4. Steam and power generation.
5. Water treating.

Figure 8 (5) shows in more detail how all of these operations are integrated to produce synthetic crude oil from tar sands at the rate of 45,000 barrels per calender day.

Before turning our attention to the performance details of the GCOS plant we would like to mention that this report was prepared in October, 1967 and is based on observations during the startup period (July, August, and September, 1967). Therefore, our data and conclusions should be interpreted as a progress report and not as a final technical evaluation.

RESULTS AND DISCUSSION

Mining

The G.C.O.S. mine is one of the largest open pit operations in North America in terms of daily tonnage. To produce 45,000 barrels per calender day of synthetic crude oil requires, on the average, 97,500 tons of tar sand per calender day. About 0.5 tons of overburden per ton of tar sand must be removed to expose the ore body. This means about 3.3 tons of ore plus overburden must be handled to produce a barrel of synthetic crude oil.

Overburden removal is accomplished by using both scrapers and a power shovel - truck combination. This operation is about 1 year ahead of the mining, so, on a short term basis, it is not critically related to daily production. The total overburden that must be moved averages 12 million cubic yards per year.

Tar sand is mined using two crawler mounted bucketwheel excavators, each with a theoretical capacity of 9,000 tons per hour and nominal average capacity rating of 5,500 tons per hour. This equipment is relatively new to the North American mining scene, although it has been extensively used in Europe, for instance in German brown coal operations.

Because of the non-homogenous nature of the tar sand deposit, G.C.O.S. operating experience with the bucketwheel excavators has varied widely. Operation at up to 8,000 tons per hour per wheel has been demonstrated. On the other hand, occasional rock seams reduce the quantity that can be mined.

Tar sand from the excavator is moved to the plant by a series of belt conveyors. Although belt conveyors have been widely used in other mine operations, there are some new problems peculiar to the handling of tar sand. An earlier paper (4) discussed the problem of tar sand sticking to the conveyor belt as noted during the operation of the G.C.O.S. test plant (1963-65). In inital operation this proved to be at least as bad as expected, if not worse. Not only did the accumulated tar sand cause unbalanced loads resulting in belt training problems; it caused considerable wear on tension pulleys, idlers, and belt scrapers because of the abrasive nature of the material. We made a number of modifications to the system that, while not a complete solution, reduced the problem to a tolerable level. Cleanup of tar sand spills around the conveyor system is an expensive nuisance.

Abnormal loads imposed on the conveyor system by rocks and large lumps of tar sand have caused some mechanical damage. This damage consisted of both broken impact idlers at the transfer points in the conveyor system and holes punched in the belt itself. Replacement of the impact idlers with larger, heavy duty units substantially reduced this problem. Belt repairs still consume maintenance manpower, and when the damage is too extensive to repair during normal shutdowns, contribute to lost production time.

In addition to the mechanical problems associated with mining, the nature of the ore body creates problems in mine planning. On the average, it takes 2.2 tons of tar sand to produce one barrel of synthetic crude oil. However, this can vary from 1.5 to 4.0 tons per barrel depending on the bitumen content of the tar sand. Similarly, the fines content (through 325 mesh) of the ore body varies so that the fresh water requirement in the extraction process can vary between 25 to 300 gallons per ton of tar sand. In turn, this causes a shift in steam demand. Maintaining stable operating conditions in the extraction plant, smooth power plant operation, and a steady flow of bitumen to the process units requires close attention to the nature of the ore body.

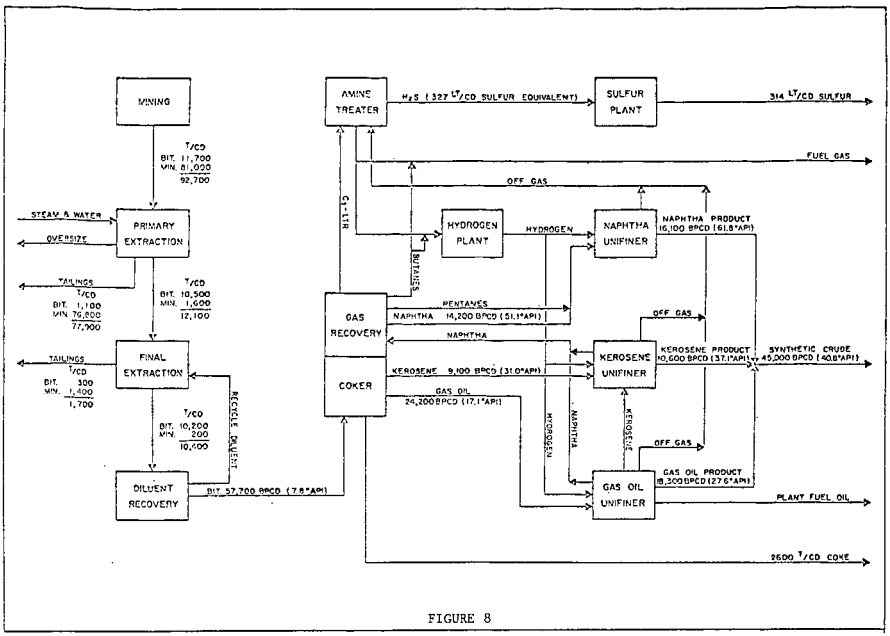

FIGURE 8

GENERALIZED FLOW SHEET SHOWING MAJOR PROCESS STEPS AND MATERIAL FLOWS

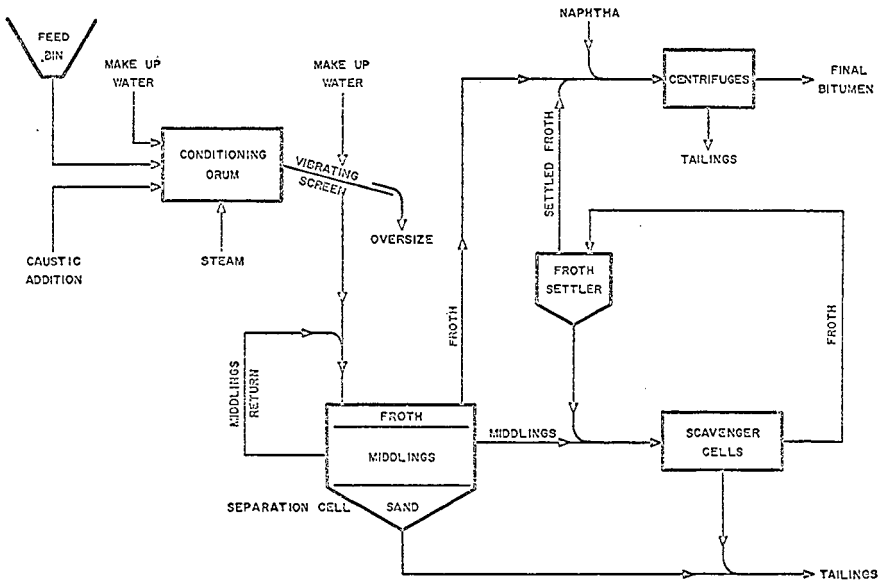

FIGURE 9

EXTRACTION PLANT PROCESS FLOW SHEET

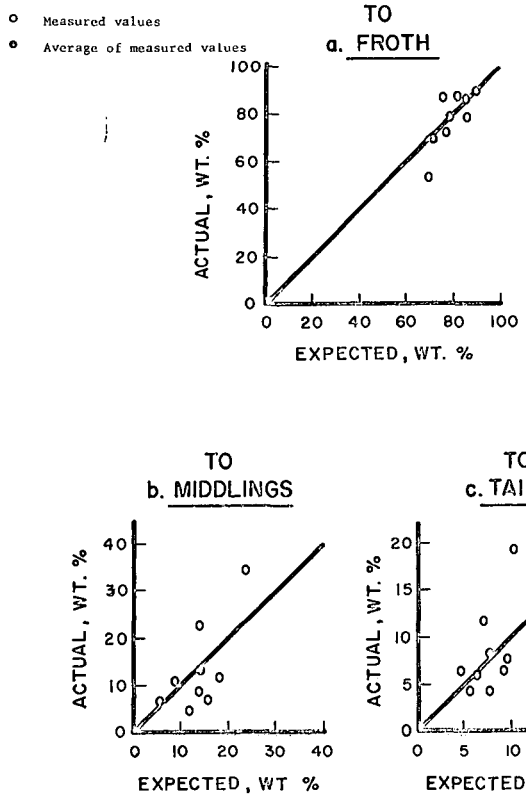

FIGURE 10
SEPARATION CELL BITUMEN DISTRIBUTION

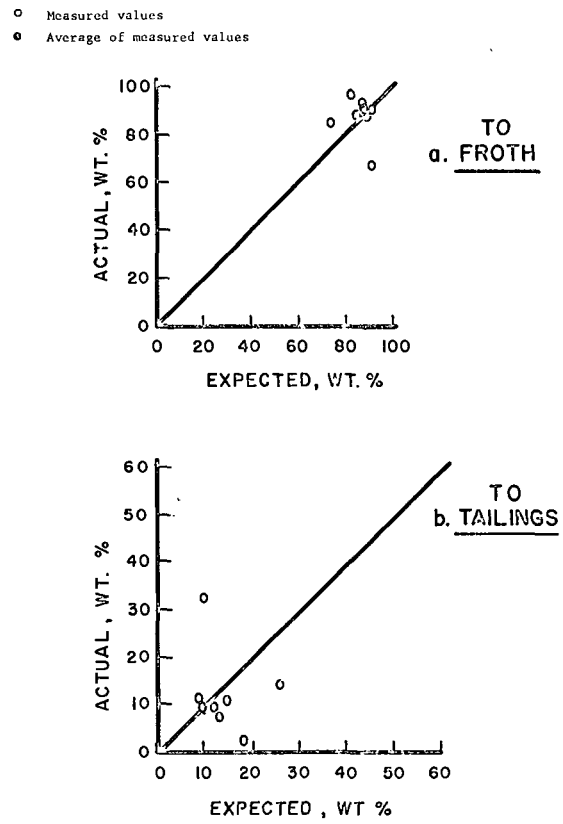

FIGURE 11
SCAVENGER CIRCUIT BITUMEN DISTRIBUTION

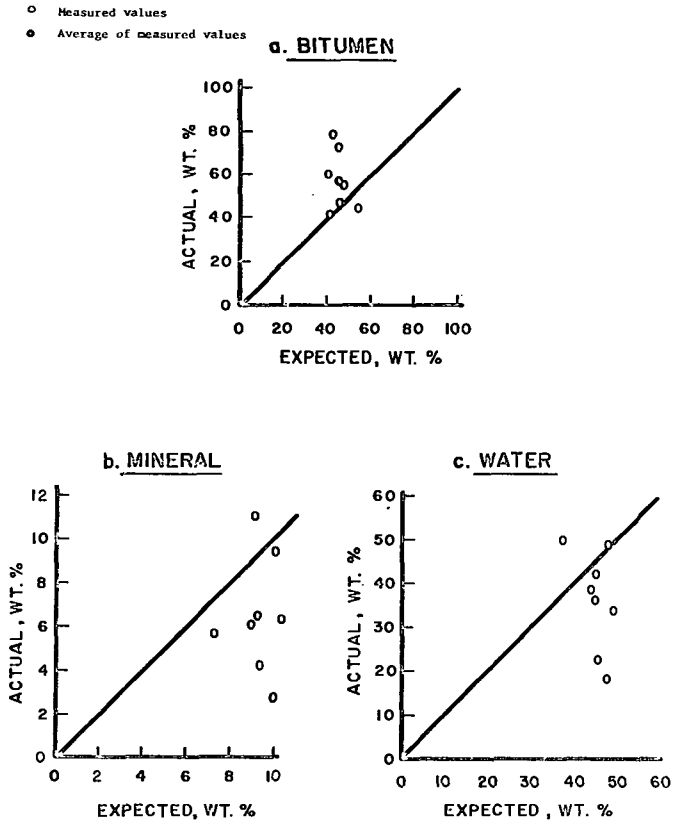

FIGURE 12
SEPARATION CELL FROTH COMPOSITION

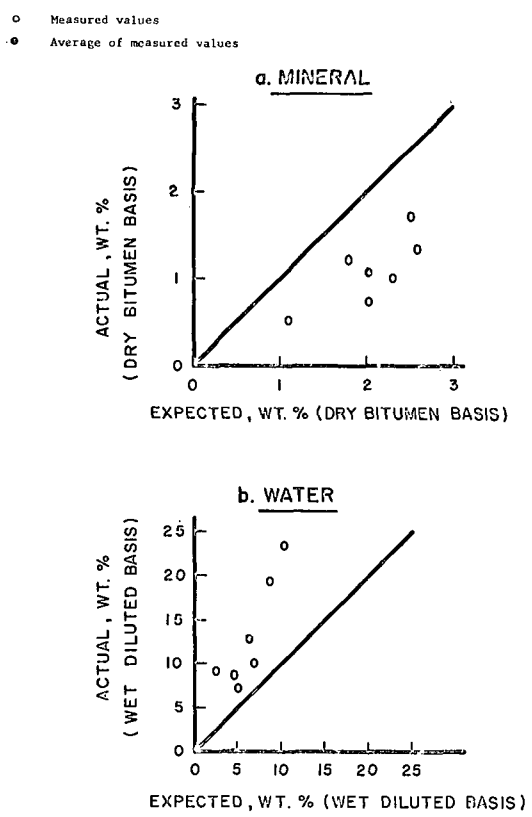

FIGURE 13
MINERAL & WATER IN FINAL EXTRACTION PRODUCT

Bitumen Extraction

Tar sand discharges from the mine conveyor system into feed bins in the primary extraction plant. As the first step in the extraction process, tar sand, caustic, and water are mixed and heated to 170 - 190°F with open steam. This operation is carried out in rotating "conditioning" drums similar in mechanical configuration to rotary kilns or rotary steam tube driers. The conditioned pulp is screened to separate rocks and lumps of unconditioned tar sand. After the addition of enough fresh and/or recycle water to convert the screened pulp to a pumpable slurry, the screen undersize is transferred to separation cells. Here an oil rich emulsion of bitumen, fine mineral, and water rises to surface and overflows into a froth collection system. Sand settles to the bottom and is discharged by a rake mechanism similar to that used in thickeners. Excess water is withdrawn as a "middlings" stream from the center of the separation cells. Part of the middlings is recycled to dilute the screen undersize and the rest is processed through air flotation scavenging cells to recover additional bitumen. Froth from the scavenger cells is an unstable water-rich emulsion of bitumen, fine mineral, and water that, upon settling, will break down into a bitumen-rich emulsion similar to that produced in the separation cells and a bottoms layer of about the same composition as middlings. Settler tailings are recycled to extinction and the settled scavenger froth is combined with the separation cell froth. This combined froth, still containing substantial quantities of fine mineral matter and water, is the product from the primary extraction step. Primary extraction tailings are diluted with cold water and pumped to the tailings disposal area.

To upgrade the froth from the primary extraction step so that it will be suitable for processing into synthetic crude, it is heated to 190 - 200°F with open steam, diluted with naphtha to reduce the viscosity and density of the hydrocarbon phase, and centrifuged.

Figure 9 (5) shows these steps schematically.

In the commercial plant, there are:

1. A four-compartment feed bin.
2. Four conditioning drums.
3. Four vibrating screens.
4. Four separation cells.
5. Thirty-six air flotation cells.
6. Two scavenger froth settlers.
7. Forty centrifuges.

To compensate for feed variations, these units are sized so that three-fourths of the installed equipment can handle the nominal capacity.

Many aspects of this approach to the recovery of bitumen from tar sand have been the subject of considerable research and small-scale plant operation over the past 30 years (8, 9, 10, 11). However, this early work did not supply sufficient information on the basic mechanism of the separation process to permit design of the G.C.O.S. plant without additional laboratory and pilot plant study (5).

The commercial plant equipment design correlations were derived by first establishing a theoretically reasonable process model and then empirically fitting the experimental data to define the constants and coefficients that would give a statistically sound representation of the relationship between equipment size and design, feed stock characterization, and process performance. Our interest at this time is in how well these design correlations represent commercial plant performance:

1. Bitumen recovery - There are four streams leaving the extraction plant that contribute to bitumen losses. These are: screen oversize, separation cell tailings, scavenger cell tailings, and centrifuge tailings. Table 1 compares plant measured losses with expected losses calculated from the design correlations.

Overall, the commercial plant gives about the recovery we expected from pilot plant performance. The only difference of any substance is in the screen oversize loss, and note that we did not have a very precise prediction for this value. Reference (5) discusses this point in considerable detail. Briefly, this is the story. Screen oversize results from tar sand lumps not broken down in the conditioning drum. The two most important factors affecting this breakdown of lumps are the rate of heat transfer in the conditioning drum and the feed lump size distribution. For our predictions, we were far from certain what the feed lump size would be. Furthermore, during winter operation some of the tar sand lumps will be frozen and this will change the heat transfer characteristics of the system. Consequently, we still do not have a complete picture of what the average year-round oversize loss will be.

Table 1 is based on averaged values for a number of steady-state operating cases. Figures 10 and 11 show in more detail operating data on the bitumen distribution in the separation

cells and scavenger cells for these cases. Note the variations in the expected values. The principal reasons for this are variations in feed bitumen content, feed fines content, and feed fines to fresh water ratio.

TABLE 1

EXTRACTION PLANT BITUMEN DISTRIBUTION (7,8/67)

Basis: a. Average bitumen in tar sand = 11.8 wt.%
b. Average < 325 mesh fines in the tar sand mineral fraction = 20.1 wt.%
c. Average water input = 0.58 tons per ton of tar sand
d. Average operating temperature = 185°F

	WT.% OF BITUMEN IN TAR SAND	
LOSSES	Measured	Expected
Screen oversize	< 0.1	0.5 to 3.0
Separation cell tailings	8.3	7.9
Scavenger cell tailings	1.6	2.0
Final extraction tailings	2.2	1.8
PRODUCT	87.9	87.8 to 85.3

As feed bitumen content varies the loss to separation cell tailings, expressed as per cent of the feed bitumen, varies inversely because this loss is (approximately) constant per ton of tar sand. As feed fines vary at a fixed fines to water ratio, the volume of middlings changes in direct proportion without much change in middlings composition. Thus more or less bitumen leaves the separation cell in the middlings stream. In a similar manner, a change in the fines to water ratio affects the bitumen leaving the separation cell in the middlings, but the relationship is more complex because this also changes middlings composition. Ideally, the process should be operated at a maximum fines to water ratio as discussed in (5) but during startup this wasn't always possible.

Our predictions of bitumen distribution in the scavenger cells are based on residence time (5). Thus any changes in the separation cell that affect middlings rate would have an inverse effect on scavenger froth yield. We've had some indication that bitumen concentration in the middlings stream should be a parameter, but this relationship hasn't been fully developed.

Within practical operating limits, we expected the final extraction plant bitumen losses to be a fixed percentage of the final extraction plant feed, so the only variation in relating this loss back to bitumen in tar sand is a slight correction for changes in primary extraction recovery. We don't consider the small difference between the measured and expected values significant. Our test plant data, used as a basis for the expected loss had a standard deviation of $\pm$ 1% and the standard deviation of the individual values that make up the average measured plant loss is $\pm$ 1.6%.

2. Primary Extraction Plant Froth Composition: On the average, the primary extraction plant froth was richer in bitumen than expected:

TABLE 2

FROTH COMPOSITION (7,8/67)

Basis: Same as Table 1.

	Actual (Wt.%)	Expected (Wt.%)
Bitumen	57.3	45.9
Mineral	6.5	9.3
Water	36.2	44.8

We do not know why the commercial plant produces this better quality froth. Figure 12 shows the individual data points that make up the average value, from the same operation as the bitumen distribution values already discussed. Note that we did not expect a great deal of variation in the froth composition. What small differences we did expect were related to the bitumen and fines content of the tar sand. In addition to a better average composition in the commercial plant product, there is a much wider variation.

3. Final Extraction Plant Product Composition - Even after the two stage centrifuge operation, the product contains some fine mineral matter and water. It is desirable to minimize these. Residual mineral is concentrated in coke produced in subsequent processing. This coke is the primary source of plant fuel, and excessive mineral makes it more difficult to pulverize and increases furnace ash. Residual water must be vaporized in subsequent processing so minimizing the water content of the product saves heat and reduces foaming problems. Figure 13 shows a comparison of plant product mineral and water contents versus what we expected at these operating conditions from our pilot plant work. The actual mineral content is lower than we expected by a factor of about 2. On the other hand, the product water content is high by about the same factor. We don't know why the mineral content is better, but subsequent to this study we did find the product water content could be improved by modifying the second stage centrifuge internals to get more even feed distribution. After this modification, we observed water contents in the 5 to 10 per cent range rather than the 10 to 15 per cent shown here. We would like to get to 5 per cent maximum water in the centrifuged product.

Tailings Disposal - Tailings from the primary and final extraction plants are pumped as a water slurry to a 700 acre diked tailings pond. Water is recovered from the pond and recirculated through the primary extraction plant. Operation has not progressed far enough to permit evaluation.

Mechanical problems - One of the major mechanical problems so far has been the tendency of the rich tar sand (>13% bitumen) to cause bridging in the feed bin. To a lesser degree, plant conveyors have encountered many of the same problems as the mine conveyors. Erosion is always a problem handling this type of material; consequently, metal wear plates or elastomer liners in critical areas were part of the original design. In some cases, it has been necessary to build up the original wearing surfaces or change to alternate materials.

At this point in the process, we have as a product a heavy (8°API) viscous (500 SSU at 210°F) oil diluted with light hydrocarbon so it can be pumped and stored in tanks. The work discussed so far, starting with mining and continuing through both extraction stages, is an adaptation of mine - ore mill technology. To upgrade this product to a suitable substitute for conventional crude oil requires further processing based on petroleum refining technology.

Upgrading Bitumen to Synthetic Crude Oil

The diluted bitumen product from the final extraction step is upgraded to synthetic crude oil by first separating the light naphtha diluent, then coking the bitumen, and finally hydrorefining the coker distillate fractions. In addition to the finished synthetic crude, these operations also yield coke for power plant fuel, gas for hydrogen plant feed and furnace fuel, supplementary fuel oil as required, make-up diluent for the final extraction plant, and hydrogen sulfide which is further processed to recover elemental sulfur.

From intermediate storage, the diluted bitumen is charged to the diluent recovery system. This unit closely resembles a conventional crude oil distillation system. Diluent is recovered as an overhead product and returned to storage for recycle through the final extraction plant. Bitumen is recovered as the bottoms product. The capacity of the system is 135,000 barrels of combined diluent and bitumen per stream day.

Bottoms from diluent recovery are fed to the coker furnaces at approximately 500°F. In passing through these furnaces, the temperature is raised to 900 - 910°F to initiate thermal cracking. From the furnaces, the bitumen discharges into delayed cokers. Coke accumulates until a drum is filled. Then that drum is cooled down, steamed to strip out residual hydrocarbon vapors, the coke dumped, and the drum preheated to prepare it for the next cycle. During the filling cycle, the hydrocarbon vapor products are continuously withdrawn. To provide a continuous flow of coker vapor product, three furnaces and three pairs of 26 foot diameter coke drums are used. At any given time, three drums (one for each furnace) are taking feed, one is cooling down, one is discharging coke, and one is being preheated.

Vapor from the coker is processed through a fractionating tower to separate it into wet gas, unstabilized naphtha (375°F end point), kerosene (375°F - 500°F), gas oil (500°F to 850°F), and bottoms (850°F+). The wet gas and naphtha fractions are further processed in a gas plant to give a C_3 and lighter gas for plant fuel and hydrogen production, a C_4 fraction which can be

used as supplementary fuel or blended into synthetic crude to control its vapor pressure, and a stabilized C_5 - 375°F naphtha fraction for hydrorefining to a synthetic crude component. The kerosine and gas oil fractions from the coker fractionator are fed directly to hydrorefining units for upgrading to synthetic crude components. The heavy bottoms fraction can either be used for furnace fuel as needed or recycled through the cokers.

The following outline is a brief summary of our experience with this portion of the G.C.O.S. plant.

1. Diluent recovery - In our discussion of the final extraction plant, we briefly mentioned the problem with foaming resulting from excess water in the diluted bitumen. This foaming problem was exaggerated in our initial operation because of the tendency of the high water content product to stratify in storage. In addition to the work in final extraction to reduce the total quantity of water, tank mixers were installed to minimize stratification.

2. Coking - Initial operation of this unit has been most satisfactory, because several potential problems that we anticipated have not so far materialized. We thought residual clay might create tube fouling problems in the coker furnaces. But after three months of operation, we inspected the tubes and found no significant buildup. Since then, there has been no measurable increase in furnace tube pressure drop. We were also concerned over the potential mechanical problems with the high pressure water jet system used for cutting coke because it had never been used in coke drums this large. However, except for one case of a water pump jammed by dirt from the water (we now use clarified water), this has not been a problem. The coke has contained more water than anticipated, thus increasing the draining and air drying time before it can be transferred to the power house bunkers, but this is not a serious problem.

The only significant operating problem related to the design of the coker system is overquenching in the bottom section of the coker fractionator. This has reduced the end point of the gas oil fraction and resulted in a loss of gas oil yield. Mechanical modifications are planned on the first opportunity and should correct this problem.

The following table compares expected and actual coker product distributions:

TABLE 3

COKER PRODUCT DISTRIBUTION (9/67)

Component	Measured wt.%	Expected wt.%
Gas (C_4 & lighter)	7.9	8.3
Naphtha	12.7	12.1
Kerosine	15.0	10.0
Gas Oil	36.2	41.4
Fuel Oil	6.0	4.2
Coke	22.2	22.7

The discrepency in gas oil yield is a reflection of the fractionator problem we just discussed. The excessive recycle that results contributes to increased kerosine yield by overcracking. The remaining kerosine comes from high end point naphtha that was used as the initial diluent inventory. Part of this material was not recovered in the diluent recovery system, thus showing up in the coker product.

3. Hydrorefining - Processing problems were minimal at startup. However, we did have a number of mechanical problems. Perfecting the seal oil system for the hydrogen recycle and booster compressors was a major one that has since been overcome.

Table 4 shows inspection data on hydrorefined synthetic crude components. The composite synthetic crude from a blend of these components is shown in Table 5, along with comparable data on pilot plant product (7). The principal differences are the low end point and the greater quantity of material in the 375 - 500°F boiling range that are results of the distillation problem we discussed earlier. When this is resolved, we think the products will be comparable.

TABLE 4

HYDROREFINED SYNTHETIC CRUDE COMPONENTS (9/67)

	NAPHTHA		KEROSINE		GAS OIL	
	Commercial Plant	Pilot Plant(7)	Commercial Plant	Pilot Plant(7)	Commercial Plant	Pilot Plant(7)
API Gravity @ 60°F	55.3	50.9	38.6	39.7	27.5	28.7
Distillation (D-86)						
IBP	162	174	358	388	498	499
5	194	260	385	398	526	512
10	206	274	398	402	540	522
30	238	282	418	411	568	561
50	278	296	438	415	588	611
70	316	310	460	423	615	655
90	369	334	496	433	675	740
95	396	344	513	448	706	785
EP	462	366	533	468	715	869
Aromatics, vol.%	-	18	12.7	13.8	25.3	29.8
Sulfur, ppm	15	50	50	50	410	800
Yield, vol.% of synthetic crude	30.8	30.6	27.2	19.0	42.0	50.4

TABLE 5

G.C.O.S. SYNTHETIC CRUDE (9/67)

	Initial Commercial Production	Pilot Plant Product
Gravity, °API	38.3	37.6
Distillation (D-86)		
IBP	162	210*
5%	221	277
10%	254	300
30%	408	379
50%	507	386
70%	588	574
90%	615	688
95%	675	738
EP	715	833
Sulfur, wt.%	.022	.030

* Pilot plant product was stabilized to C_6+, but commercial plant product is C_5+. In preparing the pilot plant sample approximately 5 vol.% of a 174°F to 210°F fraction was stripped off. There isn't any real difference in the front end.

Hydrogen Production

Amine treated coker dry gas is used as raw material for production of 63.5 mm CFD of 95.0% H2. Residual sulfur is removed by caustic washing, then the coker gas passes over a cobalt molybdenum catalyst in order to saturate olefins and convert mercaptans to hydrogen sulfide. This H_2S is then removed by passage through a zinc oxide bed at 700°F. The gas is then mixed with steam and passed over the reforming catalyst at furnace outlet conditions of 1525°F and 300 PSIG. The gas is quenched and then passed through high and low temperature shift converters. Carbon dioxide is removed by absorption in a promoted potassium carbonate solution.

The hydrogen plant was started up on natural gas. There were some problems with leaks in the system, but once these were corrected the unit performed well. Recently, the hydrogen plant operation was changed to plant gas, but we do not have any performance data yet.

Sulfur Production

Off gases from the coker and hydrorefiners are treated with monoethanolamine to remove hydrogen sulfide. The recovered H_2S is converted to sulfur in a conventional two stage oxidation plant. Little contamination of amine solution by carbonyl sulfide has been observed. Filtering and reclaiming facilities are used to maintain a clean amine system.

Utilities

The powerhouse provides all utilities for the project. Three coke fired boilers supply 2,250,000 pounds per hour of steam at 800 PSIG and 750°F. This steam is exhausted through two turbo-generators with a combined capacity of 76,500 KVA at 13.8 KV. Steam is extracted at 425 PSIG and exhausted at 50 PSIG. The higher pressure steam is used to power turbine drives in the powerhouse and refinery. The 50 PSIG steam is used primarily in the extraction plant.

The major initial operating problems were excessive superheating of the steam, creating metallurgical problems with steam piping, and fouling of boiler tubes on the fire side. Removal of some superheat tube surface eliminated the first problems. Installation of soot blowers and reduction of the ball load in the coke pulverizers to avoid over grinding coke reduced tube fouling. Control of the turbo-generators is a continuing problem, because many of the plant electrical loads are intermittent. For example, when a bucketwheel excavator completes a cut and starts repositioning itself power demand drops substantially and, the powerhouse must adjust to handle the reduced load. In as little as five or ten minutes, when the bucketwheel is repositioned, it must shift again to pick up the load.

Water treatment facilities for boiler feed water consists of a clarifier, hot lime reactors, filters and ion exchange. It is the largest boiler feed water plant in Canada and it can maintain total make-up to the boilers if required. The rather elaborate water treating facilities are necessary because at times the Athabasca River contains up to 2,500 ppm turbidity and substantial quantities of silica that the high pressure boilers cannot accommodate. This unit has operated satisfactorily.

Overall Process Evaluation

As we noted in our earlier remarks, it is too early for a complete technical evaluation of the G.C.O.S. plant. However, we do feel that this preliminary look shows that the basic process concepts are sound. The hot water extraction process had been demonstrated only at a hundred-fold smaller scale. The scaled up version performs about as expected. Coking and hydrorefining had never been applied to bitumen and products derived from bitumen except in pilot plant equipment. These also perform about as expected. What we cannot adequately evaluate is the long term mechanical reliability of these processing schemes. We've noted the major mechanical problems encountered so far, some apparently solved and others we still have. It will probably take many months, perhaps even a year or two, for a definitive mechanical evaluation to take shape.

LITERATURE CITED

(1) Government of the Province of Alberta, Oil and Gas Conservation Board; "Report to the Lieutenant Governor in Council with Respect to the Application of Great Canadian Oil Sands Limited"; 17 November 1960.

(2) Government of the Province of Alberta, Oil and Gas Conservation Board; "Supplemental Report to the Lieutenant Governor in Council with Respect to the Application of Great Canadian Oil Sands Limited"; 19 September 1962.

(3) Government of the Province of Alberta, Oil and Gas Conservation Board; "Report on an Application of Great Canadian Oil Sands Limited under Part VI and of the Oil and Gas Conservation Act"; 14 February 1964.

(4) Dor, A. A., Daly, W. J., Floyd, P. F., and Hall, F. T., "Technical Problems in the Processing of Mined Sand for Bitumen Recovery", Seventh World Petroleum Congress, April, 1967.

(5) Innes, E. D. and Fear, J. V. D., "Canada's First Commercial Tar Sand Development", Seventh World Petroleum Congress, April, 1967.

(6) Ward, D. E., "Geological Development for Mining of Oil Sands", American Petroleum Institute, Division of Production, April, 1967.

(7) Lovell, P. F., Reif, H. E., Burk, R. O., Hertel, P. H., and Abbott, B. T., The Oil and Gas Journal, August 15, 1966.

(8) Clark, K. A., Trans Canadian Institute of Mining and Metallurgy 47, 257, (1944).

(9) Clark, K. A., Canadian Oil and Gas Industries 3, 46.

(10) Clark, K. A. and Pasternack, D. S., Research Council of Alberta Report 53, 1950.

(11) Atkins, W. E., Report to the Board of Trustees of the Oil Sands Project, 1950.

JOINT SYMPOSIUM ON OIL SHALE, TAR SANDS, AND RELATED MATERIAL
PRESENTED BEFORE THE DIVISION OF PETROLEUM CHEMISTRY, INC.
AND THE DIVISION OF WATER, AIR, AND WASTE CHEMISTRY
AMERICAN CHEMICAL SOCIETY
SAN FRANCISCO MEETING, April 2-5, 1968

HOT WATER PROCESSING OF ATHABASCA OIL SANDS: I. OIL FLOTATION IN A STIRRED REACTOR

By

Walter H. Seitzer
Sun Oil Company, Research and Development Division, Marcus Hook, Pennsylvania

The laboratory separation of bitumen from Athabasca oil tar sands in hot water, was reported by Clark and Pasternak nearly four decades ago (1). The apparatus was large, requiring 17 pounds of tar sands per run. Later modifications required batches of 6.5 kilograms of sand (2,3,4). Even with the large size, these devices were able to separate only 75-85% of the bitumen from the good tar sands and less than 50% from sands containing higher amounts of clay. In order to recover more oil, the suspension of clay in water has to be passed into an air flotation cell (5).

A very simple technique was also employed by Clark and coworkers for demonstration purposes (6). As we used it, the method is to hand-stir the sands-water mixture (pulp) in a beaker over a steam bath and to add this pulp with agitation into hot water at 85°C. After the stirrer is stopped, the oil froth which rises to the surface is scraped off. This method can give good froth yields from choice samples of oil sands (14-16% bitumen) but the yields drop to 30-50% from ordinary "good" grade sands (10-12% bitumen). From sands containing high amounts of fines (mineral <325 microns in size) yields drop to 10% or less of the bitumen recovered as froth.

In order to investigate the chemistry of the hot water separation, we needed a laboratory technique which would give high yields from a wide range of tar sands and preferably from small samples. Also, the method should be as simple as possible to enable us to arrive at an unequivocal explanation of the phenomenon. The key to such a method proved to be proper agitation of the pulp, the tar sands-water mixture containing about 20% water.

EXPERIMENTAL

The reactor was an electrically heated steel reactor, cylindrical with a round bottom, 3-1/8" inside diameter. The U-shaped impeller 2-5/8" diameter, 1/4" wide, and 1-1/2" high was positioned at the bottom of the reactor to give 1/4" clearance from the wall of the reactor. For speeds up to 350 rpm, the agitator was driven by a laboratory electronic stirrer motor through chain-and-sprocket linkage. At higher speeds a direct drive through a Jacobs chuck was used. The temperature of the reactor was controlled at 85°C. automatically and monitored continuously by thermocouples.

In the normal procedure, 200 grams of tar sand were put into the heated reactor and the top bolted on. Hot water, enough to give a pulp containing 80% tar sand (dry basis) was then forced into the reactor. Enough sodium hydroxide was dissolved in the water to give a pulp having a pH of 8.2. After the material was stirred for 20 minutes, water at 85°C. was introduced to dilute down to 35% tar sand. The agitation was continued at about 50 rpm for ten minutes after which the reactor was dissembled and the froth scraped with a spatula. The watery layer was removed with suction and the sand tailings were scooped out. All fractions were weighed.

The fractions were extracted with a 4:1 mixture of benzene and methylethylbutene. Water was removed simultaneously by the Dean Stark technique. The extraction thimble was dried and weighed to calculate the mineral. To obtain the weight bitumen, the solvents were stripped from the extract. Water was determined by difference. The starting tar sand was similarly analyzed.

All samples of tar sands were homogenized by forcing the sands through 1/4" screen. To slow down their aging (6), the sands were refrigerated until used.

RESULTS

pH

The first variable studied was the effect of pH on yield of froth from high-clay tar sands.

The data in Table show a maximum in yield around pH 8.2, similar to that found in the pilot plant (5). As clay content increases, the yield becomes more sensitive to pH. Also, increasing the clay decreases the oil yield from these sands conditioned at 350 rpm.

Table I

Effect of pH on Oil Yield
Pulp conditioned at 350 rpm

Tar Sand	% Bit.	NaOH meq/100 gm. sands	pH	Yield % Bit.	% Mineral in Dry Oil
A	8.0	.31	7.6	39	14
		.62	8.1	68	12
		.94	8.2	72	12
		1.25	8.7	68	8
A + 25% Clay*	6.0	0	6.9	0	-
		.62	7.6	30	21
		1.25	8.0	62	16
		1.88	8.4	53	18
A + 25% Clay*	4.0	1.25	7.4	21	21
		1.88	8.1	31	24
		2.50	8.4	6	37

*A brown clay picked from one of the clay lenses on the surface of the open pit mine.

Stirrer Speed

The above series of experiments also revealed the fact that 350 rpm was insufficient speed to obtain high oil yields from sands containing low bitumen or, equivalently, high clay. Changing the apparatus to direct drive gave us capability to extract 90% of the oil from all of the tar sands tested as can be seen in Table II. Here no effort was made to maximize the yield over 90%. Where effort was made to maximize yields, it was found that, as the speed of the stirrer was increased, the yield of froth went through a maximum and declined. In Figure 1 the maximum for 8% bitumen sands occurs at 500-600 rpm and shows appreciable diminution at 800-1000 rpm. Higher grade tar sands give maximum yields at lower rpm and appear to be less sensitive to high stirrer speeds.

Table II

Froth Yields

Tar Sand	% Bitumen	% Total Oil - 350 rpm	% Total Oil - 500 rpm
B	12.0	94	-
C	11.6	89	-
D	11.5	93	-
E	11.2	92	-
F	10.5	81, 90	-
G	9.1	84, 87, 93	-
H	8.4	81	89, 94
F + 30% Clay	7.5	80	99

Type of Impeller

Sensitivity to stirrer speed suggests also that the oil yield should be sensitive to type of agitator. Early work in the laboratories had shown that neither the Waring Blendor nor ordinary laboratory impellers give good conditioning of the tar sands pulp. A study was made using flat-bladed turbine impellers made to standard specifications (7). Data from two turbines in Table III shows that this type of impeller is inferior to the U-shaped paddle stirrer. The double propeller with higher turbulence gives very low yields. Qualitatively, then, agitation causing high turbulence gives poor yields. This observation is supported by the rule of Rushton and Oldshue (8)

FIGURE 1

YIELDS VS STIRRER SPEEDS

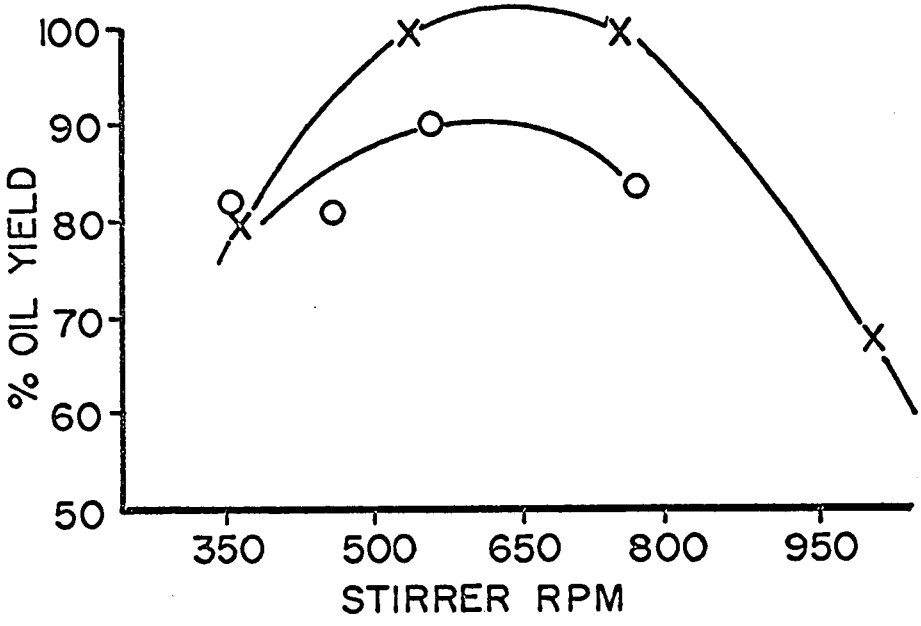

which states that flow rather than turbulence is favored in a process where the reaction rate increases with the ratio of impeller diameter to reactor diameter at constant power. By the formulas developed by Rushton and coworkers, the two turbines were using the same power at the speeds listed in Table III. In our process, the yield increases at least up to a diameter ratio of about 0.7 indicating a definite preference for flow rather than turbulence.

Table III

Type of Impeller
F Sands + 30% Clay, 7.5% Bitumen

Impeller	R.p.m.	% Oil
2-5/8" U	520	99
1-1/3" Turbine	1500	37
2-1/8" Turbine	500-700	67-62
Double Propeller	200*	18

* Run in 2" I. D. Reactor.

Other Variables

(a) Conditioning Time

Early investigations indicated that about 15 minute conditioning time was required to obtain maximum yields. Conditioning for longer times up to an hour had no effect on the yield. We standardized on 20 minutes in order to be safely out of a sensitive region. It became apparent that two events took place during the conditioning. First, the pulp was heated to 85°C. and the reagent mixed in thoroughly. Second, the hot pulp was worked intó a condition enabling the oil to rise as a froth when the sands were diluted with water (flooded).

(b) Flooding

Following Clark's admonition (4), the flooding was carried out at low stirrer speeds to prevent aeration with the accompanying increase in mineral in the froth. Early tests showed that this stirring had to be continued for about 10 minutes, otherwise oil would be trapped by the sand and not allowed to float. Merely stirring the sand with a spatula would free this oil from the sand. Work by others on similar apparatus (9) has shown that high-speed stirring during flooding actually diminishes froth yield.

(c) Air Introduction

The oil which does not float contains enough mineral to be heavier than water. One way to make this oil rise to the surface is to incorporate sufficient air to give bouyancy. Therefore, improvement in yield could imply aeration. This was tested by introducing air into the bottom of the reactor under the stirrer during the conditioning stage. The U-stirrer was operated at a lower speed in order to give some chance for yield increase by air. In fact, as is seen in Table IV, the air caused less oil to froth using either the paddle or turbine stirrer. It is thought that the froth yield was lowered because the formation of the air cavities in the pulp lowered the effectiveness of the agitation.

Table IV

Air Introduction

Impeller	R.p.m.	Air	% Yield Oil
2-5/8" U	350	No	80
		Yes	72
2-1/8" Turbine	550	No	67
		Yes	49

Instability of the Pulp

During some attempts to study other variations of hot water separation, the observation was made that the froth yield from some pulps decreased if the conditioned sands were allowed to stand before flooding. After standing for five minutes, pulps from good grades of tar sands give little or no decrease in froth yields; but allowing the pulps from poorer grade sands to stand for five minutes without agitation causes a large decrease in froth yield. Furthermore, the

effect is reversible. Reagitating the pulp restores the yield. The phenomenon is examined in Table V. With this tar sand, the yield drops nearly in half after standing for five minutes but is completely restored by restirring for five minutes.

Table V

Pulp Instability
H Tar Sand, 8.4% Bitumen

Conditioning Treatment	% Oil Yield
550 rpm, 20 minutes.	89
As above, then stop for minutes	52
Stir 20 minutes, stop 5 minutes, stir 5 minutes	94

DISCUSSION

Agitation of tar sands pulp with the paddle stirrer offers a laboratory method for separating the oil from a wide range of tar sands in hot water. The procedure can be adapted to very small batch samples and requires no recycle or further treatment of any fraction. The yield can be adjusted simply by altering the stirrer speed in order to test a variable which might improve the froth yield. We are confident that high oil yields can be obtained from poor tar sands containing only 6% bitumen and perhaps even less.

A great advantage of the technique is that the critical step -- conditioning -- is isolated and can be probed to achieve an understanding of why oil floats from tar sands in hot water. The laboratory process of Clark and coworkers (4) and the Great Canadian Oil Sands pilot plant (5) have a number of potentially interrelated steps including the recycle of the water-clay phase. Proper agitation of any of the various phases could be important to froth yield. It is most convenient to be able to vary the froth yields by controlling the agitation in one known phase.

Already just by studying a few of the obvious variables in conditioning, we can outline the requirements of frothable oil. The physics of the separation requires that, in order to float, the oil must be freed of most of the mineral and must contain enough air to make the particles less dense than water. Also, the particles must be larger than 30 microns diameter in order to float in the time allowed. One observable effect of increased clay in tar sands is to make the particles of oil smaller. When the sands are not conditioned properly these flecks remain in the water-clay layer (4).

The work here shows that as the clay increases, the vigor of agitation required to condition the pulp increases. Thus, it does not seem likely that shearing oil particles into smaller fragments is an important function of conditioning. This conclusion is born out by the fact that yields are not favored by the introduction of turbulence, a high shear phenomenon. The flotation mechanism is not ordinary air flotation where particles of material cling to the face of an air bubble. Again, turbulence would be desirable for such flotation. The low shear kneading action of the agitation would favor either working mineral out of the oil or air into the oil. No choice can be made between these alternatives except to say that the existence of a rapid decay in yield with time in unagitated pulps would favor the air distribution because of superior mobility of gases over solids. Proof of this air distribution during conditioning of good grade oil sands is the subject of a report by other workers in this laboratory (9).

ACKNOWLEDGMENT

I am glad to acknowledge the technical assistance of Mr. N. D. Morphett in the experimentation. Also, I am grateful to Sun Oil Company for permission to publish this work.

LITERATURE CITED

(1) Clark, K. A., Pasternak, D. S., I. and E. C. 24, 1410 (1932).
(2) Clark, K. A., Trans. Can. Inst. Mining and Met. 47, 257 (1944).
(3) Clark, K. A., Pasternak, D. S., Research Council of Alberta Report 53, 1950.
(4) Clark, K. A., Can. Oil and Gas Ind. 3, 46 (1950).
(5) Innes, E. C., Fear, J. V. D., Preprints of the World Pet. Congress, P. D. No. 13 (7), 133 (1967).
(6) Pasternak, D. S., Hodgson, G. W., Clark, K. A., Proc. Ath. Oil Sands Conf., p. 200, 1951.
(7) Rushton, J. H., Costich, E. W., and Everett, H. J., Chem. Eng. Prog. 46, 395 (1950)
(8) Rushton, J. H., Oldshue, J. Y., Chem. Eng. Prog. Symp. Ser. 55, 181 (1959).
(9) Bean, R. M., and Malmberg, E. W., following paper, No. II of this series.

JOINT SYMPOSIUM ON OIL SHALE, TAR SANDS, AND RELATED MATERIAL
PRESENTED BEFORE THE DIVISION OF PETROLEUM CHEMISTRY, INC.
AND THE DIVISION OF WATER, AIR, AND WASTE CHEMISTRY
AMERICAN CHEMICAL SOCIETY
SAN FRANCISCO MEETING, April 2-5, 1968

HOT WATER PROCESSING OF ATHABASCA OIL SANDS: II. MICROSCOPE STUDIES OF THE CONDITIONING PROCESS

By

Earl W. Malmberg and Roger M. Bean
Sun Oil Company, Research and Engineering Division, Marcus Hook, Pennsylvania

INTRODUCTION

This paper will consider in detail conditioning, the initial step in the hot water extraction process for the Athabasca oil sands. This term, carried over from extractive metallurgy, refers to the step in which the raw ore is converted to a form from which the desired fraction can be separated from tailings. Seitzer (1) has described experiments which showed the importance of vigorous mechanical working in producing excellent yields of froth even from grades of oil sand as low as 6 percent oil. In this paper we will be concerned with the reason why this mechanical energy input procedure is so effective and if this information can be of help in understanding procedures which are more amenable to scale-up, (for example, procedures using large-scale equipment more immediately available). From this view we had the following objectives:

(a) We needed to understand the chemistry and physics of conditioning so that scale-up could be made with confidence.
(b) A lower primary froth yield from conventional laboratory methods (2) as compared to the pilot plant must be improved or explained.
(c) We needed procedures that were comparable in all respects to large scale methods so that valid laboratory studies could be made on later steps in the process and on variations in the properties of oil sand samples.

Most workers on Athabasca oil sands have, of course, made use of the microscope (3). Early studies in our laboratory were useful, for example, in demonstrating the powerful surface forces that are operating in freeing the oil from sand particles. The need for some minimum amount of shear is easily shown. However, it was only with new techniques that we began to obtain fundamentally useful leads. The first observations were made through the glass wall of the stirred reactor. We then developed a more generally applicable method of quick-freezing samples in the pulp matrix and examining cleavage surfaces.

Observations on Bitumen Morphology in the Stirred Reactor Under High-Energy Conditions

The stirred reactor described by Seitzer (1) has the broad U-shaped blade passing within 4 mm. of the glass wall of the reactor. As the stirring rate is stopped or slowed down, a wealth of interesting observations can be made at the glass interface on the size and shape of the bitumen particle and size and distribution of air bubbles. The controlling variables are the quality of the oil sand and the amount of alkali.

EXPERIMENTAL

A Unitron low-power binocular microscope (range of magnification 5X to 90X) with inclined eye-pieces was removed from its normal stand and mounted horizontally on a heavy adjustable frame such that it could be focused through the walls of the heating bath and reactor and onto the contents of the flask. Sharp focus was only possible when walls of bath and reactor were quite close together. Lighting was provided by two 100 watt illuminators.

A Nikon-F 35 mm reflex camera fitted with a 1/2 X microscope adaptor was used to record visual observations of pulp morphology. With full illumination from two 100 watt illuminators, good photographs could be obtained at a magnification of 4 X with 1/4 or 1/8 sec. exposure using Ektachrome B film (ASA 125). In rapidly changing situations (i.e. stirring or bubble coalescence, etc.), the Nikon-F was fitted with an extension bellows and a reversed f-2 lens to give total

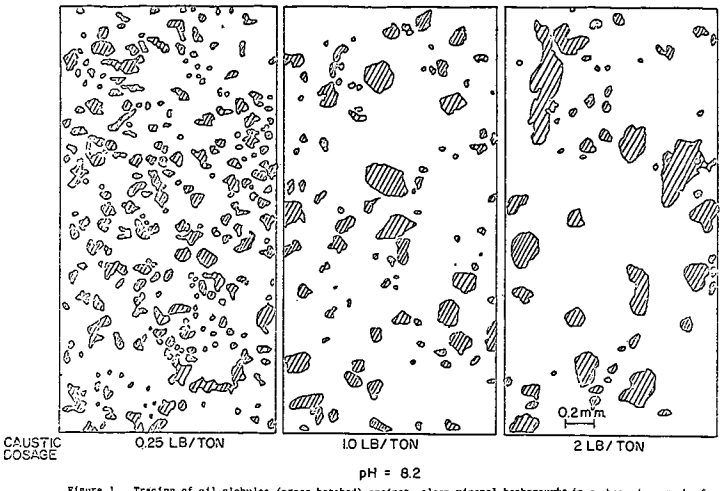

Figure 1. Tracing of oil globules (cross hatched) against clean mineral backgrounds in a photomicrograph of conditioned oil sand. Stirred reactor, 1.75 in. diameter, 1000 r.p.m. Lean oil sand, 8%

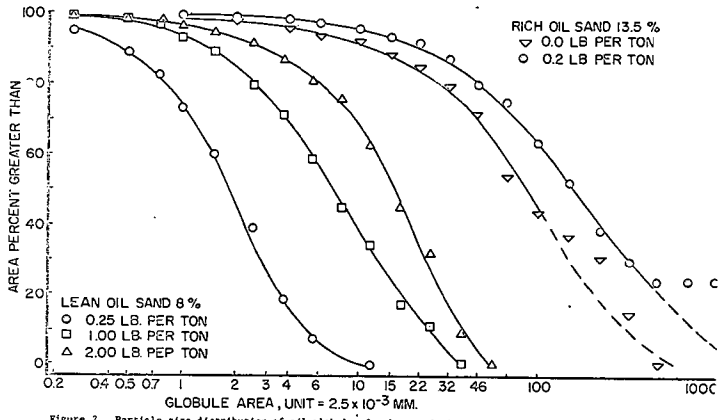

Figure 2. Particle size distribution of oil globules for lean and rich oil sand samples with variation in caustic dosage. Stirred reactor 1.75 in., 1000 r.p.m.

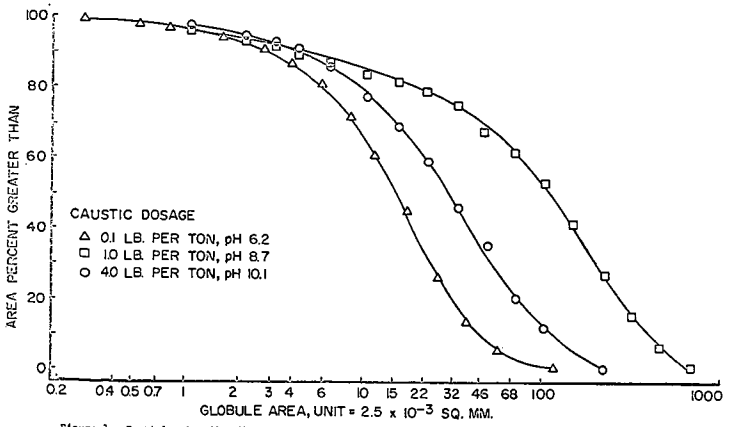

Figure 3. Particle size distribution of oil globules for an average oil sand, 10.7%, (Pit A Lot 25) as a function of pH. Stirred reactor, 3-inch, 350 r.p.m.

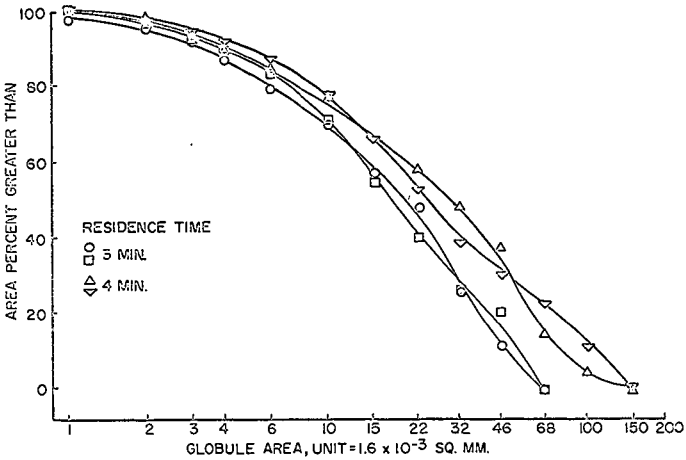

Figure 4. Particle size distribution of oil globules for average oil sand, 10.7%, (Lot 25 Pit A) with variation in residence time. Samples from FTU conditioning drum October 29, 0.55 lb/ton;pond water

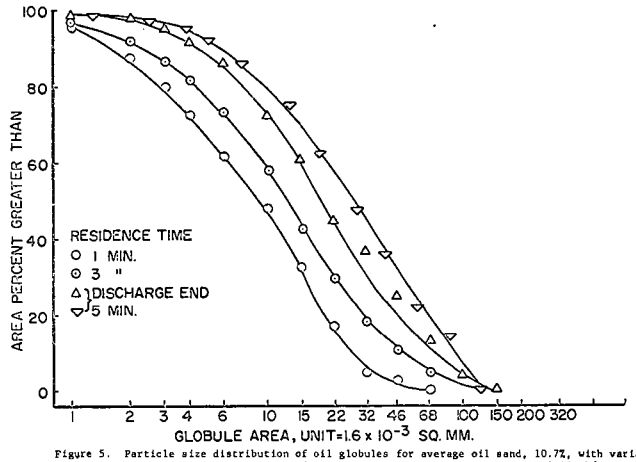

Figure 5. Particle size distribution of oil globules for average oil sand, 10.7%, with variation in residence time. Samples from FTU conditioning drum October 31, 0.45 lb/ton, fresh water.

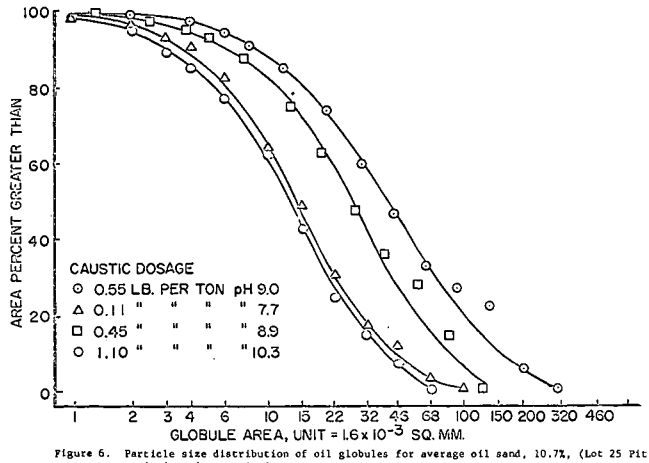

Figure 6. Particle size distribution of oil globules for average oil sand, 10.7%, (Lot 25 Pit A) with variations in caustic dosage. Samples from FTU conditioning drum discharge October 31.

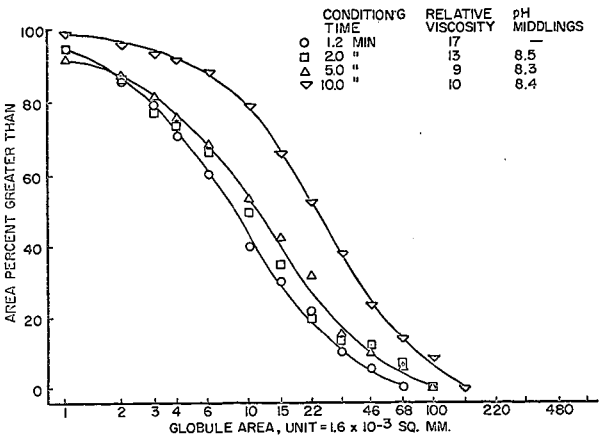

Figure 7. Particle-size distribution of oil globules for average oil sand, 10.7% (Lot 25 Pit A) with variation in conditioning time. Samples from 3-inch stirred reactor, 50 r.p.m., 0.5 lb/ton.

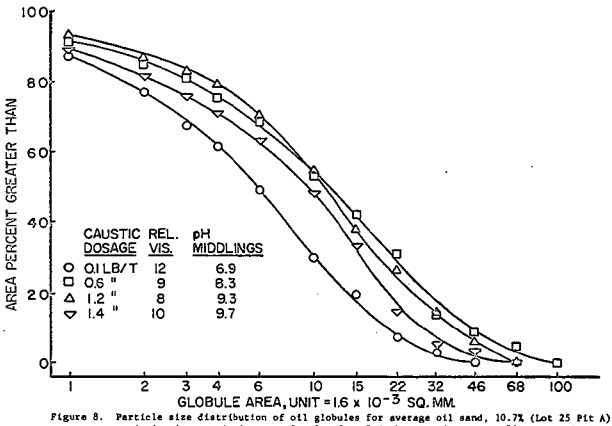

Figure 8. Particle size distribution of oil globules for average oil sand, 10.7% (Lot 25 Pit A) with variation in caustic dosage. Samples from 3-inch stirred reactor, 50 r.p.m., 5 minutes conditioning time.

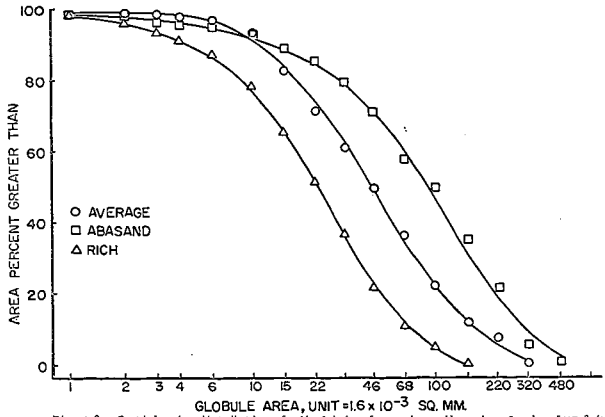

Figure 9. Particle size distribution of oil globules for various oil sands Samples from 3 inch stirred reactor, 100 r.p.m., 10 minute conditioning time, caustic dosage for optimum pH.

Sample	% Oil in Feed	Primary Froth Yield	Relative Viscosity
Average	10.0	60	11
Abasand	14.6	95	24
Rich	13.5	92	20

magnification on the film of 4.5 X. For lighting, an electronic flash was used. This arrangement was quite effective in "freezing" the action.

Visual observations and color transparency photographs provide a wealth of information that is impossible to communicate in black and white prints. Line tracings of bitumen globules of Pit C oil sand are shown in Figure 1. The progressive increase in size of the globules as caustic is added is obvious to the eye, but a description capable of finer discrimination is required if this method is to be applied widely. One solution to this problem is shown in Figure 2, in which the globule sizes from Figure 1 are plotted as a conventional size distribution. The shape of this curve and the size of the median globule provide a characterization adequate for present purposes. This method of representation will be used throughout this paper.

RESULTS

For the studies in the stirred reactor at high speed, all the observations are at steady-state conditions -- no change with time. Poor quality oil sand (Pit C, Figure 2) have in general much smaller oil globules, but the size increases as added caustic soda brings the pH up to the operating level, 8.4. The Pit A sample in Figures 2 and 3 show the characteristic larger size of an average oil sand, but with the same pH response. In addition, Figure 3 shows the decrease in oil-globule size as the operating pH is exceeded; globule size forms a rather wide flat maximum from pH 8.4 to around 10. At this high pH many average and low grade oil sands form emulsions rather than froth. This behavior is associated with a pronounced drop in the interfacial tension at this same high pH.

We had originally hoped that this globule size characterization would provide some measure of the cohesiveness of the oil globules which, in turn, might be related to froth yield. As we have seen, the high fine mineral content of low-grade oil sands is accompanied by a smaller oil globule size, and these samples in general give lower froth yields. However, when the change in globule size with pH is used as a variable, no correlation with froth yield is seen. Representative experimental results are shown in Table 1; in general, this behavior has been observed consistently over a wide range of samples. In the final analysis, working hypotheses which do not involve particle size or cohesiveness have been found to be much more useful.

TABLE 1

TYPICAL RESULTS SHOWING THE ABSENCE OF CORRELATION BETWEEN PRIMARY FROTH YIELD AND OIL GLOBULE SIZE

Caustic Soda lb. per ton	pH	Size of Area Median Globule mm^2	Primary Froth Yield
0	6.1	0.075	30
0.1	6.2	.035	49
0.25	6.7	.038	63
0.5	7.6	.150	70
1.0	8.7	.275	69
2.0	9.6	.338	75
4.0	10.1	.071	76

Further examples of this behavior are presented in Figures 9 and 10.

There were two factors observed which can account for the higher froth yields obtained from the high-speed stirred reactor. In average and high-grade oil sands, informative observations were made on the behavior of the gas bubbles in the globules of bitumen. By the squeezing action in rapid stirring of the pulp, the bubbles were made very small, perhaps less than one-hundredth of the size of the oil drop, and there were very many of them. When the stirrer was stopped, coalescence of the bubbles began immediately and within 10 to 20 seconds most of the gas was in a very few bubbles of the order of one-fourth the size of the globule. With the dynamic interchange of oil among globules which was also observed (continual coalescence and disruption of globules) a very even distribution of air was assured when flooding was performed with no time delay after the rapid stirring. Decreased froth yield is experienced when bubble coalescence is allowed to occur, and globules broken up during flooding may then yield fragments with no bubbles plus fragments containing most of the original flotation gas.

The second factor is perhaps the most important when all grades of oil sand are

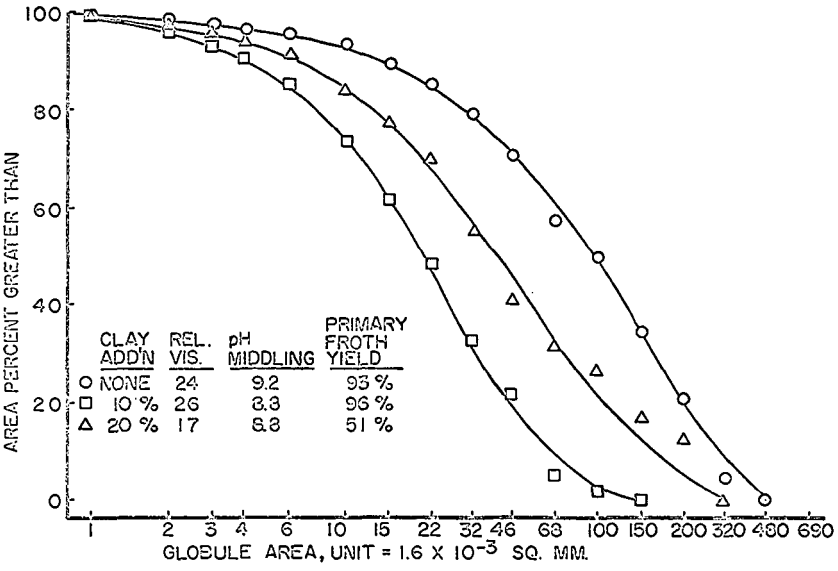

Figure 10. Particle size distribution of oil rich globules for Abasand oil sand with various amounts of seam clay added. Samples from 3 inch stirred reactor, 100 r.p.m., 1.0 lb/ton.

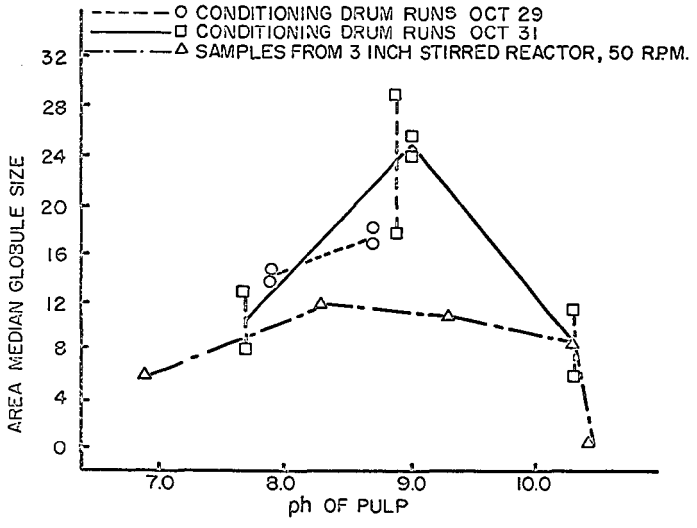

Figure 11. Summary of the change in the oil globule size distribution with pH of conditioning. Area is shown by the area median globule size.

considered. Measurement of the amount of flotation gas showed that rapidly stirred pulp contained about three times as much as pulp produced by several other procedures. Mineral contents of these pulps were all approximately the same. All other things, therefore, being equal, a higher froth yield will result from a higher content of flotation gas.

Observations on the Conditioning Drum in the GCOS Field Test Unit

Early studies on conditioning showed that the rotating drum had a rather large minimum diameter for operability, and laboratory scale work was not feasible. In order to make direct comparisons between drum and laboratory methods, a method of quick-freezing samples of pulp was developed and applied in a microscope study of conditioning in a rotating drum.

EXPERIMENTAL

Sampling Procedure

The procedure consists of quick-freezing samples of pulp, cleaving the frozen lump to produce cross-sectional surfaces for visual and photographic microscope studies, and measuring the particle size distribution of the oil globules. The sample is frozen on a flat surface cut from a solid copper bar, three quarters of an inch in diameter and six inches long; the bar is insulated except for this flat surface and is cooled in liquid nitrogen before immersion in the pulp. Efforts to detect orientation effects or effects from the sampling procedure were made in two ways. Two and three flat surfaces at right angles to each other were machined on the bars and samples frozen at each surface were examined. They were examined with cleavage surfaces parallel and perpendicular to the plane of the metal. In some cases, a partial "growth ring" effect was observed close in to the metal and these samples were eliminated. Samples were, in general, layers about one centimeter thick, and all observations corroborated the premise that the quick chill immobilized the sample the way it existed in the process of conditioning. Trial of a number of methods of sampling showed that the most satisfactory way was to stop rotation of the drum and immediately insert the sampling device at the selected point in the drum.

The cleavage planes were studied on the cold stage microscope. At magnification of 5X and 8X the depth of focus is usually adequate to give a sharp picture of the entire sample. The remainder of the magnification for measurement was done by projection of the 35 mm. color transparency. The light source was a powerful electronic flash. A number of photomicrographs were taken as the sample was allowed to warm up.

We expected that no significant observations could be made on the flotation gas bubble morphology in the frozen samples, and in general, no bubbles were seen. The rapid cooling would be expected to collapse the bubbles very rapidly since at 85°C they are predominantly steam. Photomicrographs of both surfaces of a cleavage (i.e., the mirror images) agreed quite well, showing that cleavage, in general, went through solidified bitumen particles as well as around them. In neither case could any useful observations on flotation gas bubbles be made. It should be remembered that measurements at other times showed only about one-third as much flotation gas in a conditioning drum sample as in the pulp produced in a stirred reactor at high speed.

Conditions for preparation of the pulp in the drum

These experiments were performed at a time the Field Test Unit was using a feed known as Pit A Lot 25. This sample is a mixture of lean silty oil sand plus some rich oil sand, averaging 9-10 percent oil and 17 percent fines in the mineral (< 325 mesh). For optimum froth yield, it required a dosage of 0.5 - 0.6 pounds of caustic soda per ton. From extensive experience with a wide variety of oil sands, we regard this sample as an excellent representative of feed of somewhat less than average quality. These experiments were all run at 80 percent solids (80 percent mineral plus oil, the remainder water); in general, oil or water does not separate at this composition. Although much of the Field Test Unit operation was at 70 percent solids, no differences in operation have been observed that are pertinent to this study.

Conditioning was done in a drum 2.5 ft. in diameter as already described (4) at 4 tons per hour feed rate. Alkali dosage was varied so that results would parallel the effects observed in the rapidly stirred reactor if possible. Samples were taken at the discharge end, 1, 2, and 4 feet into the drum.

Experiments were made with :

(a) fresh water used in the drum
(b) with water from a settling pond which contained 6 - 7 percent of fine suspended mineral ("pond water").

RESULTS

As already mentioned, no time rate of conditioning was detected in the rapidly stirred reactor; only steady state effects were observed. The microscope observations on frozen samples from the drum served to define a rate process of physical changes in conditioning. Samples of short residence time showed a dirty background of oil-mineral still combined with oil present as a film. There is a relatively small amount of agglomerated oil (as measured by the "percent oil agglomerated", which is simply the percent of the total area occupied by oil globules). With appreciable dirty mineral background, the accurate tracing of the droplets becomes very difficult and the results correspondingly less reliable.

Some representative results are shown in Figures 4-6. The conclusions may be summarized as follows:

1. The following aspects of conditioning as a rate process were observed.
   a. Sand becomes clean and oil agglomerates into globules of increasing size as the rolling motion of the drum applies shear and mixing.
   b. The required residence time for this process under the given conditions is about two minutes. Aside from lump ablation (4), this rate is the slowest of any of the physical or chemical processes we have observed.
2. The effect of caustic dosage, at, below, and above the amount which results in optimum pH, is the same as observed in the rapidly stirred reactor. A broad maximum in globule size is observed at and somewhat above the optimum operating pH of 8.4 (Figure 6).
3. For this particular oil sand, no differences were observed between conditioning with fresh water as compared to pond water containing 6 - 7 percent fine mineral (Figures 4 and 5).
4. The oil sand, Pit A Lot 25, is probably most similar to the Pit C sample of Figure 2. Hence the oil globule size is somewhat larger in the conditioning drum as might be expected under milder mechanical treatment.

Application to Laboratory Conditioning: The Stirred Reactor at Slow Speed

The observations on pulp from the conditioning drum led us to reconsider laboratory procedures for the conditioning step. Of continuing concern was the problem of lower froth yields from small scale laboratory conditioning as compared to the conditioning drum in the Field Test Unit. The fast stirred reactor clearly did better than the Field Test Unit in froth yield, but just as clearly was greatly different in the incorporation of flotation gas. The crux appeared to be how much energy was needed in the process and how it was applied as shear. This approach led to studies with the stirred reactor at slower and slower speeds until a sequence of photomicrographs of frozen samples was obtained which showed essentially the same rate of conditioning and other features as seen in the drum. Pulp produced by hand stirring in a beaker was also characterized by a microscope study.

EXPERIMENTAL

With a choice between freezing samples in the interior of the stirred mixture or making observations at the wall, all further work was done with the frozen samples for two reasons. The primary reason for this choice was that the progress of conditioning, i.e., the earlier stages, can be observed only in the interior, not at the wall.

The high-speed rate of stirring for the 3-inch reactor is 350 r.p.m. Upon slowing this speed to 100 and then 50 r.p.m., we reached a time scale of conditioning which was comparable to the observations in the conditioning drum. The most important parameters were again time and caustic dosage. Most of the comparison experiments were done with a sample identical with the pilot plant feed, Pit A Lot 25.

A number of additional oil sand samples were studied to confirm the observations made with the representative sample.

RESULTS

Time Effect

The time effect in conditioning that can be expressed quantitatively is the growth of the bitumen particle size during the stirring. This effect is shown, for example, in Figure 7. In

general, after about 5-10 minutes of stirring at 50 r.p.m., a steady state is reached and no further changes in the particle size distribution are observed. However, just as in the samples from the conditioning drum, the most important results are qualitative observations on the transformation of oil sand to clean mineral plus bitumen globules. The intermediate stages of small lumps of mineral plus oil and thin, yellow oil films can only be described in words. The significance of this intermediate state will be discussed in a following section.

pH Effect

A series of steady state oil globule size distributions are shown in Figure 8 that demonstrate the effect of caustic dosage. Again, as in the conditioning drum, a broad maximum in globule size is observed at and somewhat above the operating caustic dosage.

Selected oil sand samples

Although Pit A Lot 25 is an excellent representative oil sand for experimental work, a number of selected oil sands were also studied in the stirred reactor. Similar behavior was observed in all cases. We were particularly concerned in obtaining further evidence on

(a) a relation between oil globule size and primary froth yield

(b) the effect of viscosity of the pulp on the globule size

In Figure 9, the characteristic behavior of the rich oil sand from the Abasand Quarry in the Horse River Valley near Fort McMurray is shown. This sample gives very large globules of oil. This behavior may be associated with the generally much higher viscosity of the oil from this source, but any attempt at correlations of this kind immediately finds further difficulties in results such as in Figure 10.

Comparison of all the results in Figures 9 and 10 confirms the conclusion that the primary froth yield, in general, is not related to the bitumen particle size. Similarly, viscosity does not have a pre-eminent role in determining the globule size. Care must be taken to control solids contents of the pulp because decreases in globule size parallel to increases in viscosity have been observed when samples have been stirred over long periods and water lost by evaporation.

In general, although a given oil sand sample shows a consistent behavior with time and pH in these studies, wide variations among different oil sands are observed in the bitumen morphology. Many complex factors are operating to result in these differences between samples.

Application to Hand-stirred Conditioning: The Significance of Partial Conditioning

Seitzer has described some of the small scale laboratory methods of conditioning that were used in the early stages of our oil sand studies (1, 5). In an effort to understand the low froth yields from conditioning by hand stirring in a beaker, examination by microscope was applied to pulps produced by this method. Although agglomerated bitumen could be seen on the walls of the beaker during the stirring, all samples frozen in the interior of the mixture showed very little agglomeration and large amounts of dirty mineral and oil films. There were random variations in samples treated identically; no consistent pattern could be observed. Samples, in general, contained large proportions of oil not agglomerated. The significance of these results will be discussed in a following section.

Study of the Relation Between Conditioning Methods and Primary Froth Yields

The results of the preceeding experiments came to have an important bearing on one pre-eminent problem -- the low froth yield in the initially most important procedure, conditioning by hand stirring. Before this aspect is discussed, the results of a number of related experiments will serve to describe the problem and define some of the factors. Part of the difficulty results from the dichotomy of conditioning and flooding. From the viewpoint that the primary froth yield is the single most important characteristic in studying an extraction process, we are immediately confronted by the fact that the two parts, conditioning and flooding-settling, must always be part of the process for producing froth. Early studies seemed to indicate that higher pilot plant froth yield might come from quite vigorous mechanical treatment (including exposure to air) of the pulp in and after flooding. Several devices were fabricated to test this hypothesis on a laboratory scale. The results are shown in Table 2.

The most important behavior that stands out in Table 2 is -- whatever the flooding procedure -- the drum discharge produces a higher froth yield than the laboratory procedure of hand stirring in a beaker. Experiments of this kind on other types of oil sands have shown the same results: hand conditioning in a beaker, except for very high quality oil sands, gives lower froth yields than drum discharge.

TABLE 2

PRIMARY FROTH YIELD WITH VARIOUS FLOODING PROCEDURES
APPLIED TO CONDITIONING DRUM DISCHARGE AND TO HAND-STIRRED PULP

Fraction	Conditioning Drum Discharge Duplicate Runs		Laboratory Conditioning Duplicate Runs	
Flooding: Procedure A				
Percent of total bitumen in:				
Primary Froth	52	51	26	24
Middlings	28	32	54	50
Tailings	20	17	20	26
Percent mineral in:				
Primary Froth, dry basis	8	11	7	7
Flooding: Procedure B				
Percent of total bitumen in:				
Primary Froth	84	91	50	47
Middlings	11	6	29	44
Tailings	5	3	21	9
Percent mineral in:				
Primary Froth, dry basis	10	8	11	11
Flooding: Procedure C				
Percent of total bitumen in:				
Primary Froth	72	83	68	59
Middlings	26	14	23	21
Tailings	2	3	9	20
Percent mineral in:				
Primary Froth, dry basis	9	11	12	16

Flooding Procedures:

A. Simplest batch procedure, placing conditioned tar sands into hot water in mechanically stirred receiver.

B. Feeding conditioned tar sand by means of a plunger into a stirrer-water spray-rotating screen assembly, from which the flooding is completed in a stirrer-equipped beaker.

C. Apparatus as in B plus a two-foot cascade of twelve steps prior to the stirred receiver.

Oil Sand Feed

Pit A bucket wheel product, 12.3 percent bitumen; conditioning done with fresh water and caustic soda to pH 8.4. Pilot plant primary froth yield 84-88%.

At this point the correlation between this poor froth yield and the microscope observations suggested a hypothesis and some experiments to test it. If the unresolved oil-mineral or dirty mineral which is seen in frozen samples of hand-stirred pulp is present because conditioning is incomplete, then the froth yield from short-time stirred reactor experiments should be lower also. The results of these suggested experiments are shown in Table 3. The characteristic low froth yield from hand conditioning is observed again. The low froth yields from "partial conditioning" in the stirred reactor are gratifying; for these cases, microscope studies showed the same incomplete separation of oil and mineral and partial agglomeration as from hand stirring. The hypothesis was confirmed; experiments with other oil sands have given the further corroboration of this hypothesis. In addition, the utility of microscope examination of quick-frozen samples of oil sand was demonstrated.

Additional results were included in Table 3 to show the decrease in froth yield with over-treatment by caustic. Oil sands vary in this response, but in this case, emulsification of the oil occurs during conditioning at pH around 10 and froth yield drops to zero. Again, this emulsification can be observed in a microscope examination of frozen samples of pulp. That insufficient alkali will result in dirty mineral throws a valuable side-light on the usefulness of the surface forces in conditioning. At low pH many of these inherent surfactants have not been "activated", which presumably occurs by salt formation at the proper pH. Hence more

mechanical work is required. A number of results have indicated that mechanical energy (stirring of the proper kind) can be traded off for alkali.

TABLE 3

CORRELATION OF CONDITIONING, MORPHOLOGY, AND PRIMARY FROTH YIELD

Oil Sand - Pit A Lot 25, 10% Oil. Flooding: Procedure A, Table 2

Conditioning			Oil Globule Size	Flooding
Alkali dosage lb./ton	pH	Time min.	Area median size globule[1]	% of oil as primary froth
		Stirred Reactor		
I. Partial Conditioning[2] - insufficient mechanical working or alkali				
0.1	5.7	2.5	9,6	44
0.1	6.8	5.0	6	27
0.5(3)	7.6	1.2	8	27
0.5(3)	8.2	1.2	11	36
II. Adequate Conditioning				
0.5	8.5	2.0	10,10	54
0.6	8.3	5.0	11	54
0.5	8.4	10.0	23,24	54
1.0	8.9	2.5	9,10,8	60
III. Conditioning at high pH - borderline of emulsification				
1.2	9.2	5.0	11	49
1.4	9.7	5.0	9	33
IV. Conditioning at high pH - emulsification predominant or complete				
1.6	9.8	5.0	Almost completely emulsified	14
2.0	10.2	10.0	Completely emulsified	1
		Hand Conditioning		
Partial Conditioning - insufficient mechanical working[3]				
0.5	8.2	10.0	Not measurable	18
0.5	8.2	10.0	Not measurable	26

1. Area median globule size is taken from size distributions such as Figure 2 It is the value of the abscissa where curve crosses the ordinate = 50%. Multiple values are from independent duplicate determinations on the same pulp.
2. Degree of conditioning - as shown by microscope examination of frozen samples Inadequate conditioning is evidenced by the presence of large amounts of oil-mineral still in combination and areas covered by visible yellow oil films.
3. Oil sand preheated to processing temperature 85°C; time indicated is total time of stirring

The froth yields for optimum conditions in Table 3 approach those reported for separation cell froth in the pilot plant. The laboratory values are still somewhat low; experiments have established that with middlings recycle in the laboratory as used in plant scale, the primary froth yields are completely comparable. Because this aspect is more closely related to study of settling, these experiments will be reported in detail in another paper.

DISCUSSION

The goal of understanding conditioning as it is judged by the primary froth yield has been

achieved over a scale ranging from small laboratory experiments to a pilot plant at 10 tons per hour

(a) We now understand in terms of requirements for uniform shear and mixing, experiments with a scale difference of 100, 000. As might be expected, the physical factors were most important to understand; from our present understanding of the effect of shear and mixing, we would expect full-scale conditioning drums to improve on the performance of the pilot plant. The chemical factors, such as effect of sodium hydroxide in engendering surface active agents, deflocculating clay, etc., are on a molecular and interfacial level and do not vary appreciably with scale on the gross level.

(b) The microscope studies led to an understanding of the poor results of hand conditioning of oil sands. The information has been fitted into a consistent detailed picture of the extraction process.

(c) With this background of understanding of and control over the conditioning stage and returning to simple flooding procedures, we could proceed to study the next stage of the process. Future papers will describe the results of study of the settling process and further understanding of the processability of widely different oil sand samples.

Certain special topics in the present results have interesting implications which are discussed below.

1. The effect of pH: The action of caustic soda is evidenced in deflocculation of clay, forming salts with potential surfactants, and neutralizing acidic species in general. In the effect of pH on oil globule size are seen mostly secondary results. Figure 11 summarizes the results of the oil globule size measurements over the pH range of interest. The curves serve to point out one difference between the stirred reactor and the conditioning drum. The particle size is larger in the drum and the tendency to emulsification is greater in the stirred reactor because the reactor is characterized by a higher shear stress, at least at the end of the conditioning period.

2. Rate-limiting step: Conditioning in the drum and with suitable laboratory methods includes a rate process of freeing and agglomerating the oil. The drum showed a residence time requirement of about two minutes. Innes and Fear show several runs with good froth yields at residence of 0.5 minutes. However, we are describing the time in terms of immediate flooding as can be done in the laboratory. In the pilot plant the drum discharge went through a vibrating screen, a centrifugal pump, and lengthy runs of pipe before separation was allowed. This process has the slowest rate of any of the chemical or physical processes we observed in the laboratory.

3. Importance of shear properly applied: In this work the microscope observations and primary froth yield from conditioning by hand stirring testify to the need for a certain minimum shear applied in a suitable systematic way. One of the useful working hypotheses is that this extraction process is related to the problem of why bituminous pavement fails.

4. Factors directly involved in the primary froth yield: Primary froth yield, as for example in Table 2, is best understood in terms of a simple working hypothesis which we have found will explain a very wide range of empirical facts concerning the hot water extraction process. If we assume a settling medium in which Stokes law can operate, the buoyancy of the froth determines the primary froth yield. This buoyancy is determined by the flotation gas content and its distribution, the mineral held in the froth, and the density of the medium. As is well known, the pure oil has a density very close to that of water.

Dr. K. A. Clark has stated (5) that procedures such as B and C in Table 2 are inadvisable because the mineral in the froth is increased. This conclusion is based primarily on his studies with Bitumont oil sand, which is of quite high grade. Our work has necessarily been concentrated on average and poorer grade oil sand. The following modification of Dr. Clark's view is offered in order to explain our results with lower oil sands. The factors in oil buoyancy which are listed above are used plus our understanding of conditioning.

A standard flooding procedure allows a certain amount of oil to float as froth, with a given oil content. Agitation of middlings or flooded pulp in the presence of air, in general, increases the amount of flotation gas, and hence, oil with a larger mineral content can float. Primary froth yield increases and mineral in the froth increases. This behavior is observed in the column for "Laboratory Conditioning" in Table 2. This occurs because as the microscope has shown, important quantities of oil still attached to gross amounts of mineral (i.e., large sand grains) are still present. The general concept in mineral flotation is that an oil attached to a mineral provides the situation necessary for attaching the bubble of air for levitation. Perhaps the behavior first noted by Dr. Clark (6), that oil globules in the middlings will film out on the water-air surface, is part of the explanation. Whatever the mechanisms for floating, the inhomogeniety in the conditioning accounts for these results. On the other hand, in the "Drum Discharge"

column we see increases in froth yield with no detectable increase in mineral. Here it will be remembered the mixture is very homogeneous and the oil is free of major amounts of mineral. Oil globules have mineral in the form of emulsified (w/o) middlings and at best silt or clay. Quiet flooding (Procedure A) gives a much better froth yield, and the oil remaining in the middlings, resulting from an initially very homogeneous pulp, is on the borderline of floating. When the more energetic procedures of flooding are used, this oil will float readily but will not have any large amount of mineral to carry up. Confirmation of this physical picture is found in sedimentation studies. The "black layer" of oil that settles slowly and forms above the settled sand in a sedimentation from a gentle flooding is generally copious in hand-stirred conditionings. However, it is missing or very small in flooded samples from drum discharge. This unrecovered oil in these cases does not have enough mineral to cause it to sink. Further confirmation of this interpretation is described in another paper.

5. Techniques in microscope work: The use of frozen samples for microscopy proved to be a major help in studies of conditioning. Conditioning on a microscope slide does not give information on the fundamental mass-shear problem. Transferring samples of pulp to the microscope for observation invariably causes changes that vitiate the most valuable observations The quick-frozen samples were invaluable in this study of conditioning, and the technique can be applied to problems in other aspects of recovering oil from the Athabasca deposit.

LITERATURE CITED

(1) Seitzer, W. H. Preceding paper, No. I of this series.

(2) Pasternak, D. S., Hodgson, G. W., and Clark, K. A., Proc. Athabasca Oil Sands Conference, 1951, p. 200.

(3) Clark, K. A., Trans. Canadian Inst. Mining and Metallurgy 47, 260 (1944).

(4) Innes, E. D. and Fear, J. V. D., Preprints of the World Petroleum Congress, P. D. No. 13 (7), 133 (1967).

(5) The procedure was initially described and demonstrated to us by Dr. K. A. Clark.

(5) Clark, K. A., Trans. Canadian Institute of Mining and Metallurgy 47, 257 (1944). Also private communications from Dr. Clark.

(6) Clark, K. A., and Pasternak, D. S., Research Council of Alberta Report No. 53, 1949.

JOINT SYMPOSIUM ON OIL SHALE, TAR SANDS, AND RELATED MATERIAL
PRESENTED BEFORE THE DIVISION OF PETROLEUM CHEMISTRY, INC.
AND THE DIVISION OF WATER, AIR, AND WASTE CHEMISTRY
AMERICAN CHEMICAL SOCIETY
SAN FRANCISCO MEETING, April 2-5, 1968

HOT WATER PROCESSING OF ATHABASCA OIL SANDS: III. LABORATORY STUDIES ON SETTLING, MIDDLINGS VISCOSITY, AND INFLUENCE OF ELECTROLYTES

By

Earl W. Malmberg and William M. Robinson
Sun Oil Company, Research and Development Division, Marcus Hook, Pennsylvania

INTRODUCTION

The Athabasca sands yield up their oil in the hot water extraction process by floating as a froth while the sand sinks in a separation vessel. The medium in which this settling occurs is a suspension of the mineral fines in hot water called middlings. The settling may seem to involve only a simple exercise in Stokes law to predict and optimize the results. However, when detailed consideration is given to continuous large scale operations, a number of complicating factors arise. For example, economic and engineering factors dictate that the middlings be recycled through the process (1). The plant feed contains varying amounts of fine material, and their removal is accomplished through a drag stream from the middlings recycle. The magnitude of the drag stream is determined by the fines content of the plant feed and the density of the middlings. Economic and engineering factors again dictate this density be as high as settling operability will allow. The laboratory study of this critical factor directed us to some experimental parameters of primary importance in the hot water extraction process.

Conditioning Procedure Used in Settling Experiments

The second paper of this series describes a laboratory conditioning procedure whose characteristics are almost all closely comparable to the large scale apparatus of the pilot plant (2). The one remaining point of concern was the mineral content of the froth -- laboratory froth in general had a higher content of mineral. A specific procedure was discovered with the stirred reactor which solved this problem. The resolution of this last point of difference is important for the work to be presented because it gave us complete confidence that we could proceed with a laboratory study of settling; the results would be meaningful for large scale work.

EXPERIMENTAL

Conditioning is generally regarded as a process carried out at a chosen "solids content", e.g., 80 percent solids means oil + mineral is 80 percent with 20 percent water. The essence of the method used in this paper is described in Table 1 as "New Procedure". Water was added in increments at the stated intervals during the conditioning in the stirred reactor. The remainder of the procedure up to the settling process is as follows. Flooding water was added, the stirrer slowly speeded up to 300 r.p.m. and then slowly stopped. Variations in procedure such as with the rich oil sand are made when the viscosity of the mixture requires it. All operations and measurements are at 85°C.

RESULTS

The results of the stepwise addition of water in conditioning are shown in Table 1. The first results from the "New Procedure" were most gratifying in that not only was mineral low but the results were uniform. Earlier laboratory froth samples characteristically have a relatively large random variance. The experiments listed under the variations were to test the unique requirements of each stage. All the details proved to be necessary. Experiments were also performed which showed that the rate of heating or preheating had no influence on the result. In the stage at low water content, stirring produces high shear in the mixture. We believe this action is responsible for reducing the content of fine mineral in the oil globules. The action of the other essential parts of the procedure is understood in terms of the shear and the particle

size characteristics of the mineral in the froth.

Laboratory Recycle of Middlings: High-fines Oil Sand with Middlings of Normal Viscosity

In the basic laboratory operation of settling for a given batch of oil sand, the layer of froth is skimmed off, the middlings decanted after a chosen interval of settling, and the sand tailings remain in the vessel. Middlings from one run can, as chosen, be used in conditioning and flooding in the processing of the next batch of oil sand feed. In successive cycles of this process with a properly chosen "drag stream", middlings density can be built up and will proceed to inoperability. Many aspects of hot water processing, including quantitative, are formally related to multi-stage solvent extraction; laboratory batch procedure is related in this way to the continuous pilot plant. With a laboratory batch procedure, independent parameters can be set and measurements made of as many dependent variables as possible to characterize the system. We wished to examine all possible effects that might be operating in the settling, so that as wide as possible a range of characterizing variables were obtained.

EXPERIMENTAL

The "New Procedure" of Table 1 was used for the conditioning and flooding was done by adding the proper amount of water and/or recycle middlings. This stirring-for-flooding procedure is especially useful because a series of density measurements over any period of time can be made with pipetted samples, the mixture re-stirred, allowed to settle the desired time, and then decanted. The following sample sequence was used:

1. "Immediate density" - taken as soon as possible after stirring is stopped.
2. Similar sample after 2 min. settling.
3. Similar sample after 5 minutes.
4. Similar sample after 15 minutes.
5. Decanted middlings were stirred and a uniform sample taken.

The density sample was taken in a specially designed weight pipette with a large opening. The two-minute density sample was analyzed for oil and mineral.

Viscosity measurements on a suspension of mineral and oil are difficult, particularly when special rheological measurements are to be made, e.g., to detect small thixotropic effects. Early measurements in the pilot plant laboratory were made by settling the middlings for 9-15 minutes and making the measurements on the supernatent liquid. We found the procedure satisfactory and thereafter used it so that our results could be compared directly to the data from the continuous process.

Conductivity measurements are also difficult, primarily because the oil in the middlings fouls the electrodes. Two short heavy platinum wires in a fixed support proved to be rugged for cleaning and of adequate sensitivity. Analysis for oil and mineral were performed on the froth and tailings so that overall balances could be reported. Also, the primary froth yield would be used as our basic indicator to show whether in a given batch the settling was operable or inoperable. A number of intervals of settling prior to decantation were used: 0.58, 2, and 15 minutes. As will be noted in the results, the differences in behavior all were as might be expected; consequently, most of the work was done at one interval, 2 min.

RESULTS

The different facets of the experimental results resolve themselves in several major groups that are presented below.

Froth and Middlings - analytical results and other measurements:

These results from several characteristic runs are shown in Tables 2 and 3. Table 2 represents a sequence which was inoperable at the ninth cycle. The series shown in Table 3 was terminated when all signs indicated an incipient inoperability. The final middlings were then available for further detailed studies. The following points may be noted:

a. The effect of recycling middlings in increasing primary froth yield is one of the last links establishing laboratory processing as being comparable to pilot plant in yield. Evidence shows that the increase comes from the additional opportunity for oil in middlings to float as it is recycled. An alternative explanation lies in increased buoyancy from middlings of higher density. Experiments are in progress to establish which one or if both factors are important.

TABLE 1

TESTING OF CONDITIONING WITH STEPWISE DECREASE IN SOLIDS CONTENT: EFFECT ON MINERAL CONTENT OF FROTH

Conditions: 200 g. Pit A Lot 25 oil sand (10% oil) 3-inch stirred reactor, 50 r.p.m.; conditioning temperature 85°C; 200 ml. flooding water at 85°C

Procedure of Conditioning[1]	% Recovered Bitumen in Froth	Midd.	Tails	% Mineral in Froth, D.B.
Former standard procedure:				
80% solids, 10 min.	54.2	27.0	18.8	8.3
	54.3	15.7	30.0	6.7
New Procedure:				
85% 5 min ⟶ 80% 3 min ⟶ 75% 3 min ⟶ 70% 3 min	58.5	25.2	16.3	4.5
	63.2	22.7	14.1	4.6
	60.0	27.5	12.5	4.7
90% 5 min ⟶ 80% 3 min ⟶ 70% 3 min	62.6	23.0	14.4	0[2]
	70.3	19.0	11.7	4.2
Variations for Test Purposes				
85% 5 min	63.3	23.8	12.9	8.2
	64.3	20.6	15.1	7.9
70% solids 12 min	39.7	39.4	20.7	10.0
	46.6	36.2	17.2	8.5
85% 5 min ⟶ 70% 3 min	64.1	24.0	11.9	6.5
Confirmation with different type oil sand: Rich oil sand, 13.5% oil, with 20% seam clay added				
Former procedure:				
80% 10 min	63.9	23.6	12.5	5.8
New Procedure: 85% 5 min ⟶ 80% 3 min ⟶ 75% 3 min ⟶ 70% 3 min ⟶ 65% 3 min	80.2	13.0	6.8	3.0

[1] % solids in conditioning refers to oil + mineral; i.e., 80% solids in 20% water.

[2] This result may be in part analytical error, but it shows a low level of mineral.

TABLE 2

BATCH RECYCLE RUNS ON PIT A LOT 25 OIL SAND: ANALYTICAL RESULTS AND RELATED DATA

Conditions: Oil sand, 10% oil; 3" stirred reactor 50 RPM, 15 minute middlings decant, 0.6 #/ton NaOH

Cycle No.	Midd pH	Primary* Froth Yield	% of Recovered Bitumen in:* Froth	Midd	Tails	% Min. in Froth: Min.(D.B.)	Analysis of Midd % Min	% Oil
1	8.3	38.5	43.8	40.2	16.0	10.1**	7.3	3.0
2	8.3	56.2	46.1	39.5	14.4	8.3	9.1	4.1
3	8.0	56.2	43.8	44.3	11.9	10.7	10.7	4.8
4	8.2	54.8	38.2	49.7	12.1	14.0	13.6	5.6
5	8.2	56.6	39.9	46.6	13.5	14.9	14.3	5.6
6	8.4	60.1	42.0	42.8	15.2	15.1	14.9	5.2
7	8.1	62.3	39.2	51.3	9.5	13.2	15.0	5.9
8	8.2	56.2	34.8	54.3	10.9	19.0	15.0	6.3
9‡	7.8	9.5	6.7	93.3	-	62.0	42.3	5.8

*Primary froth yield is calculated on the basis of one batch input. The bitumen distribution includes oil recycled in middlings as well.

**This value is unexpectedly high and may well be in error.

‡Conditioning with middlings in place of fresh water.

TABLE 3

BATCH RECYCLE RUNS ON A SILTY OIL SAND: ANALYTICAL RESULTS AND RELATED DATA

Conditions: 200 g. September Shaley Pit A, 9% oil; 3" stirred reactor, 50 RPM; 2-minute middlings decant

Cycle No.	Caustic Loading #/Ton	Midd pH	% Primary Froth Yield	% of Recovered Bitumen in:			% Min. in Froth D.B.	Analysis of Middlings		Conductance of Decanted Middlings
				Froth	Midd	Tails		% Min	% Oil	
1	0.6	8.4	47.4	58.7	28.2	13.1	9.0	8.05	1.88	800
2	0.675	8.3	62.3	59.1	31.0	9.9	10.7	11.8	2.6	445
3	0.75	8.3	65.4	52.8	37.7	9.5	12.0	14.1	3.6	1390
4	0.75	8.5	68.5	53.4	37.2	9.4	13.2	17.6	3.6	1780
5	0.675	8.3	77.8	51.9	40.9	7.2	14.4	17.9	4.5	1890
6	0.75	8.3	62.7	49.8	42.3	7.9	13.9	19.0	4.3	2300
7	0.875	8.35	61.5	44.4	49.9	5.7	16.9	20.4	4.0	2275

b. Mineral in the froth - an important measure of the quality of the froth - is closely related to middlings density. Since conditioning was with few exceptions done with fresh water, a large portion of the mineral in the froth was incorporated in the flooding through mechanical occlusion of water.
c. The "Recovered Bitumen" results demonstrate that as inoperability is reached, the oil becomes suspended more and more in the middlings.
d. Experiments interspersed in a series in which conditioning was done with middlings rather than fresh water demonstrated that high mineral in the froth and low primary froth yield result.

Settling as measured by successive density samples:

The time sequence of density samples taken 1 inch below the surface of the settling mixture can be analyzed to indicate any normal or abnormal settling behavior. The results are shown in Table 4.

Measurements of the rate of settling of mineral particles of different known sizes would provide a clear unambiguous answer as to rheological environment that obtains in the settling process. The results in Table 4 are only part of the data required for this absolute measurement. They do, however, give a strong indication that no abnormal viscosity is present even in the last runs which preceded inoperability.

For a number of samples, particle size data are available for the final middlings. In the customary analysis, cuts are made at 43 and 2 microns. These samples are not directly from the sequences in Table 4, but are from a sample of essentially the same properties.

Cycle	Settling Time for Decantations	Sand >43 μ	Silt Fraction >2, <43 μ	Clay Fraction <2 μ
1	2 min.	0.5	42	57
9	2 min.	0.5	43	56
9	0.58 min.	4.5	52	43
2	2 min.	2.5	47	50
9	2 min.	.5	54	45

If these results are interpreted with the density differences in Table 4, then the complete Stokes law comparisons of viscosities in the early and late cycles is made. There is no evidence for a thixotropic effect in these samples. The samples vary from 6 to 20 percent fine mineral.

Mineralogical analyses by X-ray diffraction have been made on these and a number of other samples in which the mineral was fractionate by sedimentation. Aside from the expected increase in the relative amount of clay in the smaller fractions, no fractionation of any mineral species has been observed.

Measurements with the Brookfield viscometer:

Conventional measurements of viscosity were made on samples of settled middlings in a further effort to detect thixotropic and other non-Newtonian rheology. With the Brookfiled viscometer measurements for the conventional shear stress-shear rate curve can be made. No evidence could be adduced for the existence of a yield stress in these samples. The procedure was designed to measure immediate viscosity and then the viscosity which developed as the instrument was in motion. This rheopectic viscosity is related to thixotropy, but the relative time rates of development are too complex to make any direct comparison of value.

Viscosity measurements for the experiments listed in Table 3 are shown in Figure 1. Plotting viscosity against density (or percent mineral) for different oil sands is one indication we have as to how one oil sand sample may differ from another in this aspect -- how high a density may be operable. In the heading of this main section, the term "normal" viscosity is used in the sense that this September Shaley Pit A gives a relatively low visoosity for a given density. We will see in the next section some results which we have called "abnormal" viscosity. These are relative terms, and as usual, normal and abnormal are defined in terms of common experience.

Conductimetric measurements:

In recycle experiments the caustic reagent dosage will accumulate and as expected the conductance slowly increases and levels off (because of the drag stream extraction effect). The results with these samples again are noted as "normal" behavior. Occasional unexpectedly low values of conductance are of no concern because they result from electrode fouling.

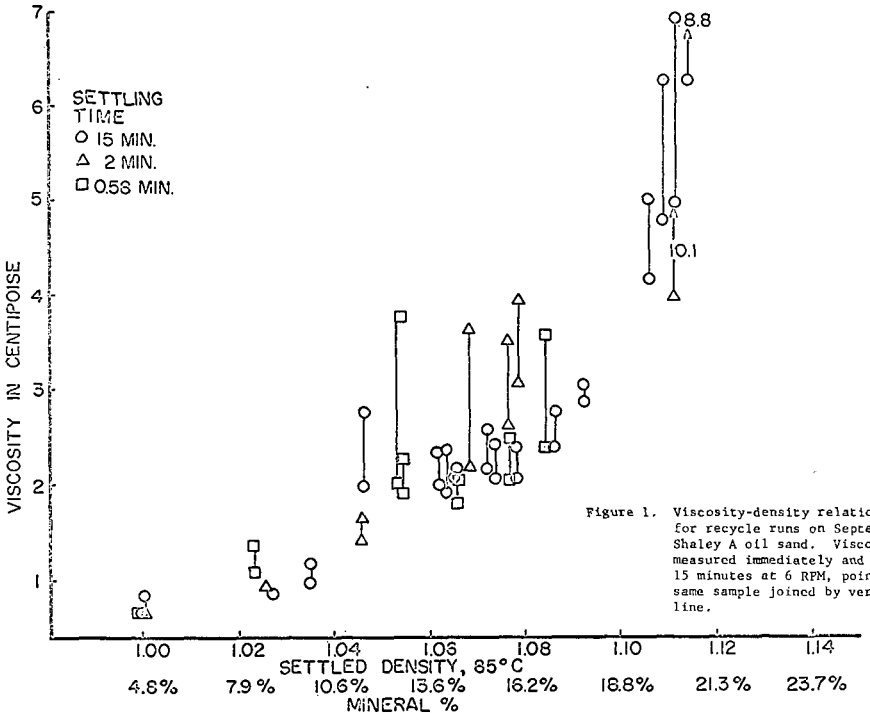

Figure 1. Viscosity-density relationships for recycle runs on September Shaley A oil sand. Viscosity measured immediately and after 15 minutes at 6 RPM, points for same sample joined by vertical line.

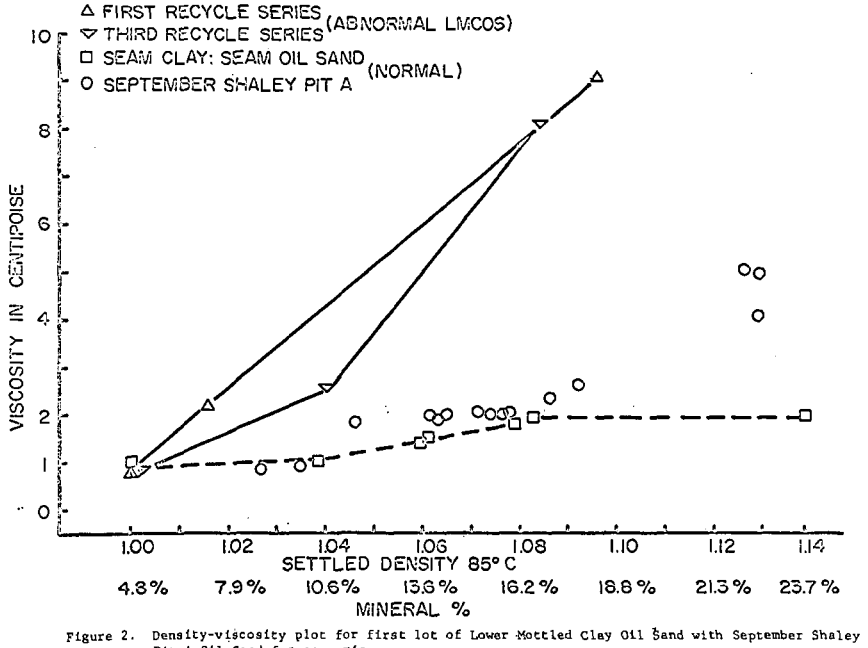

Figure 2. Density-viscosity plot for first lot of Lower Mottled Clay Oil Sand with September Shaley Pit A Oil Sand for comparison.

Laboratory Recycle of Middlings: High-Fines Oil Sands with Middlings of Abnormal Viscosity

All the laboratory studies were made with a range of different types of oil sands samples so that the general validity of results could be established.

Most of these samples have been from individual seams in the deposit, and we anticipate in general an averaging over a large number of samples. In this section will be described some samples of less common occurrence but of such extreme difference that the properties will be described in some detail.

EXPERIMENTAL

The experimental methods are essentially as in the preceding section. One additional set of data was obtained. The supernatent liquid after centrifuging all the mineral from selected middlings samples was analyzed for certain cations. Sodium, potassium, and calcium concentrations were measured by flame photometry; magnesium was determined by an EDTA titration. The cations held in the exchange capacities of various fine mineral fractions were determined by adding:

1. barium chloride to 0.05 N concentration, or
2. lithium chloride to 0.5 N and analyzing the supernatent liquid as above.

These abnormal oil sand samples were collected from a fresh face near the bottom of the escarpment on Lease 4, 25 miles down river from Fort McMurray. They appeared like a seam of clay with lumps of very rich oil sand interspersed giving a mottled appearance. There were two seams, each 8-12 in. thick, separated by about 6 ft. of rich oil sand. We were in need of high-fines samples and, therefore, chose them among others. These two samples by themselves gave essentially no froth yield although the oil content was at least 10 percent. They were mixed 1:1 with rich oil sand in order to apply the conventional procedures to test them.

RESULTS

Processing Characteristics and Middlings Viscosity of the Lower Mottled Clay Oil Sand (abnormal)

The first abnormal behavior of this oil sand was evidenced in the low froth yield by itself, as mentioned, and then even when mixed 1:1 with a very good oil sand. The results of a recycle series are shown in Table 5. A duplicate run gave essentially the same results.

An example of the extreme difference in rheological properties of this sample is shown in Figure 2. Here it will be noted that after the second recycle the immediate viscosity of the settled middlings is extremely high and as Table 5 shows, separation is not operating. The rheopectic viscosity is even more strikingly different from the immediate viscosity. In the second recycle, the viscosity reached 12-15 centipoise after 15 min. viscometer rotation at 6 r.p.m. In both types of viscosity measurement, there is a significant difference between what we have come to regard as normal behavior and the last sample we have described. For example, for a minimum operable viscosity, the allowable mineral content may be only one-half to one-third that for a sample such as Shaley Pit A. The results for this abnormal Lower Mottled Clay Oil Sand sample have been duplicated with the other seam, the Upper Mottled Clay Oil Sand.

Analysis for Cations in Middlings

The increase in conductance of the middlings during a recycle series parallels the increase in undesirable rheological characteristics. Classic studies in clay chemistry has demonstrated this effect -- flocculation by electrolytes leads to higher viscosities and non-Newtonian rheology. The effect was demonstrated in several middlings samples by removing the ionic impurities; anomalously high viscosities were no longer present in the dialyzed suspension. These data led to measurement of concentrations in the aqueous phase for selected cations, sodium, potassium, magnesium, and calcium. The pH at which the separation is carried out and the nature of the changes with time which we observed led us to eliminate other ions from consideration.

The results of analysis of middlings and the investigation of the exchange cations in the clays are shown in Table 6. The results of immediate interest are in comparing the "no recycle" samples, which are the middlings produced in the first run of a series. The Shaley Pit A shows no divalent cation whereas the Mottled Clay sample is already at 9.6 millinormal concentration. Also, this sample contains a large quantity of magnesium ion in the exchange reservoir of the clay.

Several comments are in order on these results. First, these results at the p.p.m. level

TABLE 4

SUMMARY OF SETTLING RESULTS (DENSITY DECREASE) FROM RECYCLE RUNS ON SEPTEMBER SHALEY PIT A

Time before Decantation Cycle Number	0.58 min. Second Sequence % Mineral*	D_5-C_{15}	2 min. Third Sequence % Mineral*	D_5-D_{15}	15 min. First Sequence % Mineral	D_5-D_{15}
1	7.1	0.0019	5.6	0.0009	5.2	0.0010
2	11.7	0.0060	12.0	0.0113	7.9	0.0099
3	17.2	0.0124	14.9	0.0180	9.7	0.0108
4	22.7	0.0235	16.6	0.0139	13.2	0.0099
5	23.9	0.0215	20.7	0.0160	12.8	0.0066
6	34.4	0.0373	21.8	0.0175	15.1	0.0177
7	Inoperable		31.4	0.0167	17.6	0.0228
8			Inoperable		17.7	0.0144
9					18.7	0.0177
10					17.2	0.0162
					Drag rate decreased**	
11					16.8	0.0114
12					15.4	0.0107
13					18.3	0.0118
14					23.1	0.0235
15					21.4	0.0181
16					21.2	0.0177
17					21.8	0.0169
Average-over		0.0237 last four		0.0164 last five		0.0157 last seven

* Mineral content determined from Decanted Middlings Density.

** Absolute drag rate usual 60 out of 260 ml in all except following Cycle 11 in First Sequence. Final absolute drag rate, 35 out of 260 ml.

TABLE 5

MIDDLINGS RECYCLE SERIES ON 1:1 LOWER MOTTLED CLAY OIL SAND - GOOD OIL SAND

Conditions: 3" Stirred Reactor, 50 RPM, 15 min. middlings decant
Mottled Oil Sand, 9.9% Oil; good oil sand, 13.5% oil

Cycle No.	#/Ton NaOH	Middlings pH	% Bitumen	% Recovered Bitumen in: Froth	Midd	Tails	% Min. in Froth Min(DB)	Analysis of Middlings % Min	% Oil	Conductance of Decanted Middlings
1	0.875	8.35	36.5	40.8	58.3	0.9	7.6	12.2	4.8	1000
2	1.0	8.3	29.6	21.8	65.6	12.6	11.6	16.4	9.8	1675
3	1.0	8.5	13.0	7.9	79.5	12.6	27.5	16.8	12.8	1975
4	0.875	8.4	28.2	10.2	85.7	4.1	26.6	22.5	15.6	1320

TABLE 6

DETERMINATION OF THE CATION EXCHANGE CAPACITY AND INDIVIDUAL EXCHANGE CATIONS OF CLAY IN LABORATORY MIDDLINGS

Sample	Displacing Reagent*	Total conc. of cations, mN Na	K	Mg	Ca	C.E.C. meq./100 g.
September Shaley Pit A						
No recycle	$BaCl_2$	5.8	ND	1.2	4.2	10.5
No recycle	LiCl	4.6	ND	1.0	4.7	11.5
No recycle	None	3.1	ND	ND	ND	
Fine Mineral after settling						
7th recycle	$BaCl_2$	16.9	ND	1.6	8.9	21.0
7th recycle	LiCl	14.1	ND	1.7	10.1	19.0
7th recycle	None	8.2	ND	3.9	ND	
Lower Mottled Clay Oil Sands						
No recycle	$BaCl_2$	14.5	ND	11.4	9.3	12.0
No recycle	LiCl	6.8	ND	15.8	6.4	12.0
No recycle	None	5.7	ND	9.6	ND	

*Reagent used to displace exchange cations from clay in sample. $BaCl_2$, 0.05N; LiCl, 0.5N in sample. 85°C

"None," the control, shows the amounts of cations in the aqueous phase before addition of the displacing reagent.

ND = not detected; lower limit is probably 5 ppm or less.

TABLE 7

EXPERIMENTS ON THE INTERACTION OF ADDED ELECTROLYTES AND MINERAL FINES IN THE HOT WATER EXTRACTION PROCESS

All runs at operating pH, 8.4; no recycle

Percent Added Clay	Added Mg^{++} mN	Primary Froth Yield %	% Mineral in Froth, D.B.
Mixture of high quality oil sand* with added clay			
0	0	83	0.8
30	0	63	5.7
0	2	82	6.5
30	2	5	11.1
0	6	73	9.0
10	0	91	5.1
10	6	57	2.5
September Shaley Pit A			
0	0	58	9.0
0	2	23	9.6

*This oil sand was chosen as the base because it has as close to zero fines content as we have available; 15.5% oil; less than 2% fines.

are subject to a random error, and this is evidenced by a rather large difference of the sets of sodium analysis. However, when the results of 4-5 analyses are combined additively, quite good agreement is obtained on the Cation Exchange Capacity (C.E.C.). Second, the samples with "no recycle" represent middlings as generated in the laboratory with no settling. Hence higher percentages of non-clay minerals will result in a lower C.E.C. The "7th recycle" sample represents fine mineral after settling and hence has a higher percentage clay, smaller particles, and probably a somewhat higher percentage of high exchange clays such as montmorillonite. These measurements of C.E.C. are in good agreement with the values which can be calculated from the known mineralogical composition.

Effect of Cation Concentrations on Middlings Viscosity

As an example of the effect of cations on the viscosity of clay suspensions, measurements were made on a sample of settled middlings which was normal rheology. To this sample (about 9 percent fine mineral) was added known quantities of two cations. These added cations were beyond the cations already present in the middlings from the normal procedure. The results are as follows:

	Viscosity, centipoise	
Added Cation	Immediate	Rheopectic, after 15 min., 6 r.p.m.
None	3	5
6.6 mN Na^{+}	5	75
0.7 mN Ca^{++}	5	50

These results show the effect of divalent cations as much greater than the monovalent ions, in agreement with the generalizations such as the Hofmeister series. These measurements were made to confirm that the response of the middlings clay suspensions to cations fell in the usual pattern.

Controlled Experiments on the Effect of Cations on the Extraction Process

The effect of added ions on the hot water extraction process was first reported by Clark and Pasternak (3); the Clark procedure was adopted for the Edna, California, oil sands by using a cold water wash to remove soluble salts (4). Clark's work was prompted by difficulties in processing a deposit just up the Clearwater River from Fort McMurray. Although no evidence was given, he believed them to be soluble salts present in the formation. He then showed that rather massive (by our results) doses of magnesium or calcium salts could reduce froth yields. In the experiments to test the effect of cations, Clark used oil sands of as low fines content as could be found. We agree that M^{++} concentrations of the order of 20-60 millinormal in the middlings are required to decrease froth yield for low-fines oil sands.

Three factors prompted us to design the experiment to be described.

1. Although there is a rough inverse correlation between oil content and primary froth yield, the spread of the points is very wide. For example, different oil sands of 10 percent oil content have been found that yield primary froth in the range from zero to 90 percent. An additional parameter has long been sought.
2. The behavior of medium and poor grade oil sands in processing and the properties of middlings when electrolytes have been added suggest that cations have an effect in the primary separation process as well as through increasing the viscosity for the settling step.
3. The phenomenon described in (2) is frequently associated with the mineral content of the separated oil. This mineral content is vital in determining the proportion of the oil which will float as froth. There is reason to believe that in the presence of cations, the separation of the mineral becomes less and less effective.

EXPERIMENTAL

A series of controlled experiments were organized in which the separate effects of cations and clay were evaluated and then the interaction evaluated in a further experiment. The standard procedure of conditioning and flooding was used; the additives were introduced in the first stage of conditioning. As a base for the experiments an oil sand as free from mineral fines as possible was used. Clay from a uniform seam of essentially zero oil content was used. The complete

control was not possible in the experiment on Shaley Pit A (17 percent fines), but it was used because it represents the only other important type of high-fines oil sand. Magnesium chloride was used to supply the cation because the analytical results had indicated that cation. Earlier results indicated that the Shaley Pit A had no magnesium in the initial middlings, and the seam clay yielded 2.0 mN magnesium.

RESULTS

The results of these experiments are shown in Table 7. For both of the basic types of high-fines oil sand the conclusion is unequivocal: the combination of mineral fines and a cation such as magnesium results in drastically lowered primary froth yields. The mineral content of the froth is of limited value because it is based only on the fraction of the oil that floats, and that fraction is, of course, only the portion of low mineral content. For a given sample and procedure, flotation gas content is reasonably uniform. To return to the main point, there is now clear-cut experimental evidence for an additional parameter to help us understand differences in primary froth yield. This parameter, liberation of soluble cations, is primarily effective in its interaction with mineral fines (clay).

DISCUSSION

In describing the development of the understanding of the oil sand processing in this paper, many of the points have already been discussed. In reviewing the series of experiments the following points are worthy of emphasis in summary.

1. In laboratory work with the stirred reactor, a progressively decreasing solids content yields a froth of minimum, uniform mineral content. One of the key elements seems to be high shear in a relatively viscous mixture. Conditioning with fresh water produces a better yield and quality of froth than when recycle middlings are used in conditioning.
2. The laboratory middlings recycle procedure provides an excellent tool for studying the properties of middlings. A plot of middlings viscosity against mineral content is a useful method of characterizing the settling operability of a given oil sand.
3. As inoperability is approached, the viscosity plot begins to curve upward sharply. The behavior can be understood from a simple mathematical expression of the kinetic factors involved:

   Viscosity increase (or degree of agglomeration) = constant X (mineral fines)^2

   X (soluble electrolytes)

   This expression shows that the components which accumulate during recycle jointly will produce a third order effect in the kinetics of clay agglomeration. This agglomeration results in sharp upward rise in viscosity at high levels of mineral content.
4. All comparisons we have been able to make to performance of the Field Test Unit show complete correspondence to laboratory results such as in Item 3 above. For example, electron micrographs of mineral fines show essentially the same morphology of the very fine mineral in samples from both sources.
5. The contribution of soluble electrolytes to undesirable rheological properties of middlings has been assessed in a number of ways.
   a. The increase in conductivity of the middlings in successive cycles is a good indicator of this factor. The results are in accord with the several accepted reactions of sodium hydroxide with clay.
   b. Dialysis to remove electrolytes eliminates the undesirable non-Newtonian rheology.
   c. As expected, divalent cations have 5 to 10 times the effect for monovalent cations at equivalent concentrations.
   d. Analysis of the supernatent water shows the presence of Mg^{++} in samples which have non-Newtonian rheology. These samples were "normal" oil sands after 7 recycles or "abnormal" samples in the first cycle.
   e. Determination of the exchange cations in the fine mineral of these samples shows that the abnormal samples contain large amounts of Mg^{++}.

   This and other evidence leads us to believe that these ions originate in both the exchange capacity of the clay and in the connate water.
6. If appreciable amounts of the "abnormal" type of oil sands are encountered in large

scale processing, the middlings density will have to be held at levels much lower than normal. A control on make-up water from middlings viscosity would be desirable.

7. Results of the preceeding studies suggested that soluble electrolytes could be an important parameter in the froth yield from oil sands of medium and high fines content. A set of controlled experiments showed that low levels of added electrolytes had no effect on oil sand free of fines. When clay was present, interaction of the clay and the electrolyte led to pronounced decreases in froth yield. Therefore, the primary froth yield of a given average of worse oil sand will be determined by the fines content plus the amount of (divalent) cation released to the process water.

LITERATURE CITED

1. Innes, E. D., and Fear, J. V. D., Preprints of World Petroleum Congress, P. D. No. 13 (7), 133 (1967).
2. Malmberg, E. W., and Bean, R. M., Preceeding paper, No. II of the series.
3. Clark, K. A. and Pasternak, D. S., Ind. Eng. Chem. 24, 1410 (1932).
4. Shea, R. B., and Higgins, R. V., U. S. Bureau of Mines, R.I. 4246, October, 1948.

JOINT SYMPOSIUM ON OIL SHALE, TAR SANDS, AND RELATED MATERIAL
PRESENTED BEFORE THE DIVISION OF PETROLEUM CHEMISTRY, INC.
AND THE DIVISION OF WATER, AIR, AND WASTE CHEMISTRY
AMERICAN CHEMICAL SOCIETY
SAN FRANCISCO MEETING, April 2-5, 1968

RETORTING UNGRADED OIL SHALE AS RELATED TO IN SITU PROCESSING

By

H. C. Carpenter, S. S. Tihen, and H. W. Sohns
Laramie Petroleum Research Center, Bureau of Mines
U. S. Department of Interior, Laramie, Wyoming

INTRODUCTION

Processes to recover oil from oil shale by in situ retorting are currently of great interest. Many investigators (1, 2, 3, 4, 5) have considered the possibilities of such a process because elimination of mining, crushing, and transporting the oil shale, and of disposing of the spent shale, could result in economic advantages over conventional aboveground processing. An in situ retorting technique may also make possible recovery of oil from deposits that are too deeply buried, too lean, or in beds too thin to be suitable for mining.

In situ retorting and recovery processes based on using nuclear explosions to fracture the oil shale have been discussed in the literature for several years (1, 2, 3, 4, 5). The fracturing would be accomplished by detonating a nuclear explosive near the bottom of an oil shale section at sufficient depth to insure complete containment. Following the detonation, collapse of the shale above the point of explosion would result in a nuclear chimney full of broken shale similar to a large batch retort. The size distribution of this broken shale would be different from that of any retorting charge previously investigated.

The properties of such a mass of broken oil shale are largely unknown. Predictions based on nuclear explosions in other rock types have been made about the size of a nuclear chimney in oil shale and the extent of fracturing beyond the chimney area (1, 2, 3). Assumptions based on particle size studies (3) indicate that pressure drops through a rubble column or nuclear chimney in oil shale should be low. Complete determination of the chimney characteristics, including radius, height, properties of the rubble column, and extent of the surrounding fractured area, will require a nuclear fracturing experiment in oil shale.

Following the development of the nuclear chimney, a retorting method that will recover most of the potential shale oil contained in the rubble column must be used. This method will be a batch operation capable of processing a mass of broken oil shale that will have a high bulk permeability, that will vary in size from sand-grain-sized particles to pieces several feet across, and that will vary in richness from barren shale to shale assaying 50 or more gallons per ton.

Previous research work on large-scale batch retorting methods which was done by the Bureau of Mines near Rifle, Colo. (6), studied the effects of particle size, air rates, and recycle gas rates on product recovery. Air rates studied ranged upward from 5 standard cubic feet per minute per square foot of retort cross section with recycle gas-to-air ratios of 0:1 to about 3:1. The retorts were operated using narrow particle size ranges. All fines, material smaller than 1/2 inch, were removed by screening, and the maximum particle size used was generally about 3-1/2 inches. The yield of oil from this experimental program ranged from about 60 to 90 percent of Fischer assay depending on particle size and grade of shale. This research did not include processing of large particles at low retorting rates.

The present study was started to determine the retorting characteristics of oil shale ungraded in size and varying greatly in richness. In general the oil shale charge used in the study has been mine-run material up to pieces as large as 20 inches in two dimensions. The third dimension may be as large as 36 inches, but because mine-run oil shale tends to be slabby this dimension probably averaged from 12 to 18 inches. Grade of the charge ranged from 26.0 to 48.0 gallons per ton by Fischer assay.

Air rates that have been investigated ranged from 0.58 to 1.94 standard cubic feet per minute per square foot of retort cross section. Recycle gas-to-air ratios have ranged from 0:1 to 4.27:1. These conditions have resulted in operating temperatures up to about 1,500°F. Yields of oil as high as 80 percent of Fischer assay have been obtained.

FIGURE 1. - Experimental oil shale retort.

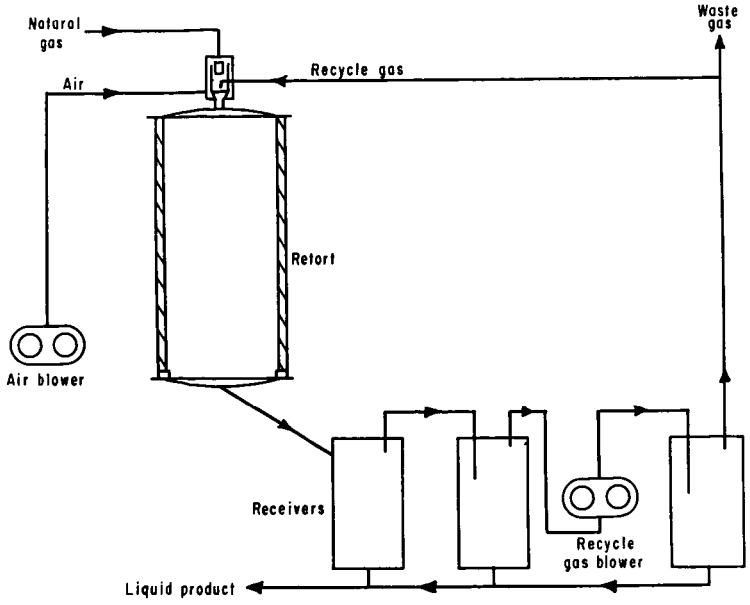

FIGURE 2.-Schematic Diagram of 10-Ton Retort.

FIGURE 3. - Block of retorted, partially burned shale.

EXPERIMENTAL PROCEDURE AND RESULTS

Apparatus

Figure 1 is a photograph of the Laramie 10-ton aboveground retort used for this investigation. The overall height of the unit is 34 feet. The retort vessel is 6 feet in diameter by 12 feet tall and has a cast refractory lining tapering from 6 inches thick at the bottom to 8 inches thick at the top. The vessel is suspended from the superstructure at three points to allow for expansion during the retorting operation. An electric hoist at the top of the superstructure, which extends 10 feet above the vessel, is used to load the oil shale charge.

A simplified schematic diagram (Fig. 2) shows the retort vessel and associated equipment. Auxiliary items are three recovery tanks, a recycle gas blower, and a primary air blower.

Located at the top of the retort vessel is a natural gas burner used to heat and ignite the shale charge. Natural gas supply for the burner is obtained from a gas line operating at about 5 psig. All of the gas supplied to the burner is measured, and samples for analysis are taken periodically.

Temperatures were measured and recorded by means of thermocouples inside thin-walled stainless steel tubes at 18-inch vertical intervals in the shale bed. Each tube or thermowell contained four thermocouples evenly spaced from the center to the outside edge of the bed. Additional thermocouples were attached to the outside shell of the retort vessel, to the gas meter, and to other points of interest. Temperatures were recorded by multipoint strip chart electronic recorders.

Rotary blowers were placed in the first two recovery tanks to agglomerate shale oil mist. The recycle gas blower was used for the same purpose, and the third tank was used for recovery of oil agglomerated by this blower.

In addition to the temperature recorders the instrumentation includes two gas flow-recorder-controllers and a process chromatograph. The flow-recorder-controllers are pneumatic instruments and were used to regulate and measure flow of recycle gas and stack gas. Gas sample inlets for the chromatograph were located at several points in the shale bed and also in the stack gas stream.

Oil Shale Charge

The oil shale charge for each experiment was prepared from mine-run shale that was obtained from the mine at Anvil Points Research Facilities near Rifle, Colo. Obtaining a representative sample of material varying widely in size and oil content is difficult, and the reliability of results based on these samples will have limits. To increase the reliability a procedure using the entire charge as a sample was developed. In this procedure the charge was segregated roughly by size into two parts, and all of the larger pieces were sampled by breaking them perpendicular to the bedding planes. The smaller pieces were sampled by a cone and quartering procedure.

Oil shale assay of the charges for these experiments ranged from 26.0 to 48.0 gallons per ton as shown in Table 1, arranged in order of increasing oil yield as a percentage of Fischer assay. Table 2 gives analyses of typical shale charges used in this study.

Since screening equipment of sufficient capacity was not available, it was necessary to determine the size distribution of each charge by separating the particles into the size catagories shown in Table 3 by actual measurement. Table 3 shows size distributions for several typical oil shale charges.

The oil shale charge was carefully loaded into the retort to avoid further breaking of the pieces. Shale particles were placed in the retort randomly in an attempt to avoid segregation by size.

Retorting

Retorting of the oil shale charge was started by heating with the natural gas burner. Length of time the burner was used ranged from a few hours to a few days. In general, external heating was not required after the top of the shale bed had been heated to about 350°F. At this temperature, stopping the flow of natural gas resulted in an immediate increase in the temperature of the shale bed because more oxygen was available for combustion of the shale.

Control of the retorting operation was based on bed temperature, on oxygen concentration in the stack gas, or on both factors. In some of the experiments a maximum bed temperature was chosen and air and recycle gas-flow rates were adjusted to maintain this temperature. In other experiments the flow rates were adjusted to maintain a minimum oxygen concentration in the stack gas and in still others to maintain a chosen oxygen concentration and a chosen temperature. In the series of experiments described here, two were made using air only with no recycle gas.

TABLE 1. - Summary of operations of the Laramie 10-ton retort

Experiment number	6	5	4	7	3	10	2	15	8	12 & 13	14	9	11
Oil yield, vol pct of Fischer assay	27.9	29.3	48.4	54.2	56.4	63.1	67.8	68.1	71.1	72.6	74.6	80.4	80.8
Fischer assay of charge, gal/ton	33.6	44.5	39.9	48.0	29.8	39.2	28.0	28.3	29.1	28.8	30.8	32.2	26.0
Air rate, scf/min/ft^2 of bed	0.84	0.71	0.84	1.00	0.58	1.06	1.33	1.94	0.85	1.04	1.11	1.23	1.36
Recycle gas-to-air ratio	3.94	4.27	0	0.92	6.90	1.34	2.67	0	0.61	0.36[1/]	0.72	0.95	0.82
Total air, scf/ton	13,900	22,429	77,057	30,511	7,349	22,953	23,306	13,727	21,965	21,566	25,530	19,666	21,150
Total recycle gas, scf/ton	55,040	95,302	None	19,780	51,188	22,503	62,204	None	10,824	4,418[1/]	18,428	16,984	12,575
Maximum bed temperature, °F	980	1,050	1,200	1,300	1,250	1,300	1,300	1,500	1,350	1,275	1,210	1,400	1,400
Selected oil properties													
Specific gravity, 60°/60°F	0.905	0.901	0.908	0.908	0.936	0.908	0.943	0.918	0.910	0.910	0.903	0.915	0.916
Pour point, °F	82	70	70	74	70	75	70	55	72	66	70	69	72
Viscosity, SUS @ 100°F	78	67	72	71	208	77	290	101	77	81	72	93	104
Nitrogen, wt pct	1.49	1.53	1.72	1.78	1.93	1.85	1.64	1.79	1.68	1.63	1.60	1.88	1.92
Sulfur, wt pct	0.81	0.80	0.98	0.86	0.78	0.86	0.60	0.89	0.91	0.80	0.78	0.76	0.77
Naphtha, vol pct of crude	1.5	3.5	5.0	6.6	1.2	7.9	0.8	7.0	7.7	6.5	7.1	6.7	4.8
Light distillate, vol pct of crude	23.8	27.0	26.5	20.5	13.4	20.9	11.5	20.5	24.0	23.7	25.3	18.5	21.0
Heavy distillate, vol pct of crude	26.8	42.8	44.2	41.5	42.2	47.9	40.9	38.4	45.9	40.7	42.8	38.2	40.3
Residuum, vol pct of crude	44.6	29.6	25.4	31.4	38.1	24.6	41.2	34.3	23.1	29.8	25.8	35.5	34.4
Gas composition, vol pct													
Nitrogen	77.6	75.3	76.6	74.0	74.7	72.3	80.0	68.1	74.3	74.0	75.3	72.5	74.0
Oxygen	4.3	7.9	8.9	4.9	10.3	6.1	6.1	2.1	4.9	4.5	6.5	3.8	3.5
Carbon dioxide	14.8	14.1	12.3	18.1	13.5	19.3	12.3	25.6	18.4	19.3	16.1	21.7	19.9
Carbon monoxide	2.0	2.0	1.4	1.6	1.1	1.3	1.1	2.6	1.5	1.2	1.3	1.5	1.5
Methane	0.9	0.7	0.6	0.5	0.4	0.7	0.5	1.1	0.6	0.6	0.5	0.4	0.8
Higher hydrocarbons	0.4	-	0.2	0.9	-	0.3	-	0.5	0.3	0.4	0.3	0.1	0.3

1/ Recycle gas was used during the last half of the run only.

Retorting runs were continued until the combustion zone reached the bottom of the retort. This point was determined from temperature measurements and also from sudden large increases in the oxygen concentration in the stack gas when these increases were caused by a decrease in the amount of carbonaceous material available for fuel. Retorting was assumed to be complete when the bottom thermocouples were at an average temperature of 900°F, and material balances were calculated over this period.

Following the retorting the shale charge was cooled in the absence of air. When cool, the spent, partially burned shale was dumped from the retort and sampled. Samples were assayed for oil content and analyzed for carbon, hydrogen, nitrogen, and sulfur. Typical analyses are shown in Table 4.

During the retorting operation liquid products were collected in three recovery tanks. Part of the liquid product drained from the bottom of the retort and was collected in the first tank. However, much of the oil left the retort as a stable mist so mechanical methods of agglomerating were required. Impellors were placed in the first two recovery tanks to agglomerate mist particles, and the recycle gas blower was used for the same purpose. Oil agglomerated from the mist was collected in the three recovery tanks. Some oil mist or vapor was vented. Although no attempt was made to recover this material, the amount was determined by adsorption of oil from a measured quantity of waste gas.

The oil and water mixture was taken from the tanks at the conclusion of each experiment, and because shale oil and water form stable emulsions both gravity and distillation were used to separate the two. After separation samples of water and of oil were analyzed. Preliminary work, which will be expanded, indicates that the water contains some soluble organic compounds as well as inorganic materials. Selected properties of the oil samples are shown in Table 1.

Gas samples taken from the retort were continuously analyzed during each experiment. These analyses were used to control the operation, and to observe the progress of the combustion zone. Average values of each constituent in the stack gas for each experiment are given in Table 1.

DISCUSSION

Oil Recovery

Oil yields from 27.9 to 80.8 percent of Fischer assay were obtained from the 13 runs shown in Table 1. The major part of these variations in yield is due to changes in the measured and controlled operating variables such as air rate, recycle gas-to-air ratio, and Fischer assay of the oil shale charge, but the remainder of the variations in yield are due to uncontrolled variables such as shale particle size distribution and location of the particles in the retort bed. The effects of these uncontrolled variables may be of major importance in the retorting of an actual nuclear chimney in oil shale.

An oil yield of 80.8 percent of Fischer assay is not as high as yields reported previously (4, 6) for other internally heated retorts using carefully sized oil shale charges. However, for ungraded charges yields would be expected to be somewhat lower.

Losses of potential oil can be attributed to several factors. One such loss is shown in the first column of Table 4, where 21.1 gallons of oil per ton remained in the discharged shale. This type of loss can be caused by channeling or by operating at gas-flow rates too high to completely retort the large pieces. Another loss is due to oil discharged with the stack gas as vapor or oil mist. The loss averages about 5 pounds per ton of oil shale charge. Improvements in the recovery system can eliminate this loss. A third type of loss may result from burning the oil as it is formed or by burning the residual organic matter before the oil has been drained away. Losses of this type may be minimized by adequate control of the process parameters including air and recycle-gas flow rates and bed temperatures.

Retorting Rate

Retorting rates covered by this study ranged between 1 and 17 pounds of shale per hour per square foot of retort cross section, depending on operating conditions. No relationship between retorting rate and oil yield was observed during this preliminary investigation.

Liquid Product Properties

In appearance, oil from the 10-ton aboveground retort is similar to oils produced by other internally heated retorts. The oil is black and viscous, has relatively high pour point, and has a distinctive odor. Selected properties of the oils are shown in Table 1. Murphy (4) has shown that oils produced in conventional retorts operating near maximum conversion have similar properties. Table 5 compares the properties of the oils discussed by Murphy and some of the oils recently

TABLE 2. - Analyses of typical oil shale charges

Sample number	6	7	14	11
Oil, Fischer assay, gal/ton	33.6	48.0	30.8	26.0
Water, Fischer assay, gal/ton	2.4	4.6	1.8	2.8
Mineral carbon, wt pct	4.81	4.55	4.96	4.51
Organic carbon, wt pct	13.28	16.79	12.43	10.27
Total carbon, wt pct	18.09	21.34	17.39	14.78
Hydrogen, wt pct	1.88	2.34	1.82	1.53
Nitrogen, wt pct	.44	.56	.39	.35
Sulfur, wt pct	.58	1.02	.79	.72
Gross heating value, Btu/lb	2642	3454	2398	2037

TABLE 3. - Particle size distribution of shale charges, weight percent

Particle size, inches	Sample number 6	7	14	11
-2	36.9	13.0	30.1	72.0
+2 -6	4.8	38.9	6.5	
+6 -12	13.9	10.3	15.9	9.2
+12 -20	14.8	20.7	18.4	6.3
+20	29.6	17.1	29.0	12.5

TABLE 4. - Analyses of discharged oil shale charges

Sample number	6	7	14	11
Oil, Fischer assay, gal/ton	21.1	0	1.0	0
Water, Fischer assay, gal/ton	1.7	0.8	0.5	0.8
Mineral carbon, wt pct	4.42	3.34	3.48	2.19
Organic carbon, wt pct	8.26	1.65	3.71	1.43
Total carbon, wt pct	12.68	4.99	7.19	3.62
Hydrogen, wt pct	1.05	0.14	0.23	0.14
Nitrogen, wt pct	0.36	0.12	0.21	0.09
Sulfur, wt pct	0.70	0.93	0.82	0.74
Gross heating value, Btu/lb	1528	153	504	137

TABLE 5. - Properties of shale oils

Properties	Conventional retorts[1] Gas-flow	Gas combustion	N-T-U	Aboveground retort[2] Experiment No. 14	11
Gravity, °API	17.3	20.0	22.0	25.2	23.0
Pour point, °F	80	85	90	70	72
Viscosity, SUS 210°F	58.0	50.4	45.8	36	38
Sulfur, wt pct	.70	.63	.80	.78	.77
Nitrogen, wt pct	2.20	2.09	1.90	1.60	1.92
ASTM distillation, °F					
Initial boiling point	225	290	196	122	122
5 percent distilled	463	446	436	348	392
50 percent distilled	641	-	662	690	735
Cut point	660	694	680	810	810
Recovery, percent	77	49	71	75	66

1/ Described by Murphy (4).
2/ Equivalent ASTM distillation was calculated from crude oil analysis distillation.

produced in the aboveground retort. The oil from the aboveground retort has a higher API gravity, lower pour point, and lower viscosity than the oils obtained from the other retorts. Sulfur and nitrogen contents are essentially the same.

Gas Composition

An average gas analysis for each experiment is given in Table 1. These gases have little fuel value and consist mainly of nitrogen and carbon dioxide. Small quantities of oxygen, carbon monoxide, methane, and higher hydrocarbons are present. The higher hydrocarbons are ethane and ethylene. Only trace quantities of propane have been observed.

Energy Considerations

An efficient batch retorting process should be able to derive most, or all, of its energy needs from combustion of the carbonaceous residue remaining on the spent shale. This residue amounts to about 25 weight percent of the organic matter that was present in the raw shale, and has a theoretical heating value of from 200 to 300 Btu per pound of raw shale. Since approximately 260 Btu are required to raise a pound of 28-gallon-per-ton raw shale to 900°F and retort it at that temperature (7), little or no heat other than that supplied by combustion of the organic residue is needed.

When retorting large particles of oil shale not all of the carbonaceous material remaining on the spent shale can be used as fuel. Figure 3 shows that a part of this material in the central portion of the larger particles may not be oxidized. Furthermore the rate of combustion may be too low to produce a useful amount or level of energy as the fuel is progressively burned from the outside portions of the particle. Therefore, in certain instances some additional fuel may be required.

The total volume of air used for these experiments varied up to 77,000 scf/ton of oil shale charge. Previous batch retorting (6) required 10,000 to 13,000 scf of air per ton. Both air and fuel requirements are related to the efficiency of the retorting system, with heat losses from the retort vessel accounting for a major part of the energy needs.

SUMMARY

Retorting oil shale ungraded as to size and oil content such as might be expected in a nuclear chimney is technically feasible. Yields as high as 80 percent of Fischer assay have been obtained by retorting ungraded shales with a maximum particle size of 20 inches in two dimensions.

The oils produced from these ungraded oil shale charges are similar to oils produced by other internally heated retorts but they tend to have more desirable properties. Their API gravities are higher, and their pour points and viscosities are lower. These more desirable properties are advantageous for transporting the oils or for further processing.

Sufficient carbonaceous material remains on the spent shale to furnish the energy requirements of the retorting process; however, in the larger particles this material may not be readily available for fuel. Air requirements for the experimental work varied widely.

ACKNOWLEDGMENT

The work upon which this report is based was done under a cooperative agreement between the Bureau of Mines, U.S. Department of the Interior, and the University of Wyoming.

LITERATURE CITED

(1) Lekas, M. A., and Carpenter, H. C., Colo. School of Mines Quarterly 60, No. 3, 7, (1965).

(2) Lombard, D. B., J. of Petrol. Technol., August, 1965, pp. 877-881.

(3) Lombard, D. B., and Carpenter, H. C., J. of Petrol. Technol., June, 1967, pp 727-734.

(4) Murphy, W. I. R., Proc. of the 2nd Plowshare Symp., Univ. of California, Lawrence Radiation Laboratories, UCLR-5678, May, 1959, pp. 80-101.

(5) Sohns, H. W., and Carpenter, H. C., Chem. Eng. Prog. 62, No. 8, 75 (1966)

(6) Ruark, J. R., Berry, K. L., and Guthrie, B., "Description and Operation of the N-T-U Retort on Colorado Oil Shale", BuMines Rept. of Inv. 5279, November, 1956 26 pp.

(7) Sohns, H. W., Mitchell, L. E., Cox, R. J., Barnet, W. I., and Murphy, W. I. R., Ind. Eng. Chem. 43, 33 (1951).

JOINT SYMPOSIUM ON OIL SHALE, TAR SANDS, AND RELATED MATERIAL
PRESENTED BEFORE THE DIVISION OF PETROLEUM CHEMISTRY, INC.
AND THE DIVISION OF WATER, AIR, AND WASTE CHEMISTRY
AMERICAN CHEMICAL SOCIETY
SAN FRANCISCO MEETING, April 2-5, 1968

REFINING OF PYROLYTIC SHALE OIL

By

D. P. Montgomery
Phillips Petroleum Company, Development Division, Bartlesville, Oklahoma

I. INTRODUCTION

Because of revived interest by both industry and government in the production of petroleum products from oil shale, a pilot-scale study of the refining of pyrolytic shale oil was made by Phillips Petroleum Company. This study used current refining technology and incorporated no novel or unproved refining steps. Only commercially available catalysts were employed.

The question to be answered was not whether shale oil can be refined to a synthetic crude and then to finished products, but what refining severity is required to reduce the nitrogen to a satisfactory level for continuous processing in a conventional refinery and what yields and qualities of the products would result.

Domestic oil shale locations and a thorough statement of the problems associated with recovering oil from these shales were presented in 1964 (7). A set of papers citing recent refining developments was published in 1966 (1). Pyrolytic shale oils are characteristically high in concentrations of nitrogen, sulfur, and oxygen; concentrations are typically two, one, and one per cent, respectively Because nitrogen is a potent poison for modern acidic type refining catalysts, its removal is of paramount importance. The oils are black, waxy, and foul smelling, with high pour points and viscosities and high concentrations of olefins and diolefins make them unstable. A detailed description of shale oil is given by Hellwig, et al (4). Facilities for refining may be non-existent at shale retort locations, since known oil shales are located in remote areas that are mountainous, arid, and cold.

For this study the most economic sequence of refining steps was postulated to be recycle coking and hydrostabilization at the retort, followed by pipeline delivery to a refinery near a marketing area. There the oil would be hydrodenitrogenated (HDN) in one or more passes, fractionated, and those distillates requiring further nitrogen reduction would be separately processed. Naphtha would be reformed and heavier distillates would be catalytically cracked. In pilot-plant operations we found that one-pass HDN of the hydrostabilized coker distillate was sufficient for distillates heavier than naphtha. In fact, the 400-650°F distillate was a satisfactory diesel fuel without additional processing. Both 400+°F and 650+°F distillates were catalytically cracked. A second-pass HDN of the hydrostabilized coker distillate was carried out, but the fractions were not further processed.

The following sections present in sequential order the experimental details, product properties, and yields for each refining step. Figure 1 is a block diagram of the processing scheme; in this figure areas separated by dotted lines represent the process steps.

II. FEEDSTOCK (RAW, PYROLYTIC SHALE OIL)

The shale oil used as raw feed was obtained by pyrolysis of a Colorado oil shale. Properties of this oil are given in Table I.

Determination of the consumption of hydrogen in many of the refining steps is important. Since this determination was based upon a balance of the hydrogen contained in feeds and products, unusual accuracy was required in analyses of the liquids processed. The requisite accuracy was attained by comparing the nuclear magnetic resonance spectra of protons in feedstocks and products and relating these spectra to those of pure hydrocarbons of approximately the same hydrogen content. A statistical study of this procedure by R. S. Silas of Phillips Petroleum Company has shown that hydrogen content can be determined to $\pm$ 0.05 per cent, at a 95 per cent confidence level (8).

TABLE I

COKING

Conditions: 14 psig, 810 F, 0.208 vol[a]/coker vol-hr.

Yields, % R.S.O.	Wt.	Vol.
Hydrogen	0.09	
Hydrogen Sulfide	0.11	-
Methane	1.39	-
Ethylene	0.42	-
Ethane	1.16	-
Propylene	0.67	-
Propane	0.87	-
Butylenes	0.67	1.0
i-Butane	0.14	0.2
n-Butane	0.44	0.7
Pentane and Heavier	81.43	85.5
Coke	12.61	-
	100.00	87.4

Properties	RSO[b]	Coker[c] Dist.	Coke
API Gravity	19.5	26.9	
Pour Point	+75	+40	
Vis., CS@100	-	5.05	
" " @210	-	1.55	
Aniline Point	-	83.6	
Mol. Wt.	-	252	
Br. No.	-	45.3	
Carbon Res, wt %	3.08	0.4[d]	
Composition, wt %			
C	84.6	84.3	89.5
H	10.84	11.30	3.4
S	0.61	0.54	0.32
O	1.5	1.2	2.34
N	2.2	2.0	4.5
Ash			0.55

[a]Coke drum filled in 32 hours.

[b]No free water was observed in the raw shale oil.

[c]Not stabilized.

[d]From another run.

TABLE II

HYDROSTABILIZATION

Conditions: 470 F (455 inlet, 485 outlet, exothermic Δ T), 500 psig, 0.89 LHSV, 1150 SCF hydrogen/bbl coker distillate, Filtrol 475-8 catalyst (pre-sulfided cobalt-molybdenum on alumina).

	Yields			
	% Coker Distillate		% R S O	
	Wt	Vol	Wt	Vol
Hydrogen	-0.71[a]		-0.58	
Water	0.07	0.1	0.06	
Hydrogen sulfide	0.02		0.02	
Methane	0.03		0.02	
Ethane	0.01		0.01	
Propylene	0.01		0.01	
Propane	0.02		0.02	
Butylenes	0.01		0.01	
i-Butane	0.01		0.01	
n-Butane	0.01		0.01	
Pentanes and heavies	100.52	101.7	81.8	86.8
Total	100.71	101.8		

Properties of C_5 + Liquid	
API Grav.	29.0
Pour Point, F	+40
Vis 100 F, CS	4.51
" 210 F, "	1.46
Aniline Point, F	94.7
Bromine No.	37.2
Composition	
C	84.3
H	11.93
S	0.49
O	0.83
N	2.0

[a]Hydrogen Consumption 414 SCF/bbl feed

Distillation (Corr. to 1 atm)	
IBP	120F
10%	330
20%	412
30%	476
40%	516
50%	561
60%	608
70%	655
80%	708
90%	769
EP	900

TABLE III

HYDRODENITROGENATION & FRACTIONATION OF

HYDROSTABILIZED COKER DISTILLATE

Conditions: 1500 psig, 812 F, 1.002 LHSV, 5200 SCF hydrogen/bbl feed, Harshaw 4303-E catalyst (nickel-tungsten on alumina, pre-sulfided)

	Yields			
	% of Feed		% of Raw Shale Oil	
	Wt.	Vol.	Wt.	Vol.
Hydrogen[a]	-3.41		-2.79	
Water	0.92		0.84	
Hydrogen sulfide	0.31		0.25	
Ammonia	2.42		1.99	
Methane	1.21		0.99	
Ethane	1.21		0.99	
Propane	1.16		0.96	
i-Butane	1.96	3.1	1.61	2.7
n-Butane	0.91	1.4	0.77	1.2
C_5-180 F	3.29	4.3	2.71	3.7
180-400 F	30.78	34.9	24.96	30.1
400-650 F	44.96	47.3	36.86	41.3
650+ F	4.28	14.8	11.66	12.9
Total	103.41	105.8	84.59	91.9

[a]Hydrogen Consumption 1970 SCF/bbl

TABLE IV

PROPERTIES OF HYDRODENITROGENATED LIQUID PRODUCTS

	Total Liquid Product[a]	C_5-180F	180-400F	400+ F	400-650F	Chicago Area Diesel Fuel Spec.	650+ F
API Gravity	42.7	76.8	51.3	36.1	37.5		34.9
C, wt %	86.06	-	85.79	-	-		-
H, wt %	13.84	-	14.19	-	-		-
N, total ppm wt.	917	10	240	710	695		-
N, basic, ppm wt.	-	-	-	415	-		100
S, ppm wt.	60	110	10	11	30	4000 max.	-
RON, Clear	-	61.4	32.8	-	-		-
RON, +3 ml TEL	-	82.2	61.4	-	-		-
Cetane No.	-	-	-	-	50.2	50 min.	-
Pour Point F	-	-	-	+45	-15	-15 max.	+95
Saturates[b]	69.8	-	-	67.8	-		-
Aromatics[b]	27.5	-	-	26.2	-		-
Olefins[b]	2.7	-	-	6.0	-		-
Paraffins	-	-	47.7	-	-		-
Monocyclicnaphthenes	-	-	34.5	-	-		-
Dicyclicnaphthenes	-	-	2.4	-	-		-
Benzenes	-	-	13.2	-	-		-
Heavy Aromatics	-	-	2.2	-	-		-
ASTM Color	-	-	-	-	<1.0	2 max.	-
Vis, 100F, SUS	-	-	-	-	36.1	33 min. 45 max.	-
" 210F, CS	-	-	-	1.46	-		3.21
Mol. Wt.	-	-	-	234	-		340
Carbon Res., Ram., Full range	-	-	-	0.03	0.01	0.02 max	0.1
Carbon Res. Rams., 10% Btms.	-	-	-	-	0.18	0.15 max	-
Copper Corrosion	-	-	-	-	Sl. tarnish	3 max.	-
Flash Point, F, P. M.	-	-	-	-	210	150 min.	-
Storage Stability, Dupont (Nalco) pad rating	-	-	-	-	7	7 max.	-

[a]Snap sample taken after 100 hrs continuous operation - contains 0.4 wt % C_3+C_4's.

[b]By FIA Analysis - olefins not reliable.

TABLE V

HYDRODENITROGENATION OF NAPHTHA

Conditions: 1500 psig, 698F, 0.988 LHSV, 4730 SCF hydrogen/bbl feed
Harshaw 4303-E catalyst (nickel-tungsten on alumina, presulfided)

	Yields, Percent			
	Feed		Raw Shale Oil	
	Wt	Vol	Wt	Vol
H_2[a]	-1.23		-0.31	
C_1	0.33		0.08	
C_2	1.25		0.31	
C_3	1.35		0.34	
iC_4	1.44	2.1	0.36	0.7
nC_4	1.18	1.6	0.29	0.5
C_5^+[b]	95.68	97.3	23.92	29.3
	101.23	101.0	25.30	30.5

[a]Hydrogen Consumption - 627 SCF/bbl
[b]Separator liquid product, not stabilized

TABLE VI

PROPERTIES OF NAPHTHA AFTER HDN

		ASTM Distillation	
API Gravity	54.0	IBP	246
RON, Clear	20.0	5	262
RON, +3ml TEL	52.8	10	272
Paraffins	46.9	20	282
Monocyclicnaphthenes	46.6	30	294
Dicyclicnaphthenes	5.5	40	306
Benzenes	1.0	50	320
Bromine No.	<0.1	60	332
C wt%	84.93	70	344
H wt%	15.07	80	357
N ppm wt	1.5	90	372
S " "	8	95	382
As ppb wt	10	EP	402
Pb " "	13		

TABLE VII

REFORMING OF NAPHTHA-CONDITIONS AND YIELDS

OF NAPHTHA FEEDSTOCK

Conditions: (All runs with same portion of initially new U.O.P. R-5 Catalyst)

Test	1		2		3		4		5		6	
Temp., [a]F	806		829		853		878		908		954	
LHSV	2.96		2.89		2.96		2.96		2.95		2.96	
Moles H_2/naphtha	8.35		8.52		8.21		8.59		8.72		8.59	
Press., psig.	500		500		500		500		500		500	
Yields:	wt	vol	wt	vol	wt	vol	wt	vol	wt	vol	wt	vol
H_2	1.81		1.84		1.89		2.05		1.86		1.01	
C_1	0.30		0.48		0.82		1.26		2.13		3.49	
C_2	0.89		0.96		1.22		2.24		4.03		6.98	
C_3	1.48		1.78		2.52		4.32		6.70		11.50	
iC_4			0.06	0.1	0.98	1.3	1.12	1.5	1.97	2.7	2.67	3.6
nC_4	0.98	1.3	2.43	3.2	2.41	3.1	3.03	4.0	4.26	5.6	7.71	10.1
C_5^+	94.54	91.5	92.45	89.6	90.16	87.1	85.98	82.8	79.05	75.5	66.64	62.8
Total	100.00	92.8	100.00	92.9	100.00	91.5	100.00	88.3	100.00	83.8	100.00	76.5
Hydrogen Prod, SCF/bbl	905		920		946		1038		931		507	
Yield-Oct. No. (Liq. vol% x RON, +3) $\times 10^{-2}$	59.0		76.7		78.1		77 3		74.0		64.1	

[a] Mean reading of nine evenly spaced TC's in catalyst bed

III. PILOT PLANT AND PROCEDURE

Coking and Hydrostabilization

Raw shale oil was pumped through a preheater into the bottom of the coking vessel, made from a 20-in. length of 8-in. diameter pipe and closed with weld caps. The coker was vertically mounted in a two-section furnace, with each section separately controlled. Within the coker was a concentric thermowell for determining the temperature at any height. Heaters were set so that incoming feed and outgoing distillate were in the range 800-850°F.

Coker distillate passed through a heated line to the flash still; temperature in the flash zone was 665°F. Product gases were cooled in an external condenser and the condensate was metered, sampled, and collected. A regulator ahead of the gas meter held the still pressure at 10-12 psig and also determined coker pressure. Distillate was condensed and flowed into a water knockout, from where it was pumped to the hydrostabilizer. Bottoms were continuously recycled to the coker.

Coker distillate was mixed with metered hydrogen, preheated to 450°F, and fed to the hydrostabilizer. Reactants passed down-flow through a one-gallon reactor filled with pre-sulfided catalyst, Filtrol 475-8. A temperature increase of 30°F was noted as reactants passed through the bed. Effluent was cooled and the gas and liquid phases separated in the chamber of a liquid-level controller. Pressure was maintained at 500 psig by action of a regulator on tail gas from the separator (75°F). This gas was sampled and metered, as was the gas evolved from the liquid discharged from the separator. The liquid product was sampled and held for HDN operations.

Hydrodenitrogenation

The composited, hydrostabilized liquid was mixed with 5200 SCF hydrogen per barrel, preheated to 750°F, and passed downflow over the bed of pre-sulfided Harshaw 4303-E catalyst, heated by a five-zone furnace. A sharp increase in temperature of 50°F occurred at the bed top. The remainder of the reactor was virtually isothermal at 812°F and 1500 psig. The space velocity was 1.0 liquid volume per hour. To prevent effluent lines from plugging with deposits of ammonium sulfides, water was injected into the effluent at a rate of 50 ml/hr. A high pressure tail gas from the liquid-gas separator (ambient temperature) was sampled and metered. Similar measurements were made on the gas desorbed when pressure on the liquid was reduced to atmospheric.

As 10-gallon portions of liquid product accumulated, each portion was fractionated into gas (butanes and lighter), C_5 to 180°F and 180 to 400°F distillates, and 400+°F bottoms. The 180 to 400°F distillate was feed for naphtha HDN and reforming, and the 400+°F bottoms were catalytically cracked. Corresponding distillates and bottoms from each distillation were composited and analyzed. A 10-gallon portion of the 400+°F bottoms was further fractionated at 20 mm pressure to yield a 400 to 650°F diesel fuel and 650+°F bottoms for catalytic cracking.

Hydrodenitrogenation of Naphtha

The 180 to 400°F distillate obtained by fractionation of the initially hydrodenitrogenated oil comprised the feedstock naphtha. Other than the use of a fresh portion of catalyst (pre-sulfided), and a bed temperature of 700°F, the apparatus and procedure were the same as in the initial HDN operation. Since little nitrogen and sulfur remained in the naphtha feedstock, water was not injected into the reactor effluent.

Reforming of Nitrogen-Free Naphtha

The total liquid product from naphtha hydrodenitrogenation was used as feedstock without stabilization. A 300 ml bed of fresh U.O.P. R-5 catalyst was used, and the reactants were preheated in a tube furnace to reaction temperature. All tests were carried out at 500 psig, with nominal values of 8/1 for hydrogen/naphtha (molar) and 3.0 for liquid hourly space velocity. Reactor effluent was cooled by exchange with tap water and charged to a gas-liquid separator at 75°F. Samples of reformates were caught at 500 psig and stabilized to yield butane-free reformates and gases composed of butanes and lighter components. Tests were performed in the chronological sequence 2, 3, 4, 5, 6, and 1 of Table VII.

Cracking of Gas Oils

Both 400+°F and 650+°F oil from the first-pass HDN were catalytically cracked. Properties of these oils are given in Table IV. The catalyst was an equilibrium catalyst withdrawn from a refinery FCC reactor and was composed of 75 per cent Filtrol-800 and 25 per cent of a mixture of other catalysts.

The confined bed cracking apparatus was described by Johnson and Stark (6). Measured

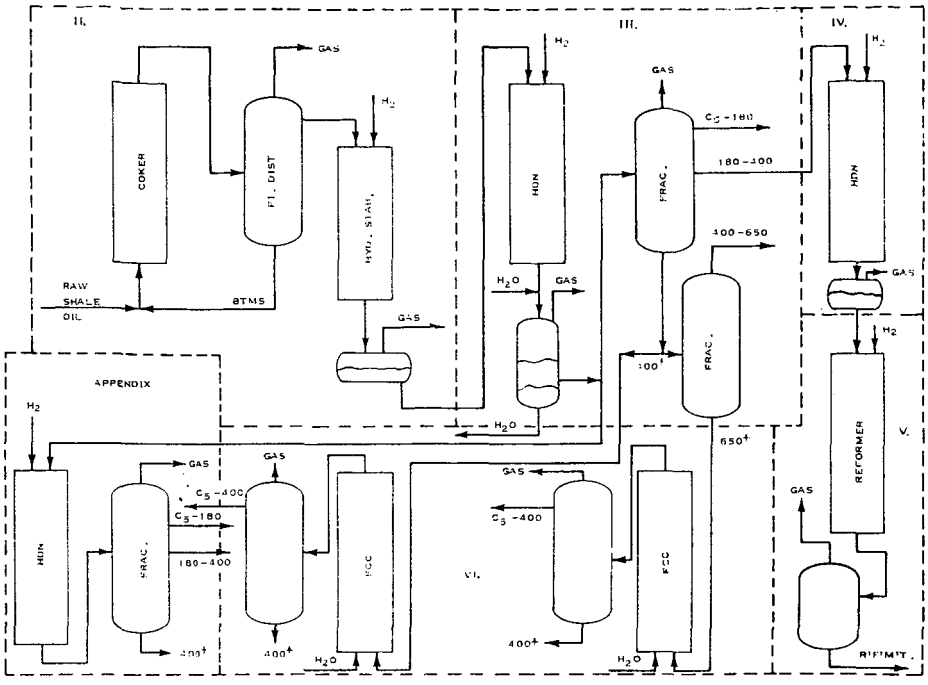

FIGURE 1
PROCESS SCHEME

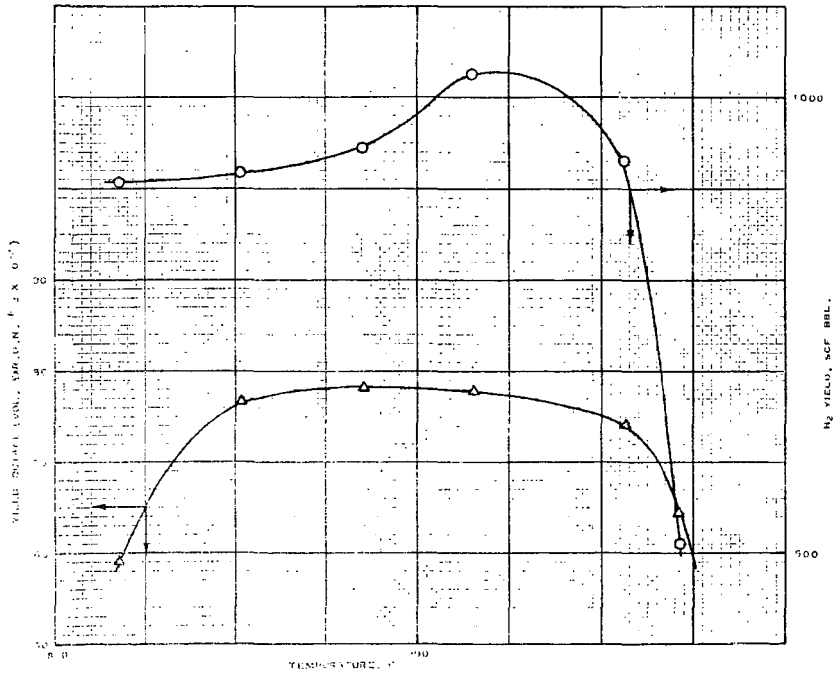

FIGURE 2
REFORMING TEMPERATURE VS.
YIELD - OCTANE AND H_2 YIELD

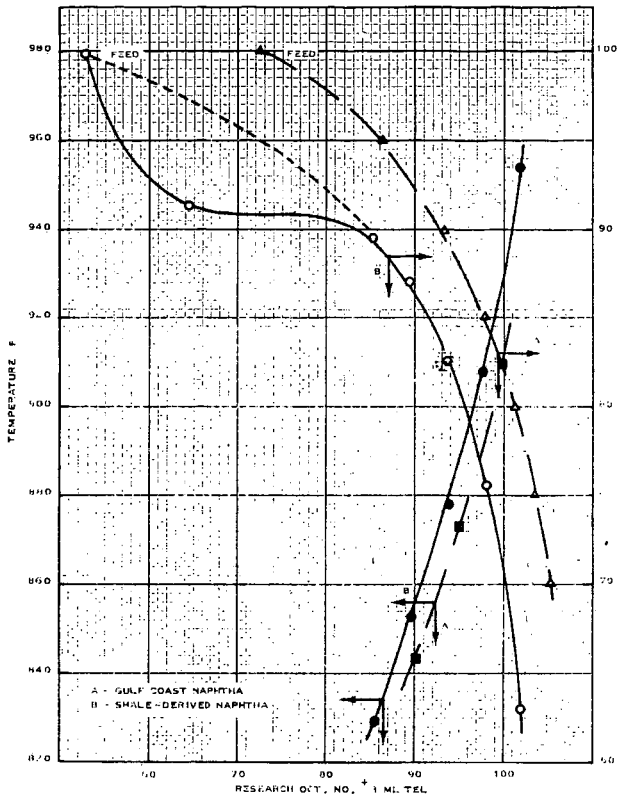

FIGURE 3
REFORMATE OCTANE VS.
TEMPERATURE AND YIELD

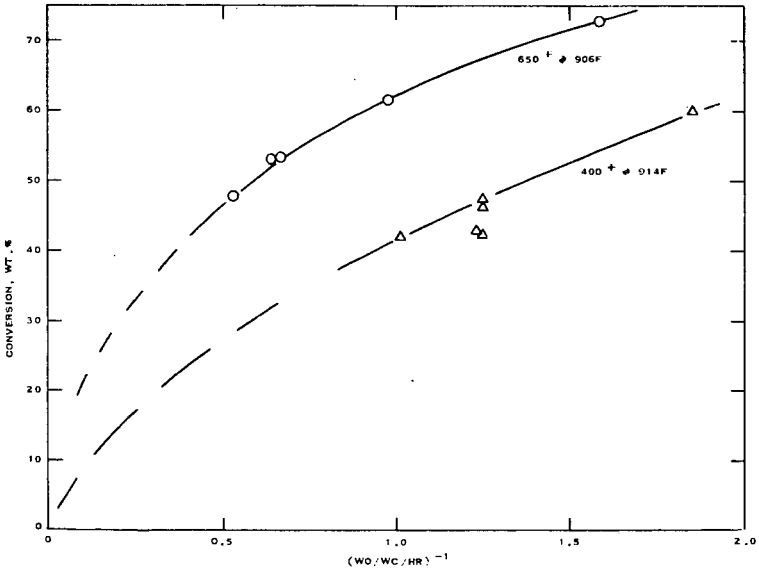

FIGURE 4
FCC CONVERSION VS.
RECIPROCAL SPACE VELOCITY

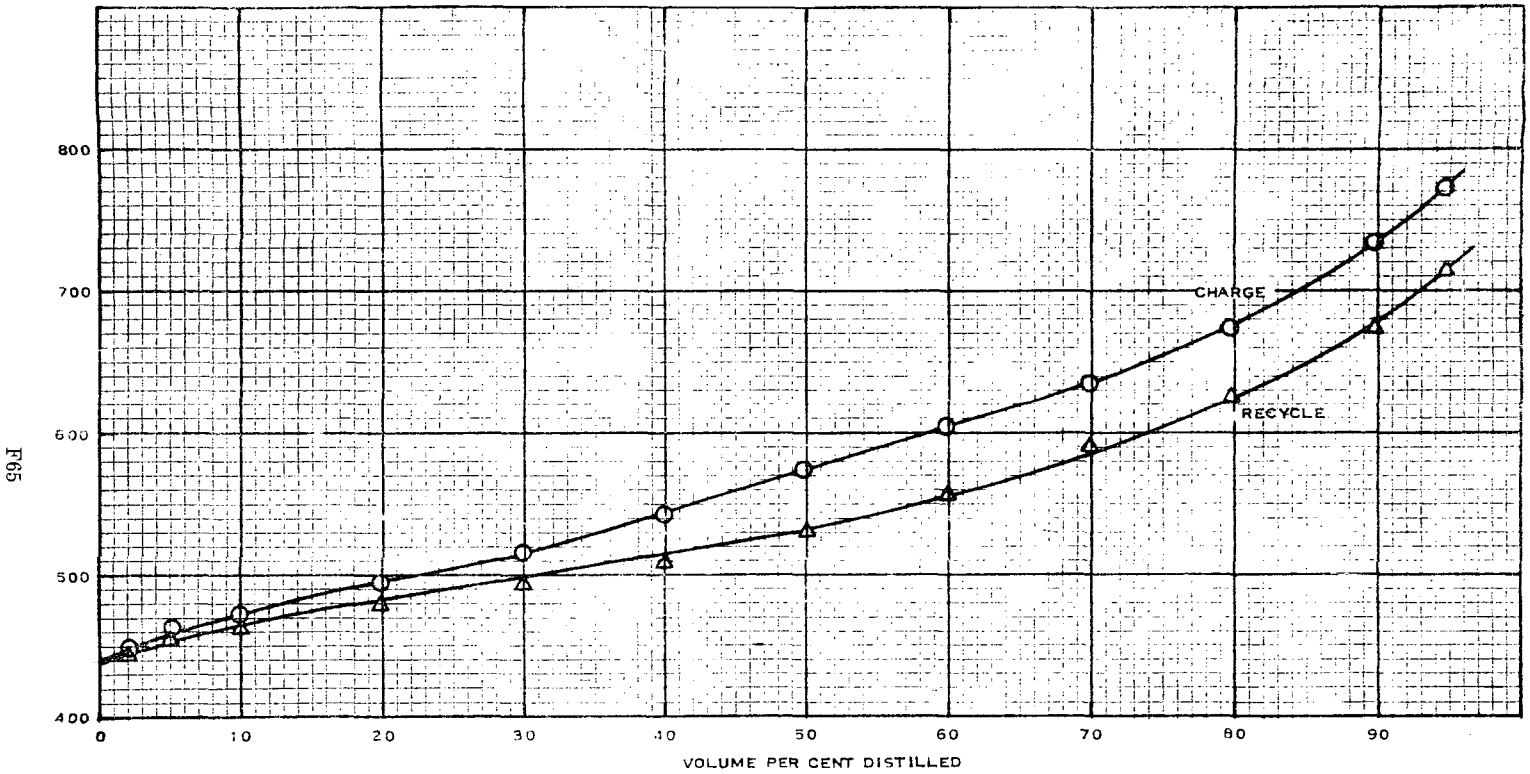

FIGURE 5
DISTILLATIONS OF FCC
CHARGE (400^+ F) AND
RECYCLE

TABLE IX

Catalytic Cracking of 400+ HDN Product

Conditions: 914F, 10 psig, 0.8 Wo/Wc-hr., 16.2 lbs H_2O/bbl, 33 min. cycle, 0.93 Cc, K. C. equil. cat. (75% F-800)

Yields, Percent	Feed Wt.	Feed Vol.	Raw Shale Oil Wt.	Raw Shale Oil Vol.	Properties of Liq. Prod.	Gaso.[b]	400+
H_2	0.11	63.8 SCF/bbl	0.05		API	56.5	32.6
C_1	0.99		0.48		RON,0	92.2	-----
$C_2^=$	0.57	191 " "	0.28		RON+3	98.9	-----
C_2	0.96		0.47		MON,0	----	-----
$C_3^=$	2.29	3.70	1.11		MON,+3	87.8	-----
C_3	1.14		0.55		ASTM Dist		
$C_4^=$'s	2.98	4.11	1.45		IBP	119	-----
iC_4	2.80	4.19	1.36	2.26	2	----	444
nC_4	2.11	3.05	1.05	1.69	5	137	455
C_5-400F Gaso.	28.43	31.8	13.82	17.2	10	151	461
400+ C.C.	54.20	53.1	26.3	28.6	20	168	478
Coke	3.42	---	1.66		30	185	492
Total	100.00				40	205	509
Total Gasoline[a]		45.1		24.2	50	227	530
					60	254	560
Conversion	45.8	46.9			70	282	590
					80	307	626
					90	338	674
					95	358	716
					EP	405	----
					BMCI	----	40.1

[a] (C_5-400 F Gasoline) + 1.7 (Vol $C_3^=$ + Vol $C_4^=$)

[b] Contains no alkylate

TABLE VIII

REFORMING OF NAPHTHA-PROPERTIES OF REFORMATES

Test	1	2	3	4	5	6
IBP	224	192	161	136	129	120
5	251	226	212	188	167	176
10	265	251	239	216	189	191
20	279	274	262	246	220	214
30	291	282	276	264	245	235
40	304	296	292	280	265	253
50	318	304	307	296	282	271
60	333	326	322	314	299	289
70	346	342	338	328	318	308
80	358	358	354	346	338	328
90	374	378	375	371	366	358
95	388	401	399	402	401	385
EP	416	430	437	449	452	422
API Gravity	48.1	48.3	47.7	47.1	45.5	43.5
Octane Nos.						
RON, Clear	51.6	69.0	74.9	83.1	90.9	97.6
RON, +3	64.4	85.6	89.7	94.0	98.0	102.1
MON, Clear	52.0	65.0	68.8	75.2	82.4	86.7
MON, +3	64.4	78.2	82.2	85.2	87.6	91.4

TABLE X

Catalytic Cracking of 650+ HDN Product

Conditions: 906F, 10 psig, 1.89 Wo/Wc-hr, 15.9 lbs H_2O/bbl, 16.5 min. cycle, 0.93 Cc, K. C. equil. cat (75% F-800)

Yields, Percent	Feed Wt	Feed Vol	Raw Shale Oil Wt	Raw Shale Oil Vol	Properties of Liq. Prod.	Gaso.[b]	400+
H_2	0.06	34.2SCF/bbl	0.01		API	64.4	31.4
C_1	0.47		0.06		RON,0	90.3	----
$C_2^=$	0.36	101.2	0.04		RON,+3	97.7	----
C_2	0.51		0.06		MON,0	----	----
$C_3^=$	2.76	4.96	0.32		MON,+3	87.5	----
C_3	0.90	-----	0.11		ASTM Dist		
$C_4^=$'s	3.42	4.64	0.40		BP	104	----
					2	----	459
iC_4	3.39	5.13	0.40	0.66	5	115	492
					10	128	551
nC_4	1.02	1.50	0.12	0.19	20	143	672
					30	158	699
C_5-400F Gaso.	32.40	38.5	3.80	4.93	40	177	----
					50	201	723
400+ C.C.	52.11	51.1	6.10	6.59	60	229	746
					70	263	747
Coke	2.60	-----	0.30	-----	80	294	763
					90	331	793
Total	100.00				95	354	816
Total Gaso.[a]		54.8		7.0	EP	391	----
					BMCI	--	28.6
Conversion	47.8	48.6					

[a] (C_5-400 F Gasoline) + 1.7 (Vol $C_3^=$ + Vol $C_4^=$)

[b] Contains no alkylate

quantities of steam and oil were pumped into the catalyst bed, and non-condensed products were metered and analyzed by gas-liquid chromatography (GLC). Coke deposits were determined by analysis of the regeneration gases. After fractionation of condensed products, fractionation gases were analyzed by GLC.

Cracking was carried out at 10 psig, a nominal steam-oil ratio of 15 pounds/barrel, and cycle times to accomplish a value of 1.0 wt per cent for the mean carbon content of the catalyst ($\bar{C}c$). Space velocities were varied to determine the WHSV conversion relationship, as shown in Figure 4. The 650+°F oil was cracked at 906°F; the more refractory 400+°F oil was cracked at 914°F.

IV. RESULTS AND DISCUSSION

Coking and Hydrostabilization

Table I contains data characterizing the raw shale oil, conditions of coking, and yields and properties for products of the coker. The porous, friable coke was easily removed from the coker. Hydrostabilizer yields and product properties are given in Table II. The reported data are for 32 hours of operation. Recovered gases plus hydrostabilized liquid equalled 100.8 weight per cent of the 214.5 pounds of raw shale oil fed. Catalyst coke was not determined.

Charging raw shale oil to the flash still rather than to the coker would reduce the volume of coker feed. Also, shale oil components of coker distillate boiling range would not undergo degradation in the coker. However, this mode of operation could not be practiced because an insoluble, organic material separated from the flash-still bottoms and plugged transfer lines. The nature of this insoluble matter was not determined.

Coker distillate with a higher end-point would be possible, but this might make hydrodenitrogenation more difficult. Over all yields would probably be little affected by increasing coker distillate end-point. The coker distillate was immediately hydrostabilized in the pilot plant to insure against its properties changing radically while awaiting further processing. Commercially, this step may not be required because retained samples of coker distillate did not show any obvious changes, such as precipitates or increased viscosity, after 6 months storage in glass. Elimination of hydrostabilization, however, may require a higher severity operation in the subsequent hydrodenitrogenation step and would certainly increase hydrogen consumption during HDN.

If coking and hydrostabilization take place at the retort site, three economies may be possible. First, unsold coke could be mixed with raw shale charged to the retort so that coke combustion could provide heat otherwise derived by burning, and thus prevent loss of oil precursors in the shale. Second, steam reforming of coker (flash) gas could provide hydrogen in excess of that needed for hydrostabilization. Third, additional heat could be obtained by adding air to the retort gases, followed by burning of carbon monoxide and hydrocarbons in the retort gas.

Hydrodenitrogenation of Liquid Product from Hydrostabilization

Yields and properties of the various fractions from HDN are given in Tables III and IV. A material balance was calculated for a 6.75-hour period, during which products exceeded hydrocarbon feed by 4.1 wt per cent. Hydrogen consumption and yields of hydrogen sulfide, ammonia, and water were calculated from feed and product contents of hydrogen, sulfur, nitrogen, and oxygen, respectively.

Carbon on the catalyst was not determined until the second pass of HDN operation was completed (not reported in detail because of its ineffectiveness). At that time carbon content of the catalyst was 2.2 per cent. No decline in catalyst activity was observed.

The value of this HDN process can be seen in the high qualities of the product fractions, particularly the diesel fuel (400-650°F). No further processing would be required to market the diesel fuel, and its volume was 41 per cent of the raw shale oil. Either the 400+°F or 650+°F bottoms could be charged to a catalytic cracker although it may prove desirable to market the 400-650°F as diesel fuel. The light gasoline (C_5-180°F) from coker distillate HDN was of a modest octane number (82.2 RON + 3), but the small volume of this fraction would not upset pooled octane number of a refinery.

The conditions for this hydrodenitrogenation process were suggested from unpublished results of N. J. Kertamus. However, catalyst studies by Falk and Berg (2) indicated that nickel-tungsten promoters were best for HDN. Our results validated and extended these studies to show that high concentrations of these promoters gave best HDN. Since plant costs would be reduced if only one HDN catalyst were utilized, such a single catalyst should have maximum HDN activity, and for this reason Harshaw 4303-E was chosen. After 100 hours of operation, a snap sample of total liquid product contained 917 ppm nitrogen; this was comparable to the combined,

total product and indicates no catalyst aging took place.

Although the results obtained were satisfactory for the purposes of our study, better yields and properties might be realized after further exploratory study. For instance, most of the hydrogen consumed (1970 SCF/bbl) was taken up by saturation reactions, not by direct reactions of nitrogen elimination. The hydrogen contents of feed and products bear this out; it was also evidenced by the heat released. Had the feed nitrogen been present as pyridine, for instance, only 830 SCF of hydrogen would have been required to convert the pyridine to pentane and ammonia.

Naphtha Hydrogenitrogenation

Table V cites the conditions and yields of products from the naphtha hydrogenitrogenation. The properties of the liquid product from the gas separator were similar to the naphtha charge except for the nitrogen content which was reduced from 240 ppm to 1.5 ppm (see Tables IV and VI). The liquid product was not stabilized, because unstabilized liquid from first-pass HDN contained only 0.4 per cent propane plus butanes, and tail gas from the present operation contained even less hydrocarbons than that from HDN of the total coker distillate. At the end of the naphtha HDN, coke-on-catalyst was 0.7 per cent.

The goal of naphtha HDN was to reduce the nitrogen content of the product naphtha to a level permissible for long-term reforming. This goal was achieved, since the naphtha product contained 1.5 ppm nitrogen. An alternate route to nitrogen-free naphtha by two-stage HDN of total coker liquid reduced the naphtha only to 7 ppm, too high a level to sustain long life of a platinum reforming catalyst.

This HDN was run at 700°F and 1500 psig. These conditions had been found to be near optimum for cycle oils and may not be optimum for this feedstock. However, since most of the hydrogen consumed in naphtha HDN is recoverable in subsequent reforming, the effects of pressure and temperature upon hydrogen consumption probably have little economic significance.

Catalyst aging was not studied. The low level of catalyst coke (0.7 per cent) at the end of the operation indicated a long period of satisfactory use. The catalyst can be regenerated.

Reforming of Nitrogen-Free Naphtha

Material balances were calculated for separator products from each test and were in the range 96.5 to 100.7 wt per cent. Fractionation balances were virtually 100 per cent For yield calculations, separator gases were allotted the same isobutane to normal butane ratio as was found for the fractionation gases.

Table VII contains detailed test conditions, yields of products based on feeds, and yield-octane values. Properties of the reformates are given in Table VIII. Figure 2 shows that both hydrogen production and yield-octane are nearly optimum at 910°F. Octane numbers of reformates are plotted against yields and temperatures in Figure 3.

Because the reformer feedstock contained virtually no aromatics and was about 50 per cent naphthenic, volumetric yields of reformate were low at high octane levels. At the high temperatures required for maximum octane reformate, cracking reactions caused a loss of reformate and a lowered hydrogen yield. Although less severe treating of naphtha during HDN would have increased the aromatic content of the reformer feed and would have resulted in less loss upon reforming, the yield based on raw shale oil would have been about the same since the severe HDN increased naphtha volume.

In Figure 3, data from reforming of a Gulf Coast naphtha, which was slightly lower in overall boiling range, are shown together with that from the shale-derived naphtha. Relations of octane number to reformer temperature and yield were found to be similar for the two naphthas. The yield-octane number (RON + 3) curve for the shale oil reformates exhibits an inflection at low octane. This is not observed in corresponding plots for reformates of straight run naphtha. Research clear octanes of the shale reformates (not shown) also show the inflection. In addition, plots of specific gravities vs octanes for these reformates are similarly S-shaped. A possible explanation for this abnormality is that the naphthenes of the shale-derived naphtha were virtually all cyclohexanes, with little cyclopentanes. This seems reasonable since the naphtha was obtained from hydrotreating reactions accompanied by much saturation of aromatic rings and the HDN catalyst was low in isomerization activity. In contrast, the cyclopentanes of straight run naphthas usually equal or exceed the quantities of cyclohexanes (3). With platinum reforming catalysts, Hettinger and co-workers showed that cyclopentanes isomerize to cyclohexanes much more slowly than the latter dehydrogenate to benzenes (5). Also, the rates for paraffin isomerizations are comparable to the rates for conversion of cyclopentanes to cyclohexanes. Consequently the initial reforming reaction of the shale oil naphtha may have been the rapid and almost complete dehydrogenation of cyclohexanes to benzenes, with abrupt volume decrease. In support of this,

results in Figure 2 show that hydrogen yield at the mildest condition was almost equal to the maximum yield of hydrogen. As temperature was increased, no cyclopentanes were present to isomerize and dehydrogenate at accelerated rates. Instead, paraffin isomerization (and dehydrocyclization) took place with increase of octane number but with little increase in product density or hydrogen yield. At severe conditions, hydrocracking eliminated alkyl groups with accompanying hydrogen consumption and resultant increase in aromaticity, density, and octane number.

Catalytic Cracking of Gas Oils

Tables IX and X contain yields and properties of products from both feedstocks cracked at about 50 per cent conversion. Total volumetric yields of gasoline were calculated as the sum of observed gasoline volumes plus additional volumes potentially available by alkylation and polymerization of propylenes and butylenes. Since the synthesis gasolines were not actually produced and blended with FCC gasolines, the yields based on raw shale oil were calculated from densities of FCC gasoline, and gasoline properties were determined for FCC gasolines alone.

At the 50 per cent conversion level, gasolines from both cracking stocks were of high octane number, 99 RON + 3 from the 400+°F and 98 RON + 3 from the 650+°F stock. Yields were greater for the 650+°F feed. On the other hand, gasoline from the 650+°F stock represented only 4.9 vol. per cent of the raw shale oil vs 17.2 vol. per cent for the lighter stock, because the quantity of 650+°F stock was smaller. Potential gasoline from alkylation of C_3 and C_4 olefins was 2.1 vol. per cent of shale oil for the 650+°F and 7.0 vol. per cent for 400+°F.

Both feedstocks were sufficiently free of nitrogen, sulfur, and carbon residue as to be desirable cracking stocks. Both were paraffinic; the 400+°F had a Bureau of Mines Correlation Index of 27 and the 650+°F a value of 19. A real difference was found in the more refractory nature of the 400+°F stock as shown by the longer cycle times and higher temperature required for cracking. Figure 5 shows that the higher boiling components of the 400+°F feed were preferentially cracked, since the recycle is lower boiling than the feed. Probably a better alternate to the cracking of this stock would be the sale of the 400-650°F portion as diesel fuel, or hydrocracking of the entire 400+°F stock.

CONCLUSIONS AND SUMMARY

1. The steps for converting Colorado pyrolytic shale oil into saleable products were:
   a. recycle coking combined with hydrostabilization;
   b. hydrodenitrogenation and fractionation;
   c. hydrodenitrogenation of naphtha from (b);
   d. reforming of product naphtha from (c);
   e. catalytic cracking of gas oil from (b).

   These steps were perhaps not performed at optimum conditions, since for most operations conditions were pre-selected and effects of process variations were not determined. The maximum temperatures and pressures of 914°F and 1500 psig were well within the limits of conventional refining processes.
2. The hydrostabilization step may not be required commercially.
3. Nitrogen content of reformer feed and cat cracker feed (650°F+) were reduced to satisfactory levels, 1.5 ppm total N and 100 ppm basic N respectively. These stocks could be processed in conventional refinery units.
4. The 400 to 650°F material from the denitrogenated coker distillate was suitable for diesel fuel.
5. Yields of hydrogen, coke, hydrocarbons, and non-hydrocarbons, for one set of operating conditions and based on raw shale oil were:

Process (see below) (wt %)	A	B	C	D	E	Total
Hydrogen	-0.49	-2.79	-0.31	0.44	0.01	-3.14
Hydrogen sulfide	0.13	0.25				0.38
Water	0.06	0.84				0.90
Ammonia		1.99				1.99
Methane	1.41	0.99	0.08	0.51	0.06	3.05
Ethylene	0.42				0.04	0.46
Ethane	1.17	0.99	0.31	0.96	0.06	3.49
Propylene	0.68				0.32	1.00
Propane	0.89	0.96	0.34	1.61	0.11	3.91
Butenes	0.68				0.40	1.08
i-Butane	0.15	1.61	0.36	0.47	0.40	2.99
n-Butane	0.45	0.77	0.29	1.02	0.12	2.65
Coke	12.61				0.30	12.91
C5-180°F Gasoline		2.71				2.71
Reformate				18.91		18.91
FCC Gasoline					3.80	3.80
400-650°F Distillate		36.86				36.86
FCC Cycle Oil					6.10	6.10
						103.19

A. Recycle coking to 850°F end point followed by hydrostabilization at 470°F, 500 psig, and 0.9 LHSV.
B. Hydrodenitrogenation of hydrostabilized coker distillate at 812°F, 1500 psig, and 1.0 LHSV.
C. Hydrodenitrogenation of 180-400°F naphtha from B at 700°F, 1500 psig, and 1.0 LHSV.
D. Reforming of naphtha from C at 500 psig, 3 LHSV, and 945°F to yield 75.5 vol % of 98.0 RON + 3 reformate.
E. Cat cracking of 650+ gas oil from B.

LITERATURE CITED

1. Chem. Eng. Prog. 62 No. 8, 49 (1966).
2. Falk, A. Y., and Berg, L., "Tungsten as a Hydrodenitrogenation Catalyst", Fifty-eighth Annual Meeting AIChE, December 5-9, 1965.
3. Haensel, V., "The Chemistry of Petroleum Hydrocarbons" 2, 189-219, New York, N.Y. 1953.
4. Hellwig, K. C., Feigelman, S., and Alpert, S. B., Chem. Eng. Prog. 62, No. 8, 71 (1962).
5. Hettinger, W. P., Keith, C. D., Gring, J. L., and Teter, J. W., Ind. Eng. Chem. 47, 719 (1955).
6. Johnson, P. H., and Stark, C. P., Ind. Eng. Chem. 45, 849 (1953).
7. Oil and Gas Journal, 62, No. 10, 65-81 (1964).
8. Silas, R. S., private communication.

JOINT SYMPOSIUM ON OIL SHALE, TAR SANDS, AND RELATED MATERIAL
PRESENTED BEFORE THE DIVISION OF PETROLEUM CHEMISTRY, INC.
AND THE DIVISION OF WATER, AIR, AND WASTE CHEMISTRY
AMERICAN CHEMICAL SOCIETY
SAN FRANCISCO MEETING, April 2-5, 1968

APPLICATION OF A MICRO RETORT TO PROBLEMS IN SHALE PYROLYSIS

By

A. W. Weitkamp and L. C. Gutberlet
Research and Development Department, American Oil Company, Whiting, Indiana

INTRODUCTION

Research on the pyrolysis of oil shale (a non-shale rock that contains little or no free oil) has been popular in recent years. Despite a century of experience in the commercial production of shale oil in Scotland and elsewhere, and multifarious suggestions for effecting heat transfer, the retorting process had been little improved with respect to the considerable portion of the potential oil yield that had been lost because of excessive coke formation. The idea of using hydrogen under pressure to increase the yield and improve the quality of shale oil had been reduced to practice in the laboratory as early as 1932 (9). More recently, intensive effort has been aimed at the eventual commercialization of hydro-retorting (14).

Much of our existing knowledge of the composition of shale oil--mainly from research at the Bureau of Mines--has been reviewed by Thorne (16). The oil is highly olefinic, contains large proportions of sulfur, oxygen, and nitrogen compounds, and smells bad. It is further characterized by an inability to be totally reevaporated to the vapors from which it was originally condensed (17). Possibly the liquefaction of the vaporized pyrolysis product is accompanied by chemical condensation reactions.

Efforts to elucidate the chemistry of the pyrolysis process have not been entirely successful. Studies of the kinetics of shale pyrolysis have yielded apparent activation energies ranging from 13.6 to 48.5 kcal./mol, but mostly above 40 (5). The conclusion is usually drawn that most of the oil- and gas-forming reaction involves the breaking of carbon-carbon bonds. The reaction is rather more complicated than a simple first-order reaction. Most shales contain a small amount of organic matter that can be extracted with solvents and consists of an array of C_{13} to C_{33} hydrocarbons (16) along with other material. The amount of extractibles is greatly increased by heating at moderate temperatures--275 to 325°C. Credit for this discovery goes to S. R. Zimmerly (M. S. Thesis, Univ. Utah, 1923) (10). This primary decomposition process, leading to solubility, was believed to be the rupture of thermally unstable crosslinks.

Quite independently, Kogerman and Kopwillem (9) in 1932 described the pyrolysis of Estonian kukersite in terms of the initial formation of a soluble, non-volatile, semisolid intermediate substance at temperatures below 360°C. At higher temperatures, according to their view, the intermediate is cracked to oil, gas, and large amounts of coke; but if the reaction is carried out under a hydrogen pressure of 250 kg/cm^2 (3560 psi) in the 380-410°C range, practically no coke is formed although coke does begin to be formed at higher temperatures, e.g., 440-450°C.

More recently, Hubbard and Robinson (6) and Allred (1, 2) have accepted the idea of a "bitumen" intermediate and have expressed the mechanism as a sequence of two reaction steps.

$$\text{kerogen} \longrightarrow \text{bitumen} \dashrightarrow \text{oil} + \text{gas} + \text{coke}$$

Unfortunately, these terms are not well defined. "Kerogen" is an insoluble coal-like material with an empirical formula approximating $C_{200}H_{300}SN_5O_{11}$. The name literally means "producer of wax". The intermediate "bitumen" is a nondescript derivative of kerogen that has been thermally degraded to the point of solubility but not of volatility. "Shale oil" is the waxy liquid or solid obtained by cooling the vapors that result from pyrolysis.

Recently Hill and Dougan (5) reported on the low temperature pyrolysis of in situ shale with heated methane as the retorting fluid. Based on these studies and attendant laboratory experiments as well as published data, they suggested that at high temperatures (450-620°C) bitumen and oil are produced more rapidly than they can escape from the pores in which they are located. The diffusion-limited rates of product evolution thus account for the low apparent activation energies (13-25 kcal). During the time the initial products are confined in the pores,

polymerization occurs and subsequent decomposition of the polymer yields on the average higher molecular weight products than the primary oil. The following mechanism was proposed for high temperature pyrolysis:

$$\text{kerogen} \longrightarrow \text{bitumen} \longrightarrow \text{polymer} \longrightarrow \text{oil} + \text{gas} + \text{coke}$$

However, at lower temperatures (below 427°C) the "polymer" was not necessarily an important intermediate. The activation energy for the decomposition of kerogen was said to be between 40 and 41.7 kcal; and for the decomposition of bitumen, 42.5 to 48.5 kcal.

Experimental approaches to the study of shale pyrolysis have been many and varied. Included among the few that have operated on very small samples are the thermogravimetric method (0.25–2.00 g) used by Allred (1, 2) for kinetic studies, and a combination pyrolysis-gas chromatographic method (100 mg) used by Bordenave, et al, (3) to study the C_1 through C_{11} portion of the product.

We have carried out an experimental program to learn more about what happens when oil-shale is heated in hydrogen or an inert atmosphere.

A versatile micro-scale (10–20 mg) retorting system has been developed. With suitable auxiliary equipment, the entire product can be examined. On the basis of kinetic experiments and some product composition data, we have concluded that diffusion-limited processes may be quite important, both in the kinetics and the chemistry of product formation.

At best, shale pyrolysis is a highly complex process that begins with the transfer of heat to a hard, non-porous rock--generally in pieces of substantial size--and ends with a residue of highly porous, friable ash. Not only is diffusion important (15) but its importance changes during the pyrolysis. The time it takes heat to diffuse into a substance that has the thermal conductivity of firebrick, and the time it takes product to diffuse out of a structure that initially has no pores is significant. Indeed, data presented by Allred (2) on the effect of particle size show that doubling the particle diameter increases by about a factor of four the time required for 95% completion of pyrolysis. The increased seriousness of the diffusion limitation at high temperatures noted by Hill and Dougan should only be compared at equal conversions. However, the extent of conversion, whether at high or low temperature, is the more important variable because porosity develops only as products leave the matrix.

It is the purpose of this paper to describe our micro-scale retort, to present some experimental results, and to suggest some possibilities and limitations for additional applications.

EXPERIMENTAL

The oil shale for the retorting experiments was a 28 gal./ton (Fisher Assay) sample obtained from the Green River Formation in Colorado. It was crushed and screened to a particle size of 48 to 65 mesh. Detailed analyses for similar shales have been reported (7).

Apparatus

Several systems for pyrolysis of organic compounds couples with gas chromatography have been offered commercially. None of these had sufficient control over the temperature and heating rate for kinetic studies. Preliminary experiments were done with a commercial dual column gas chromatograph with thermal conductivity detectors and designed for linear temperature programming from -65 to 400°C. As the program developed, it became evident that none of the features of this otherwise excellent instrument were particularly well-adapted for the study of shale pyrolysis. The lower limit, -65°, was not nearly cold enough for the trapping and analysis of light hydrocarbons such as methane. The upper limit of 400°C was too low for the completion of programmed temperature pyrolysis and was just at the beginning of the interesting range for isothermal pyrolysis. The linearity of temperature programming was adequate for analytical gas chromatography but was not precise enough for kinetic studies. The thermal conductivity detectors were not suitable for either kinetic or composition studies because of sensitivity to water in the products of pyrolysis. Furthermore, the oven temperature required to prevent condensation in the product transfer line (375°C) was much too high for efficient thermal conductivity detection. Dual column operation to compensate for column bleed turned out to be ineffective because no known substrate could withstand the high temperatures required for elution of the recondensation products of shale pyrolyzate. In the final version we used either no column at all (kinetic experiments) or a series of columns from which product could be eluted at safe temperatures.

The apparatus as it eventually evolved is shown schematically in Figure 1. It consisted of a pyrolysis tube mounted in a GLC oven equipped with a hydrogen flame ionization detector.

The oven served as a heater for transfer line A as well as a heated environment for pyrolysis chamber C, and also served as a programmed temperature heater for the GLC analysis of products in Traps 1, 2, and 3. Traps 2 and 3 also served as fractionating columns.

The pyrolysis unit is shown in Figure 2. It consisted of a well-insulated 30-inch length of 1/8-inch o.d. thinwall stainless steel tube with electrical connections for resistance heating. One lead was attached at the mid-point and the other to the two ends. The high current at low voltage necessary for resistance heating was supplied by a 5-volt transformer in series with a Powerstat (0-100 volt variable autotransformer). The temperature was controlled with a time proportioning device (TempTendor, API Instruments Co., Chesterland, Ohio) designed for isothermal operation. However, it was readily adapted as a linear temperature programmer by simply replacing the set knob with a sprocket and driving with a slow speed motor.

The manostat and flow controller (See Figure 1) for use with hydrogen or deuterium consisted of two ordinary hydrogen pressure regulators; the one at the inlet to the pyrolysis chamber reduced cylinder pressure to the desired operating pressure (500 psig); the downstream one, at the outlet from the last trap, reduced pressure from the operating pressure to some lower value appropriate to the pressure drop across the metering orifice. The metering orifice consisted of a 15-foot length of 0.01 inch i.d. copper tube. Hydrogen flowed at 50 ml./min. with the pressure drop set at about 35 psi. When helium was to be used as the retorting fluid at atmospheric pressure, the flow was controlled by the flow controller of the GLC unit, usually at 35 or 50 ml./min.

The trapping system consisted of three traps in series; each consisting of a length of 1/8-inch o.d. thinwall stainless steel tube coiled to fit inside a 1/2 pint Dewar. Trap 1 consisted of an 18-inch section filled with 50-mesh glass microbeads; Trap 2 contained a 30-inch section packed with 1% polyphenyl ether (nominally heptamer) on Chromosorb G; Trap 3 was a 6-foot column packed with Poropak Q (unsupported polystyrene, 50-80 mesh powder).

Procedures

Kinetic data were obtained by taking the product through the heated transfer line directly to the detector. The choice of hydrogen flame detection limited retorting fluids to inert gases (helium) at atmospheric pressure. The operation could be either temperature programmed--usually 4°C/minute--or isothermal. In the isothermal operation at temperatures from 100 to 400°C, the temperature was raised in a progressive stepwise manner and held at each level for an extended period. Above 400°C, reaction was much faster and a fresh shale sample was used for each temperature.

Composition data were obtained by collecting the product in the traps and subsequently chromatographing each trap. The operation could be either temperature programmed or isothermal. The retorting fluid could be either hydrogen or deuterium or an inert gas (helium) under atmospheric or elevated pressure.

During a pyrolysis run Trap 1 was at ambien temperature while Traps 2 and 3 were cooled with liquid nitrogen. At the completion of pyrolysis the gas inlet was reconnected to the helium flow controller and, with helium flowing at 35 ml./minute, Trap 1 was heated by programming the oven to 180°C at which point the product had been eluted through C_{28}. Further elution was prevented by immediately cooling Trap 1. At this point Trap 2 contained all products from C_1 through C_{28}. Trap 2 was warmed by replacing the liquid nitrogen Dewar with one containing water at ambient temperature for two minutes. This operation transferred the C_1 through C_6 hydrocarbons to Trap 3. Since all valves had been eliminated from the product zone, each trap was mounted in the oven by means of Swagelock connectors and chromatographed in turn.

The glass bead column (Trap 1) was chromatographed merely for the purpose of obtaining a material balance. Its main function was to keep high boiling components out of Trap 2. Stripping of the glass bead column required temperatures up to 415°C. We have observed in other experiments that the stripping is accompanied by thermal decomposition, from which we conclude that some condensation or polymerization had occurred following the initial pyrolysis. It is not known whether the polymer in the glass bead trap was due to polymerization that occurred within the liquid film on the glass beads, or whether polymer was formed earlier and got into the glass bead column by entrainment in the sweep gas.

The polyphenyl ether column (Trap 2) was chromatographed from ambient temperature to about 220°C at 4°C/min. for recovery of the C_6 through C_{28} components. Separation was adequate for analysis by carbon number. The maximum temperature is well below the onset of column bleed (ca. 250°C) so that columns are long-lived and dual column operation is unnecessary.

The Poropak Q column (Trap 3) contained the C_1 through C_6 hydrocarbons. With this strongly retentive substrate, only methane was eluted at subambient temperature. By simply replacing the liquid nitrogen Dewar with an empty Dewar, the methane was eluted in six or seven

FIGURE 1

APPARATUS FOR PYROLYSIS
OF OIL SHALE AND ANALYSIS OF PRODUCT

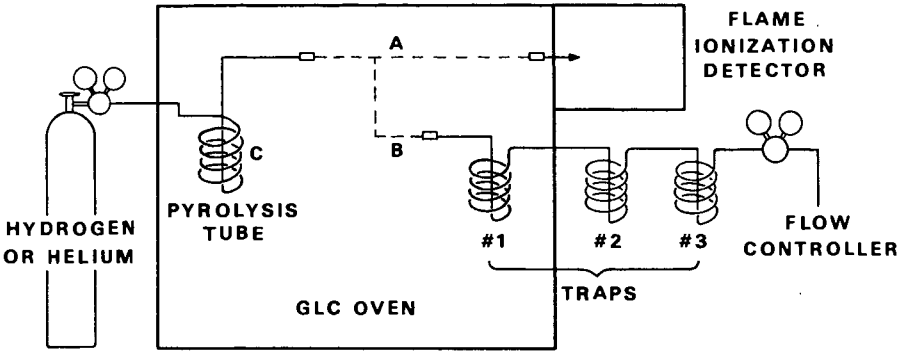

FIGURE 2

PYROLYSIS CHAMBER AND CONTROLS

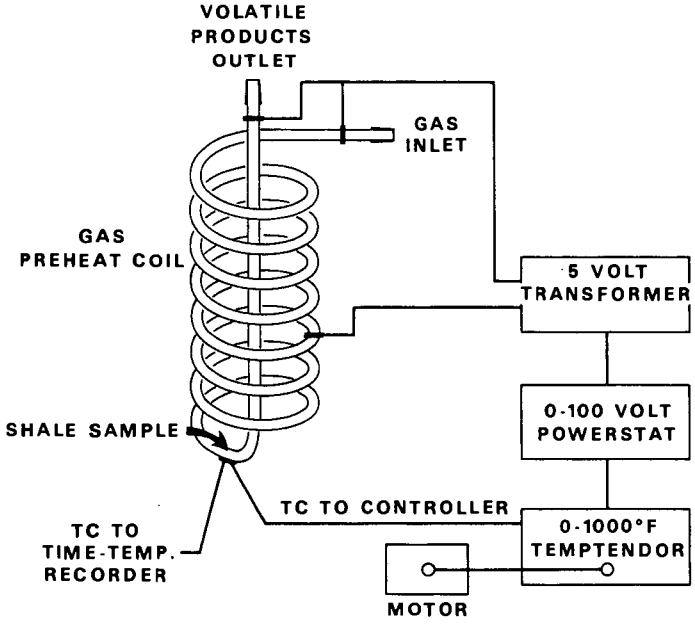

FIGURE 3

STEPWISE ISOTHERMAL PYROLYSIS OVER THE TEMPERATURE RANGE, 108 TO 416°C

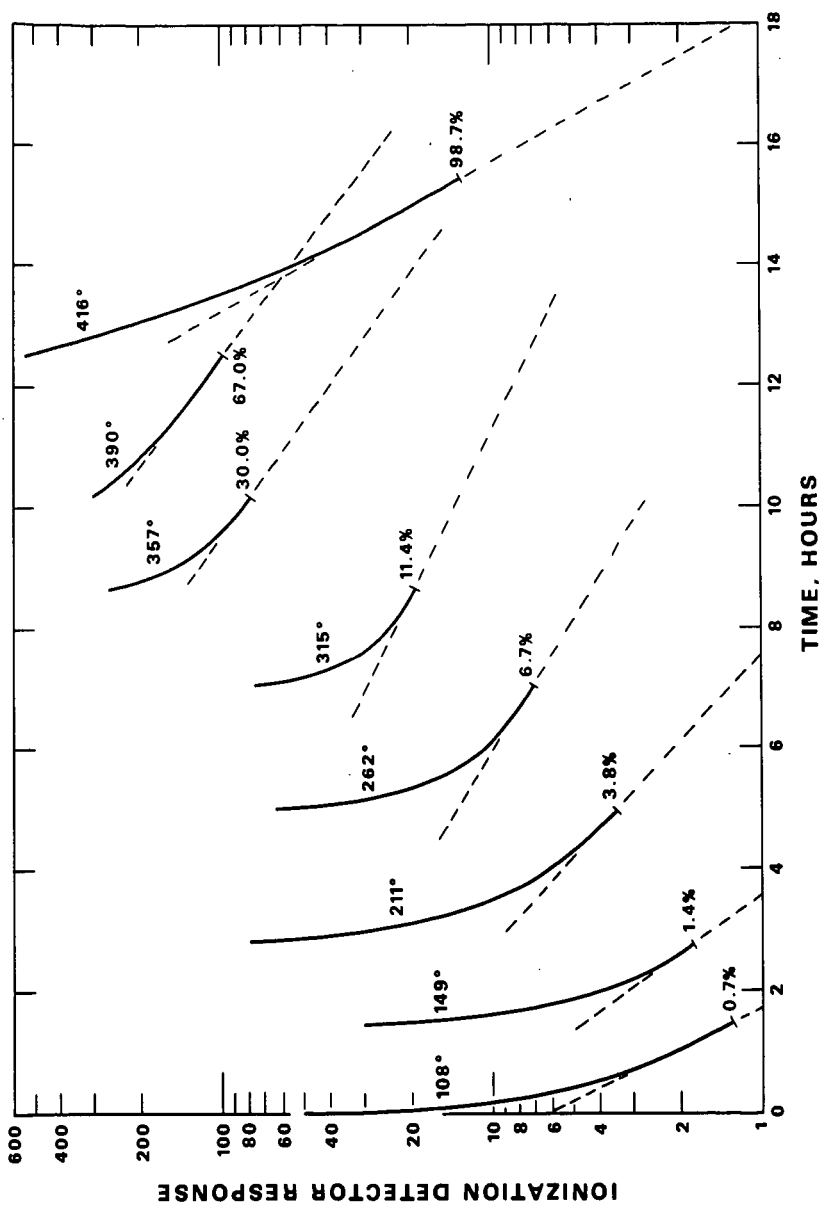

minutes, after which the Dewar was removed and the GLC oven was programmed to 180°C at 4°C/min. The remaining components were eluted in the order: ethylene, ethane, propylene, and propane. Isomer separation is complete. The C_4's, C_5's, and C_6's were completely separated by carbon number but the isomers overlapped. The C_4 olefins were separated from the C_4 paraffins and from each other on a benzyl cyanide-silver nitrate column prepared by the ASTM standard procedure.

EXPERIMENTAL RESULTS

Isothermal Pyrolysis

Heat transfer to the small sample of small shale particles, each of which was in contact with the surface of the pyrolysis tube, was so efficient that deficiencies in the thermal control were more readily detected by changes in the rate of product formation than by variations in the observed temperature. The entire temperature range--from the lowest at which product was detected (ca. 100°C) to decomposition rates that were too fast to be measured accurately--was covered. At temperatures much below 400°C, decomposition was never quite complete even after prolonged heating. At any given temperature an initially high rate of product formation settled down to the essentially exponential decay that is characteristic of a more or less first order reaction.

A typical isothermal experiment covering the lower part of the temperature range is detailed in Figure 3. The shale sample (196 mg.) was heated at a sequence of temperatures in a helium stream, the product being swept directly to the flame ionization detector. The amplified output of the detector was replotted on a semi-log scale to show the exponential first-order decrease following the initially more rapid decline in product rate. The heating was continued at the lined-out condition to establish the slope for later extrapolation to "ultimate yield" at that temperature. At the conclusion of each period the temperature was quickly increased and the process repeated at successively higher temperatures until the decomposition was complete. The temperature and percentage yield of product actually obtained in each interval are recorded on the graph. The results of extrapolation to infinite time in two such experiments are plotted in Figure 4. The term "ultimate yield" comprises only the organic compounds to which the flame ionization detector responds. Such products as hydrogen sulfide, ammonia, carbon monoxide, carbon dioxide, and water are excluded. The ultimate yield increased exponentially with temperature until the point of complete decomposition of the kerogen was reached at about 400°C. The ultimate yield approximately doubles in each 42°C temperature interval.

Isothermal pyrolysis rates in the range above 400°C were very fast. Estimates of the time required to reach 50%, 90% and 99% conversion are given in Table I. By way of comparison, the programmed temperature (4°C/min.) pyrolysis reached 50% conversion at about 428°C, at which point the rate constant was about 13%/min.

Table I

ISOTHERMAL PYROLYSIS RATES AT HIGH TEMPERATURE

	Minutes to Indicated Conversion		
Temp., °C	50%	90%	99%
430	2.5	14	60
440	1.5	7	30
450	0.8	5	21
460	0.5	3.7	16
470	0.3	3	14
480	-	2.6	12
490	-	2.3	11
500	-	2.1	10
510	-	1.9	9.3
520	-	1.7	8.7
530	-	1.6	8

At high conversions, i.e., near the end of the reaction, the rate of product formation was slow enough for the kinetics to be followed. Plots of the product yield as a function of time for about the last 13% of the product at selected temperatures between 417 and 485°C are shown in Figure 5.

FIGURE 4

ULTIMATE PRODUCT YIELD AS A FUNCTION OF PYROLYSIS TEMPERATURE

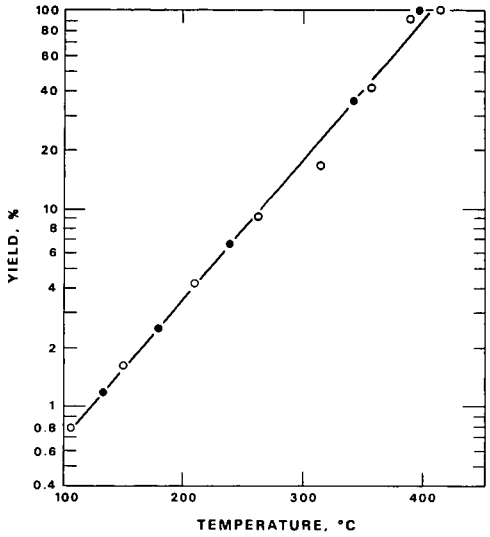

FIGURE 5

RATE OF FORMATION OF THE LAST 13% OF PRODUCT

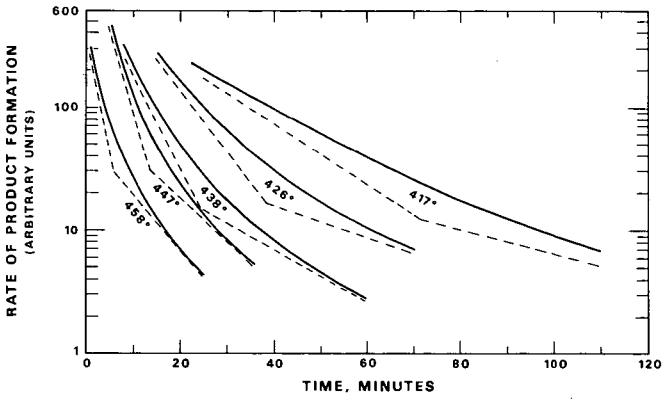

FIGURE 6

GLC TRACE FOR OIL SHALE PYROLYSIS

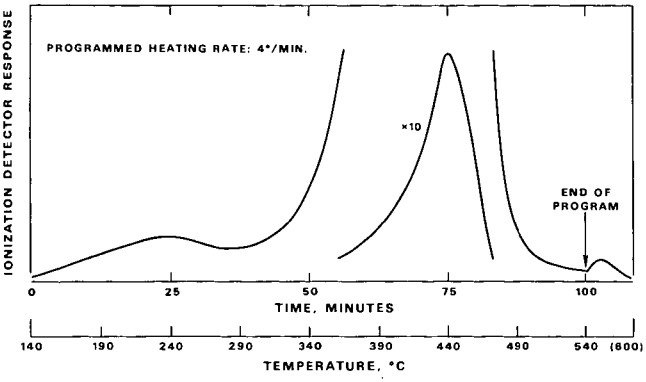

Programmed Temperature Pyrolysis

A GLC trace for a programmed temperature experiment is reproduced in Figure 6. The products of pyrolysis of a 21.4 mg sample of shale were swept to the flame ionization detector while the temperature was increased from 80 to 540°C at the rate of 4°C/minute. In contrast with the isothermal experiments, the rate of kerogen decomposition is steadily increasing. The rate of product formation also increases and passes through a maximum at about 440°C. Product formation is nearly complete at 540°C and after a short period at 600°C, no more is detected. A remarkably similar plot was obtained by Allred (2) by a thermogravimetric method.

By integrating the area under the curve from left to right, one obtains the cumulative yields as a function of temperature that are shown in Table II. By integrating in the opposite direction, i.e., from right to left, one obtains ratios of the instantaneous rate of product formation at any temperature to the amount of product yet to be formed. These "rate constants" for the "decomposition of kerogen" are also listed in Table II.

Table II

RATE CONSTANTS AND CUMULATIVE PRODUCT YIELD AS A FUNCTION OF TEMPERATURE

Pyrolysis Temp., °C.	K, Wt. %/min.	Cumulative Yield, Wt. %
170°	0.067	0.34
186	0.090	0.64
204	0.113	1.02
220	0.122	1.49
236	0.145	2.01
252	0.131	2.56
268	0.099	3.01
284	0.106	3.40
300	0.132	3.83
316	0.192	4.42
332	0.340	5.38
349	0.615	6.91
366	1.096	9.9
383	2.07	15.1
400	3.80	23.2
417	7.19	37.5
425	11.62	47.0
434	18.77	60.6
442	25.80	75.0
451	33.27	87.0
468	24.47	97.4
485	12.75	98.9
502	9.10	99.3
519	9.36	99.5
536	8.62	99.7
(600)		(100.0)

Methane comprises about 3% of the total product. A "methane only" experiment was carried out by pyrolyzing 52 mg of shale and simply trapping all heavier products in an 18-inch section of 1/8-inch o.d. copper tube, coiled to fit into a 1/2-pint Dewar and inserted between Trap 1 and the flame ionization detector (See Figure 1). Whereas methane is held indefinitely on organic substrates at liquid nitrogen temperature, the empty tube condensed and held C_2 and higher products but did not retain any methane. The transmit time for methane through the traps was under 60 seconds and tailing was not a problem. The GLC trace for methane was generally similar to that for total product, except that little or no methane was produced below about 275°C. The 3% of total product that appeared below 275°C must therefore have been produced by a mechanism different from the one that produced methane. Both curves peak at about 440°C. A distinction should be made between the rate of product formation (detector response) and the rate constant for kerogen decomposition (rate of product formation relative to amount of product yet to be formed, i.e., amount of kerogen remaining). The rate constants reach their maxima at about 450°C, at which point the cumulative yield of methane was only 31% compared with 87% for total product. The cumulative yield of methane as a function of temperature and the rate

FIGURE 7

PROGRAMMED TEMPERATURE PYROLYSIS OF SHALE

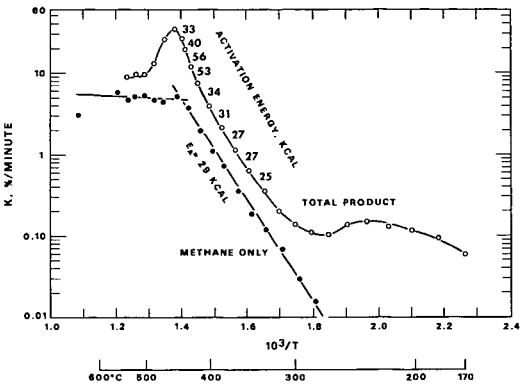

FIGURE 8

ISOTHERMAL PYROLYSIS OF ACTIVATION ENERGY OF SHALE

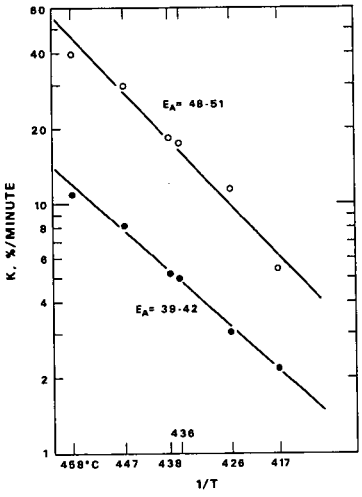

FIGURE 9

ACTIVATION ENERGY FROM MICRORETORTING

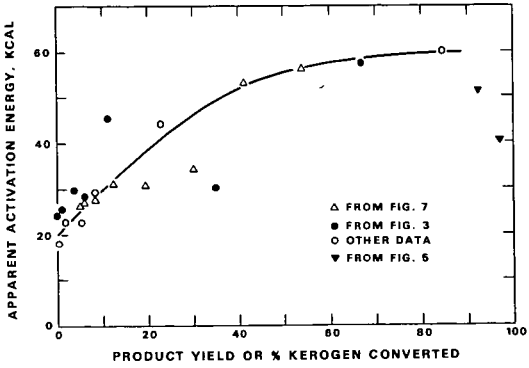

constants as a function of methane-yet-to-be-produced are in Table III.

Table III

RATE CONSTANTS AND CUMULATIVE METHANE YIELD AS A FUNCTION OF TEMPERATURE

Pyrolysis Temp. °C	K, %/min.	Cumulative Yield, %
280	0.015	0.03
295	0.028	0.10
312	0.065	0.26
330	0.112	0.52
346	0.180	1.04
362	0.335	1.90
380	0.700	3.4
395	1.05	4.8
412	1.90	11.0
430	3.60	18.8
448	4.98	31.4
466	4.43	44.6
484	4.53	53.7
503	5.06	62.6
519	4.94	69.6
535	4.49	75.2
555	5.5	79.7
(650)		(100)

To evaluate the effect of mineral constituents on the pyrolysis reaction, limited work was done on kerogen that had been concentrated by extracting the shale with hydrochloric acid to remove carbonates, hydrofluoric acid and remove silicates, ammonia to remove mineral acids, and $CHCl_3$ and benzene to remove natural bitumen. Pyrolysis gave a GLC trace very similar to that for raw shale, including a few percent of low temperature pyrolyzate. However, this product contained much larger proportions of normally gaseous hydrocarbons. The possible mechanistic significance, i.e., the effect of infinite porosity, was not appreciated at that time and unfortunately a "methane only" experiment was not done.

Product Composition

High retorting temperatures are known to give increased proportions of light paraffins and aromatic compounds (4). The kinetic experiments described in the foregoing section confirmed the earlier report of Bordenave, et al, (3) that the composition of the product also changes with the extent of pyrolysis. Thus, in a programmed temperature experiment, nearly 70% of the methane was in the last 13% of the product.

Many experiments were carried out in which the product was trapped and examined by gas chromatography. In one set the shale was heated isothermally in a helium stream for 30 minutes at each of a series of temperatures, much as in Figure 3, and the products were collected separately for each temperature. In the first few fractions, representing the first few percent of product, a rather narrow distribution of carbon numbers that shifted to higher values with increasing temperature suggested cuts from a simple distillation. Thus, a product collected at 126°C was mainly C_{11} to C_{15}; at 200°C at least 90% was in the C_{14} to C_{22} range; at 220°C it was largely C_{20} to C_{24}; at 275°C it was mostly C_{22} to C_{26}, but traces of methane and other light products were beginning to appear. At 303°C the main product was C_{25} to C_{31} but the cut-off at C_{31} was sharp and the amount of light products had increased. At 325°C and higher, a dramatic change occurred. The C_{31+} fraction was large and considerable amounts of methane and other products gave a continuous spectrum of GLC peaks.

A large peak between C_{17} and C_{18} and perhaps other smaller but outstanding peaks may be members of the isoprenoid series. Odd-numbered normal hydrocarbons are also a little more abundant than the even-numbered members. In isothermal pyrolysis at a given high temperature the initial product is lower in methane and richer in higher molecular weight components than the later portions.

Pyrolysis Under Hydrogen or Deuterium Pressure

The pyrolysis conditions selected for present purposes were: temperature programmed at 4°C/minute, 500 psig hydrogen (or deuterium) pressure with a sweep rate of 50 ml/minute (measured at atmospheric pressure).

Typical product distributions obtained under 500 psig hydrogen are compared in Table IV with that obtained with helium at atmospheric pressure. Also included are data reported by Schlinger and Jesse (14) for a large pilot plant operation in which the hydrogen pressure was in the range of 1000 to 2000 psig--flow rate not specified--and the shale was crushed so that the largest chunks did not exceed 4 inches in diameter.

Table IV

PRODUCT DISTRIBUTION FROM RETORTING IN HYDROGEN AND HELIUM

Component, Wt.%	Sweep Gas: Helium	Hydrogen: Present Work[a]	Hydrogen: Schlinger & Jesse
Methane	3.0	22.8	6.2
Ethylene	1.9	3.8	
Ethane	1.6	8.0	3.3
Propylene	1.6	4.7	
Propane	1.1	12.0	2.4
C_4	2.7	6.9	0.8
C_5	2.9	3.3	0.1
C_6	3.0	3.5	22.7[b]
C_7 - 12	15.8	12.2	
C_{13} - 28	40.9	21.6	64.5[b]
C_{29}+	25.4	1.2	

(a) The actual yield in hydrogen was 193% of that in helium.
(b) Estimated to a weight basis from the reported ASTM Distillation.

The effect of hydrogen in our experiments was to increase the over-all yield to about 190% of that with helium. The increase was reflected in every category except the C_{29}+ fraction. The yield of methane was increased enormously. So were those of ethane and propane, but not at the expense of ethylene and propylene. The absolute yields of ethylene and propylene were actually about 3.8 and 5.7 times larger, respectively, in the presence of hydrogen than in the presence of helium.

The substitution of deuterium for hydrogen offered an intriguing possibility for the study of mechanism. Unfortunately, our deuterotorting experiments yielded only fragmentary data. Isotopic analyses of methane, ethylene, ethane, propylene, and propane are possible by high-resolution mass spectrometry, although the C_3 hydrocarbons require the highest resolution of which the instrument is capable. Fortunately, in the spectra of the butenes, the difference in ionizing voltage between the C_4H_8+ (parent) and C_4H_7+ ions is sufficient to permit isotopic analysis by conventional low-resolution mass spectrometry.

The few available bits of data are shown in Table V. In a low-deuterium-pressure experiment (160 psig, 50 ml/minute flow) all possible isotopic species of methane and ethane were present. The major species of methane were CH_3D (methane-d_1) and CD_4 (methane-d_4). The most abundant ethane was C_2H_5D (ethane-d_1). In another experiment at 500 psig deuterium pressure, an isotopic distribution was obtained on cis-butene-2. All possible isotopic species were present. Whatever mechanisms may be operative, the end result was to substitute some or all of the hydrogens with deuterium without saturating the double bond. The k's in the tabulation amount to a statistical analysis. The random k's are computed from the coefficients of the binomial expansion of $(h+d)^8$; the observed k's are computed from the experimental results

such that

$$k_1 = \frac{d_1^2}{d_0 \times d_2} \quad , \text{ etc.}$$

Comparison of the random and observed k's shows a small but significant preference for even numbers of deuteriums in the olefins.

Table V

ISOTOPIC SPECIES IN METHANE, ETHANE AND CIS-BUTENE-2 FROM DEUTEROTORTING SHALE.

Isotopic Species	Methane %	Ethane[a] %	cis-Butene-2 %	k_{obs}	k_{random}
d_0	19	12	30.6		
d_1	23	24	18.9	0.75	2.29
d_2	16	20	15.6	1.24	1.75
d_3	16	16	10.4	0.86	1.60
d_4	26	12	8.1	1.17	1.56
d_5		8	5.8	0.83	1.60
d_6		8	5.0	1.72	1.75
G_7			2.5	0.40	2.29
d_8			3.1		

(a) Not better than ± 4.

DISCUSSION

The changes of product rate with temperature from which activation energies are calculated were measured in a variety of kinetic experiments. The results can be correlated over three broad ranges of conversion: 0-40%, 40-87%, and 87-100%.

Activation Energies

Isothermal pyrolysis experiments, such as the example in Figure 3, in which the temperature was increased stepwise yielded apparent activation energies from incipient pyrolysis to about 85% conversion. Because the time intervals were short and the temperature increases moderate, one should not expect large changes in the structure of the kerogen or in the nature of the product being formed during the short intervals of abrupt temperature increase.

The programmed-temperature experiment (Figure 6) yielded a set of rate constants that gave the Arrhenius plot shown in Figure 7. Activation energies were calculated from the slopes at selected temperatures in the range of 316 to 440°C (4.4-75% conversion). The anomalous decline in the rate constants for the last 13% of product in the programmed temperature pyrolysis (Figure 7) is explained by the fact that these rate constants are expressed on a weight-yield rather than a molar basis. The increase in lower molecular weight products, and especially methane, must reflect changes in the structure of the uncracked residue as it approaches coke. The change in slope suggests negative activation energies. However, reasonable values for this region can be obtained from the isothermal pyrolysis data in Figure 5 by treating the product rate curves as a linear combination of a fast and slow reaction, i.e., fast and slow on a weight yield basis. The "slow" reaction becomes rate-controlling at about 96-97% conversion. The Arrhenius plot in Figure 8 for the rate constants of these reactions gives apparent activation energies of about 40 for the slow reaction and 50 for the fast reaction.

Apparent activation energies from the isothermal and programmed-temperature experiments are plotted in Figure 9 as a function of the extent of pyrolysis. The initially low values rise as pyrolysis proceeds, and reach the 50-60 kcal/mol range after 40% conversion. This corresponds quite closely to the point at which Allred (1) inferred from the data of Hubbard and Robinson (6) that the decomposition of kerogen to bitumen was complete. From here forward, the reaction appears to follow first-order kinetics and the observed activation energies are in excellent agreement with the 57.1 kcal reported by Keith, et al, (8) for the thermal cracking of a petroleum gas oil. The agreement is good enough to suggest that the last 60% or so of the pyrolysis may be relatively uncomplicated rupture of carbon-carbon bonds. However, when high temperatures are used in the later stages of reaction, the rate of product formation increases faster than the rate of diffusion, even though porosity is high; hence the drop in apparent activation energy.

Evidence for Diffusion Effects

In a diffusion-limited system the apparent activation energy should rise as the effects of diffusion are reduced. Thus, the good heat transfer characteristics of the micropyrolysis reactor, the small shale particle size, the small sample size, and the high sweep rate all tend to minimize the delay of getting product out. The activation energy in a large part of the reaction approaches 60 kcal and is the highest so far reported. The thermogravimetric method used by Allred (1, 2) utilized a finely powdered shale and a larger sample size, but depended largely on diffusion to get the product out of the sample bucket. His highest reported activation energy in the temperature range of 430-475°C was 40.5. Only a slight effect of sample size over the range of 0.25-2.00 grams was noted.

The presence of "natural bitumen" in small amounts in raw shale, the conversion of kerogen to more bitumen by the low temperature thermolysis of weak bonds, and--as will be proposed later--the occurrence of diffusion-controlled recombination reactions are all factors that affect the kinetics in the early stages of pyrolysis.

The elimination of high molecular weight products from the rock matrix during pyrolysis at low temperatures is diffusion-limited because of low porosity. The stepwise isothermal pyrolysis of 48-65 mesh shale at temperatures below 325°C gave a series of distillation-like fractions. They covered a molecular size range that was remarkably like the C_{13} to C_{33} range reported by Thorne (16) for solvent-extracted natural bitumen. That diffusion was a limiting factor is shown not only by the progression of molecular sizes with increasing temperature, but also by the observation that a C_{28} fraction could be stripped from a glass bead packed column at 180°C but required a temperature 100°C higher to be stripped from small shale particles. The same lack of porosity that interferes with volatilization into the gas stream could also interfere with the extraction of natural bitumen with solvents. We have observed that extraction of the shale before pyrolysis actually made little difference in the amount (ca 3%) of low temperature pyrolyzate. Even more strangely, concentrated kerogen that had been freed of most of the minerals by extraction with acid (HCl and HF) and then further extracted with boiling chloroform and boiling benzene still yielded the low temperature material. Extraction at high temperatures under pressure has long been known to give larger bitumen extracts, but this may be a combination of low-temperature thermolysis and solvent extraction.

A very significant effect of diffusion is apparent in the differences in product yield and composition resulting from the use of hydrogen as retorting fluid. Shale particle size seems to have a considerable effect on the efficiency with which hydrogen interacts with the pyrolysis products.

Free Radical Reactions

The thermal cracking process is considered to involve free radicals. In an inert sweep gas the free radicals may disappear by routes different from those in hydrogen. Data pertinent to the effect of hydrogen on product yield and composition are in Table IV. Some fragmentary results on the incorporation of deuterium in some of the smaller molecules are in Table V.

The high yields of methane, ethane, and other light products under hydrogen pressure, and the high content of the mono-deutero species (methane-d_1, ethane-d_1) argue for the importance of methyl, ethyl, and other small free radicals in the over-all reaction. There is no telling how many free radicals disappeared by coupling, but evidently a good many reacted with deuterium:

$$CH_3 \cdot + D_2 \longrightarrow CH_3D$$

$$C_2H_5 \cdot + D_2 \longrightarrow C_2H_5D$$

Quite a few appeared as undeuterated species, probably by abstracting hydrogen from a nearby organic molecule or from molecular hydrogen formed in the pyrolysis reaction.

$$CH_3\cdot + R\text{-}H \text{ or } H_2 \longrightarrow CH_4$$

Incidentally, the increased yield of light products at high pyrolysis temperatures may be a result of the increased availability of hydrogen due to the dehydrogenation of aliphatic precursors of aromatic compounds.

The large methane-d_4 content may well reflect the deuterogenation of coke in the latter stages of pyrolysis. The last 70% of the methane was produced along with the last 13% of the total product when the pyrolysis was done in helium. At that stage the shale is highly porous and would offer relatively little resistance to the diffusion of deuterium into the particles.

The major isotopic species in the cis-butene-2 is the undeuterated molecule. One could postulate that the most important reaction of the butyl radical is loss of an atom of hydrogen, possibly due to abstraction by another radical, or disproportionation.

$$C_4H_9\cdot \longrightarrow C_4H_8 + H\cdot$$

The tendency toward even numbers of deuteriums in cis-butene-2 suggests that olefin biradicals, or even diolefins such as butadiene, might be involved in a sequence of hydrogenation-dehydrogenation reactions while slowly diffusing from the developing pores.

The product distributions in Table IV can now be The product distribution obtained by Schlinger and Jesse (14) by hydrotorting large chunks of shale is not grossly different from the product distribution we obtained by retorting small shale particles with a high helium sweep rate. Unfortunately, data on the pyrolysis of large particles in an inert gas were not included. Nevertheless, Schlinger and Jesse reported a considerable absorption of hydrogen, and their product is probably quite paraffinic. The product distribution in our hydrotorting experiment is profoundly different. The yield of gaseous hydrocarbons is much increased and the $C_{29}+$ component is almost non-existent. Evidently the improved diffusion in the micropyrolysis reactor had about the same moderating effect, in the presence of helium, on the recombination reactions as the 1000-2000 psi hydrogen pressure had in the large reactor with large pieces of shale.

Comparison of the C_5+ product in the three cases shows:

	C_5+, Wt.%
Helium Retort	88.3
Micro-hydrotort	41.8 (x 193% = 80.6)
Large-scale Hydrotort	87.3

In terms of the recovery of liquid fuels from shale, the reduction in loss to coke was more than compensated by increased yields of normally gaseous hydrocarbons. The actual yield of liquid products was slightly reduced. Perhaps the optimum process will provide for a controlled amount of radical recombination.

ADDITIONAL APPLICATIONS OF THE MICRO TECHNIQUE

Because of the ease and speed of microretorting, many possibilities exist for coupling it with all sorts of specialized detection systems. Thus, one could pursue elusive details of reaction mechanism or examine the effects of process variables on product components or product distribution. As examples of the kinds of phenomena that might be examined are the following observations: a) a tendency of sulfur compounds to be formed relatively early and nitrogen compounds relatively late in the pyrolysis, and b) a tendency for the product from hydrotorting to have higher ratios of nitrogen compounds to sulfur compounds than are observed in the product from inert gas retorting.

Especially useful should be the selective sulfur (11, 12) and nitrogen (13) detectors recently developed. In the programmed temperature mode of operation, one could continuously monitor the rates of production of sulfur or nitrogen compounds. With selective traps one might monitor particular compound types, such as basic or non-basic nitrogen, or individual compounds like H_2S, NH_3, H_2O or CO_2. In isothermal operation the same sort of thing could be done to determine whether reaction orders for sulfur- or nitrogen-containing products were the same as for hydrocarbons. In any of the variants where products are trapped and component analysis is done

subsequently, the individual sulfur and nitrogen compounds can in many cases be identified as well as measured.

Combinations of a suitable GLC column with selective traps could be further coupled with mass spectrometry for a great variety of studies, particularly with deuterium as the retorting fluid--we have only scratched the surface. One can only wonder about the isotopic compositions of the other butane and butene isomers. Would straight-chain components be more or less deuterated than branched-chain or cyclic compounds? What would be the isotopic composition of water, ammonia, or hydrogen sulfide? What would be the effect of process variables such as temperature, heating rate, particle size, and deuterium pressure on deuterium incorporation?

CONCLUSIONS

Pyrolysis of oil shale on a micro scale is a technique with much potential and some accomplishment.

The pyrolysis reaction appears to be a somewhat diffusion-limited first order reaction whose kinetics are complicated by the possibility of more than one bond-breaking step in going from kerogen to oil, gas, and coke.

The extent of diffusion-control diminishes during the course of the reaction as the shale changes from impervious rock to highly porous ash, and increases at high heating rates because products are generated faster than they can diffuse out of the pores.

The effect of hydrogen in hydrotorting is to compete with condensation reactions. The result is increased yields of lighter products and less coke formation.

The use of deuterium gave results that are consistent with a free radical mechanism. The thermal free radicals may become stabilized by the gain or loss of a D or H atom or, depending on the extent of diffusion control, may recondense to form heavier product.

LITERATURE CITED

(1) Allred, V. D., Chem. Eng. Progr. 62 (8), 55-60 (1966).

(2) Allred, V. D., Quart. Colorado School Mines 59 (3) 47-75 (1964).

(3) Bordenave, M., Combaz, A., Geraud, A., "Influence of the Origin of Organic Matter and Its Degree of Evolution on the Pyrolysis Products of Kerogen", Third International Congress on Geochemistry, London, Sept. 26-28, 1966.

(4) Dineen, G. U., Chem. Eng. Progr. Symp. Ser. 61, No. 54, 42, (1965).

(5) Hill, G. R., and Dougan, P., Quart. Colorado School Mines 62 (3) 75, (1967).

(6) Hubbard, A. B., and Robinson, W. E., U.S. Bur. Mines Rep. Investigations, No. 4744 (Nov. 1950).

(7) Jones, D. G., and Dickert, J. J., Jr., Chem. Eng. Progr. Symp. Ser. 61, No. 54, 33, (1965).

(8) Keith, P. C., Jr., Ward, J. T., and Rubin, L. C., Am. Petrol. Inst. Proc. 14M (III), 49, (May, 1933).

(9) Kogerman, P. N., and Kopwillem, J., J. Inst. Petrol. Techn. 18, 833, (1932).

(10) Maier, C. G., and Zimmerly, S. R., Univ. Utah Bull. 14, 62 (1924).

(11) Martin, R. L., and Grant, J. A., Anal. Chem. 37, 644, (1965).

(12) Martin, R. L., and Grant, J. A., Anal. Chem. 37, 649 (1965).

(13) Martin, R. L., Anal. Chem. 38, 1209 (1966).

(14) Schlinger, W. G., and Jesse, D. R., Quart. Colorado School Mines, 62 (3), 133, (1967).

(15) Thiele, E. W., Am. Scientist 55, 176, (1967).

(16) Thorne, H. M., Quart. Colorado School Mines 59 (3), 77, (1964).

(17) Zelenin, N. I., "Composition, Properties and Utilization of Shale Tar in Chemistry and Technology of Combustible Shales and Their Products" Publ. 6, Transl. by Israel Program for Scientific Translations, 1962, 21-32.

JOINT SYMPOSIUM ON OIL SHALE, TAR SANDS, AND RELATED MATERIAL
PRESENTED BEFORE THE DIVISION OF PETROLEUM CHEMISTRY, INC.
AND THE DIVISION OF WATER, AIR, AND WASTE CHEMISTRY
AMERICAN CHEMICAL SOCIETY
SAN FRANCISCO MEETING, April 2-5, 1968

MODIFIED FISCHER ASSAY
EQUIPMENT, PROCEDURES AND PRODUCT BALANCE DETERMINATIONS

By

L. Goodfellow, C. E. Haberman and M. T. Atwood
The Oil Shale Corporation, 1700 Broadway, Denver, Colorado 80202

INTRODUCTION

Fischer assay is a procedure for determining the yield of oil from oil shale or similar material by programmed pyrolysis and collection of products. The major use of the procedure has been in establishing the values of shale properties.

There are many versions of the assay method. The original work on the adaptation of the Fischer retort to oil shale assay was reported in 1949 by K. E. Stanfield and I. C. Frost (Report of Investigation 4477). The routine procedure used by the Bureau of Mines in Laramie involves simultaneous, automated operation of twelve retorts and gives produced oil and water yields but does not measure the evolved gas (1). A procedure for determining product balances was published by the same author (2), which provided for collection and weighing of the product gas, while collecting the produced oil and water as usual. Product gas analyses were reported. A similar procedure was published by J. Ward Smith (3), along with data from very careful, complete material balance studies. Data from replicate runs were examined statistically.

The Fischer assay apparatus in use at The Oil Shale Corporation permits collection of oil and water in the usual manner and allows for gas collection in either an inverted graduated cylinder for simple volume measurement or in an evacuated gas receiver for both volume measurement and analysis by gas chromatography. The equipment was developed primarily for use in support of the 1000 ton per day Parachute Creek semi-works retorting facility, operated by TOSCO, rather than for core analysis. We have investigated the effects of shale particle size and terminal retorting temperature on oil yield and have carried out detailed studies on balances for total material and for carbon, nitrogen and sulfur.

EXPERIMENTAL

Sample Preparation

A basic requirement of good Fischer assay is to start with a sample of shale which is completely representative of the material being investigated. This is best accomplished by reducing the material to fine mesh size and thoroughly blending.

The size of sample required for a specific ore size can be determined by using directions prepared by A. F. Taggert (4). The selected quantity of shale is prepared as follows:

1. If the sample size is large, grind it in a "Jaw-crusher" or "Chipmunk" crusher to minus 1/2-inch size.
2. Stage grind the minus 1/2-inch material to a nominal minus eight mesh using a "coffee-mill" grinder. Each grinding stage should lead to a finer grind, with the minus eight mesh material screened out and only the remaining plus eight mesh material recharged to the mill. Grinding in one stage can result in overheating the sample.
3. Blend the sample using a pad blender and normal blending techniques.
4. Split the blended sample on a Jones Riffle to approximately one gallon.
5. Grind, using an appropriate pulverizer, to minus 65 mesh. (We have found the 6-inch Raymond Mill produced by Combustion Engineering to be satisfactory.)
6. Blend the pulverized sample and split out needed samples on a Jones Riffle.
7. Dry the sample to constant weight at room temperature. Overheating the sample in a drying oven will result in reduced oil yield.

Operation of Equipment

The apparatus is described in Figure 1. One hundred (100) grams of dried oil shale are placed in a 7-ounce aluminum can which is then placed in the retort, and the retort head is bolted in place using an aluminum gasket for sealing. The charged and sealed autoclave is placed in the Transite heater case equipped with electric heating elements, and the glassware is attached as indicated. The calibrated centrifuge (receiver) tube is immersed in ice water, and ice water is also pumped through the water condenser. The apparatus is checked for leaks by placing under vacuum and observing any changes in an attached vacuum gage. The system is then purged with nitrogen.

Stopcocks are arranged so that the produced gas goes either to the inverted graduated cylinder for routine assay or to the glass gas bomb for complete material balance assay. In the latter case, the mercury switch manometer is set to open the solenoid valve whenever the system pressure exceeds ambient pressure. The opening of the solenoid valve allows gas to flow into the evacuated gas bomb until the system pressure is below ambient, at which time the mercury switch is activated and the solenoid valve is closed.

The heating schedule (below) is started and maintained by manual control of a Variac which feeds power to the electric heating elements in the retort heater case.

Time, minutes	Temperature (°F)
5	113
10	212
15	311
20	419
25	536
30	662
35	761
40	860
45	914
50	932
50 - 70	932
off	

At the end of the heating cycle a nitrogen purge is conducted. If the product gas has been directed into the inverted graduated cylinder the two liquid levels are equalized and the volume reading taken before purging. Nitrogen is then passed through the gas heater and through the retort to force oil remaining on the retort side arm down into the oil receiver. If the evacuated glass gas bomb was used, the hot nitrogen purge is directed similarly through the retort and finally into the gas bomb. From the total volume of the gas bomb and the gas chromatography analysis of the contained gas, the nitrogen contribution can be ascertained and the true product gas quantity determined. As stated below, we have found that nitrogen is not a product of oil shale retorting.

The glass adapter and oil receiver, previously tared, are removed from the retort and water condenser and weighed. The weight increase represents water plus oil. The oil receiver is then separated from the adapter and warmed and centrifuged. The water layer is removed in a tared syringe and weighed, allowing calculation of the weight of oil. The specific gravity of the oil is determined, and the oil and water yields are calculated in gallons per ton of shale. The gas yield is also calculated in SCF per ton.

RESULTS AND DISCUSSION

Statistical Analysis of Data

Forty-two (42) Fischer assays were run in routine fashion by the same operator on a single raw shale sample utilizing gas collection in the inverted graduated cylinder. Data obtained are shown in Table I.

When this work was done the water was determined by visual observation of the calibrated centrifuge tube receiver. Since then we have begun removing the centrifuged water layer in a tared syringe and determining the water by weight difference. This improved procedure should reduce the uncertainty in water yield and, to a lesser extent, the uncertainty in oil yield.

Figure I.

Modified Fischer Assay Equipment

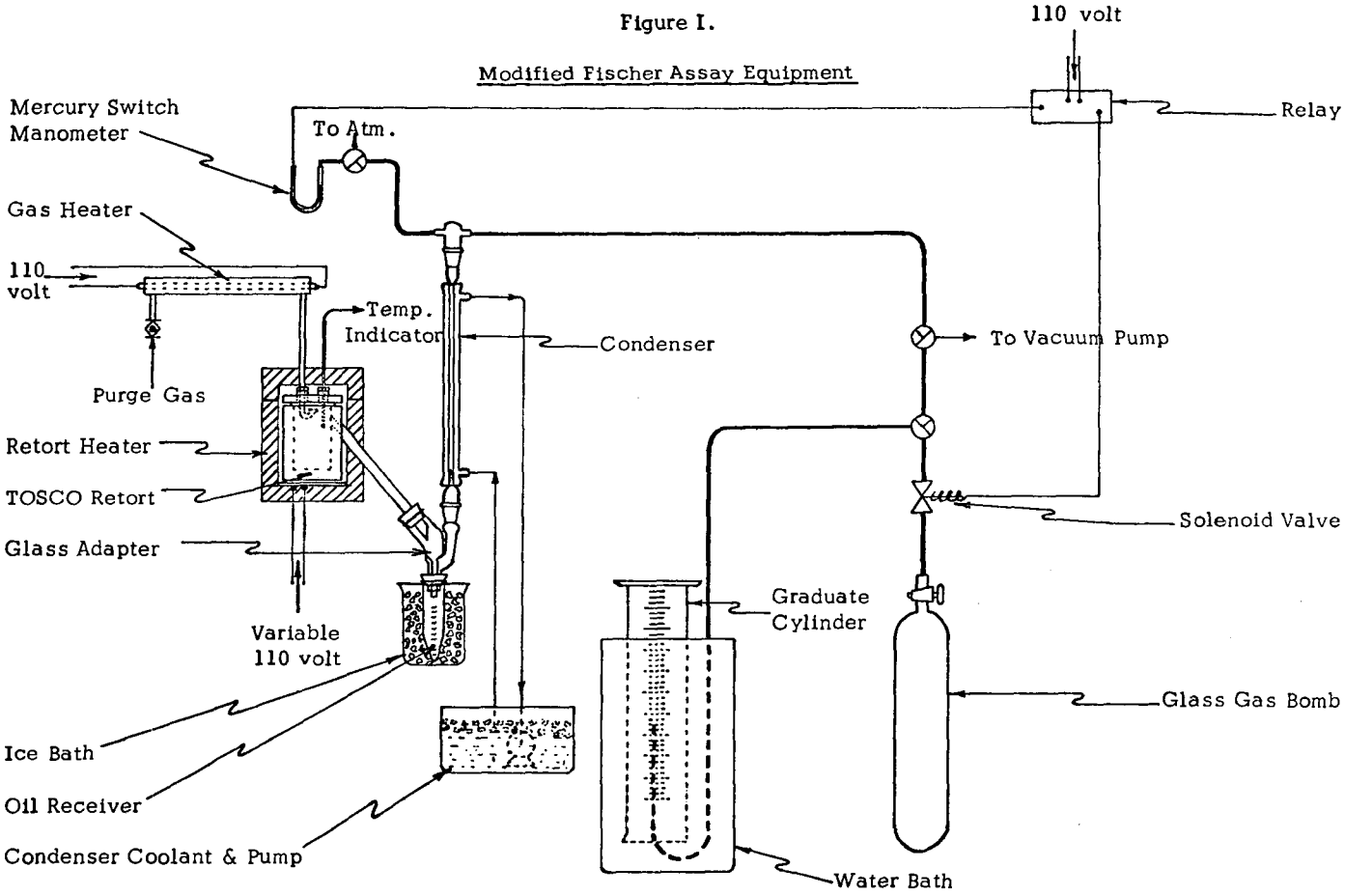

TABLE I

Results of Forty-Two Replicate Fischer Assays

	Arithmetic Mean	Mean Deviation	Standard Deviation
Oil Yield (gallons per ton)	33.17	0.237	0.291
Gas Yield (SCF per ton)	1028	33.3	45.6
Water Yield (gallons per ton)	2.82	0.28	0.33

Material and Carbon Balances

A sample of 33 gallon per ton oil shale was used in a complete product balance study. The Fischer assay procedure utilized gas recovery in the large, evacuated gas bomb followed by complete gas chromatography analysis. The normalized gas analysis is shown in Table II

TABLE II

Fischer Assay Gas Analysis

Component	Mole %
Hydrogen	36.4
Carbon Monoxide	3.6
Carbon Dioxide	18.0
Hydrogen Sulfide	2.9
Methane	17.2
Ethane	7.1
Ethylene	3.3
Propane	3.2
Propylene	2.9
iso Butane	0.1
n-Butane	1.0
Butenes	1.7
C_5's*	1.4
C6's*	0.7
C_7's*	0.3
C_8's*	0.1
C_9 and heavier	nil
Total	99.9

* Assumed molecular weight is calculated as Cn H (2n + 1).

The raw shale and spent shale were analysed for total carbon by the conventional combustion procedure (5). Inorganic carbon was determined by measuring carbon dioxide released by reaction with hydrochloric acid (6). In raw shale and spent shale the organic carbon value is the difference between total carbon and mineral carbon. Total carbon in the gas was calculated from the total amount of gas and from the analysis shown in Table II. The mineral carbon in the gas was calculated from the difference in mineral carbon values between the raw shale and spent shale, assuming this difference was represented by a portion of the carbon dioxide in the gas (Table I). The remainder of the carbon dioxide in the gas is assumed to be of organic origin. We have found in normal Fischer assay that somewhat more than half of the carbon dioxide in the gas is derived from pyrolysis of inorganic carbonates. J. Ward Smith (3) found in eight replicate runs, with 26 gallon per ton shale, that an average of 50% of the carbon dioxide in the gas was inorganic derived.

The total product balance and total carbon balance are shown in Table III. The organic and inorganic carbon balances are given in Table IV. The contribution of retort water contents to the carbon balances is very small and can be ignored.

It would be straightforward to obtain a hydrogen balance around Fischer assay, but the value of the information would be questionable. There is no reasonable way to distinguish organic hydrogen from hydrogen present as water in the mineral matrix.

Nitrogen and Sulfur Balances

The same raw shale as used above was subjected to additional total product balance

TABLE III

Product Balances*

	Total Product		Total Carbon	
Material	Weight (lbs) In	Weight (lbs) Out	Weight (lbs) In	Weight (lbs) Out
Raw Shale	2000		430	
Spent Shale		1648		177.2
Oil		252		213.4
Gas		70.5		38.4
Water		23		- - -
Total	2000	1993.5	430	429
% Deviation		0.32		0.23

* Based on one ton of raw shale, 33 gallons per ton Fischer assay oil yield.

TABLE IV

Organic and Inorganic Carbon Balances*

		Organic Carbon			Inorganic Carbon		
Material	Weight(lbs)	Wt.% Organic Carbon	Weight(lbs)In	Weight(lbs)Out	Wt.% Inorganic Carbon	Weight(lbs)In	Weight(lbs)Out
Raw Shale	2000	16.43	330.6		4.97	99.40	
Spent Shale	1648	4.94		81.4	5.81		95.75
Oil	252	84.69		213.4	- - -		- - -
Gas	70.5	49.25		34.7	5.24		3.69
Water	23	- - -		- - -	- - -		- - -
Total			330.6	329.4		99.40	99.44
% Deviation				0.36			0.04

* Based on one ton of raw shale, 33 gallons per ton Fischer assay oil yield.

TABLE V

Sulfur Balance*

			Sulfur	
Material	Weight (lbs)	Wt.% Sulfur	Weight (lbs) In	Weight (lbs) Out
Raw Shale	2000	0.75	15	
Spent Shale	1656	0.63		10.4
Oil	250	0.88		2.2
Gas	52	5.42		2.8
Water	22	0.03		nil
Total			15	15.4
% Deviation				2.7

* Based on one ton of raw shale, 33 gallons per ton Fischer assay oil yield.

TABLE VI

Nitrogen Balance *

Material	Weight (lbs)	Wt.% N (as NH_3)	Weight (lbs) In	Weight (lbs) Out
Raw Shale	2000	0.56	11.20	
Spent Shale	1648	0.34		5.60
Oil	252.8	2.21		5.59
Gas				nil
Water	23.0	1.87		0.43
Total			11.20	11.62
% Deviation				3.8

* Based on one ton of raw shale, 33 gallons per ton Fischer assay oil yield.

TABLE VII

Screen Size vs. Oil Yield

Screen Size (U.S. Standard)	Wt.%	Oil Yield (gallons per ton)	Size Wt.% X Oil Yield
+10	78.6	38.3	30.1
-10 to +20	11.9	35.7	4.2
-20 to +40	4.7	34.1	1.6
-40 to +80	2.6	32.5	0.8
-80	2.2	32.7	0.7
Head Assay*	100	37.2	37.2

Yield by Head Assay*	37.2 gallons per ton
Yield by Fraction Assay	37.4 gallons per ton
Variance	0.5%

*Oil yield of undivided, original sample.

TABLE VIII

Effect of Terminal Temperature on Product Yield

(Raw Shale Sample 01-1132)

Terminal (maximum) Temperature (°F)	Oil Yield (gallons per ton)	Water Yield (gallons per ton)	Gas Yield (SCF per ton)
875	35.1	2.4	810
875	35.6	2.4	835
900	37.4	2.9	940
900	37.9	2.9	925
932	38.0	2.8	1260
932	37.9	2.4	1360
932	37.4	2.9	1260
932	37.2	2.2	1330
932	37.7	3.0	1165

Fischer assays, and the charge materials and products were analyzed for nitrogen and sulfur. The nitrogen contents of the raw shale, spent shale, water and oil were determined by conventional Kjeldahl analysis. The sulfur contents of raw shale and spent shale were determined by combustion in a Leco furnace. The sulfur content of the gas was calculated from the hydrogen sulfide content, as determined by gas chromatography. The oil was analyzed for sulfur by X-ray fluorescence. Sulfur in water was assumed to be sulfide and was determined by iodimetric titration.

The amount of nitrogen remaining in the spent shale was unexpected since inorganic nitrogen compounds have not been reported in Green River formation oil shale.

Ammonia is never found in gas produced by shale retorting because of its rapid reaction with both carbon dioxide and hydrogen sulfide in the vapor phase. It is believed that all of the produced ammonia ends up in the retort water.

Independent tests on Fischer assay equipment and at the Parachute Creek semi-works facility, operated by TOSCO, have shown that molecular nitrogen is not a product of shale retorting.

Effect of Shale Particle Size on Oil Yield

A sample of crushed shale of random particle size distribution was separated into various screen fractions, and the individual fractions were subjected to the usual sample preparation and Fischer assay. The results are given in Table VII.

The general decrease in oil yield with decreasing particle size is evident. This trend was observed in every case which we investigated.

Variation of Product Yields with Terminal Retorting Temperature

The standard retorting time-temperature schedule is described above in the experimental section. It calls for leveling off the retorting temperature at 932°F (500°C) after 50 minutes, maintaining this temperature for an additional 20 minutes and then shutting off power. A brief investigation was made of the effect of varying the terminal temperature on product yield distribution. In each case the time cycle was unchanged, but the maximum temperature was leveled off as soon as it was reached. Data are given in Table VIII.

The 875°F temperature does not permit complete retorting of the oil. There seems to be little difference in oil yield between the two higher temperatures. The difference in gas yields between the two higher temperatures is likely due to formation of more carbon dioxide from inorganic components at the 932°F temperature.

LITERATURE CITED

(1) Hubbard, Arnold B., U. S. Dept. of the Interior; Bureau of Mines, Report of Invest. 6676 (1965).

(2) Hubbard, Arnold B., Fuel 41, 49-54, January, 1962.

(3) Smith, J. Ward, U. S. Dept. of the Interior; Bureau of Mines, Report of Invest. 5932 (1962).

(4) Taggert, A. F., "Handbook of Mineral Dressing", Chapter 19, p. 22, John Wiley and Sons, 1966.

(5) 1967 Book of ASTM Standards, Part 19, pp 33-38.

(6) ASTM D-1756-62, 1967 Book of ASTM Standards, Part 19.

JOINT SYMPOSIUM ON OIL SHALE, TAR SANDS, AND RELATED MATERIAL
PRESENTED BEFORE THE DIVISION OF PETROLEUM CHEMISTRY, INC.
AND THE DIVISION OF WATER, AIR, AND WASTE CHEMISTRY
AMERICAN CHEMICAL SOCIETY
SAN FRANCISCO MEETING, April 2-5, 1968

THE CONSTITUTION OF TASMANITES

By

R. F. Kane
University of Tasmania, Australia

INTRODUCTION

Thirty years ago, the plenary session of the first Conference on Oil Shale and Cannel Coal (1) adopted a resolution that a standard nomenclature for oil shale was most desirable and that a suitable classification should be secured. No such scheme has ever been adopted. One of the difficulties of any system based on the nature of kerogen itself, has been the virtual absence of recognisable features in the organic matter of the rock, the biological progenitor having been so macerated and metamorphosed that little of the original structure remains. One notable exception is the oil shale called tasmanite, which has characteristics so different from normal that, for over a century, it was believed to be utterly dissimilar from all others. In their early classification, Down and Himus (6) regarded tasmanite as unique and placed it in a separate category.

The purpose of this paper is to record the nature and thermal behaviour of this peculiar oil shale, large deposits of which were, until recently, regarded as endemic to Tasmania. However, in 1966, Tourtelot, Tailleur and Donnell (16) described a particularly rich, although not so distinctive, deposit which has been found in Alaska. This paper deals exclusively with the Tasmanian deposit. The chemistry of the Alaskan material will be the subject of a later contribution.

It is outside the scope of the paper to discuss the geological features of tasmanite as these have been amply covered elsewhere (14). For completeness, however, a summary is given.

RESULTS AND DISCUSSION

Occurrence and Nature

Tasmanite occurs as a single dichotomous seam, or two closely associated seams, about 5 feet thick in the Upper Permian in a relatively restricted area in northwestern Tasmania, fairly close to the coast. It would appear that the boundary of the deposit followed roughly the coast of the Permian sea and was associated with shallow waters of the early coastal islands. Above and below the tasmanite are mudstones associated with pebbly conglomerates. Insignificant patches of tasmanite have also been observed at other isolated places in northern Tasmania as well as on the mainland of Australia. There is no recorded occurrence in southern Tasmania.

The mineral matrix consists largely of fine silicaceous marlstone, silica particles and clay, together with small amounts of carbonates and sulphides. The total mineral matter varies between 50% and 90% of the entire rock, with a corresponding specific gravity range of 1.2-1.6.

The composition of the ash does not vary very much with the richness of the seam and adventitious inclusions of quartz, grit and pyrite are to be found throughout the deposit. A range of representative analyses (various authorities) of the ignited mineral matter is shown (% w/w) in Table 1.

The rock itself is grey-brown in colour, soft, fissile and combustible. When examined closely, many samples of tasmanite have a minute speckled appearance made up of innumerable orange spots just visible to the naked eye. These discrete particles are tasmanite "kerogen".

The Organic Matter

The organic matter of tasmanite is different from any other rock type and consists nearly entirely of numberless yellowish clearly differentiated small discs embedded in the mineral matrix. The discrete particles, when viewed under the microscope perpendicular to the bedding plane, appear, when whole, as translucent disc-shaped bodies, roughly 1/2 mm in diameter with a creased and sculptured surface (see Figure 1. A satisfactory vertical section is shown in Ref. 6, Figure 3). In transverse section, innumerable distorted overlapping flattened sausages

are observed and it is not unreasonable to assume that the undistorted entities were nearly spherical in shape and have become flattened and creased under geological pressure. The nature of the surface sculpturing and the spore morphology have been discussed by Singh (15) and Wall (17). Opinion on the exact nature of the "spore cases" has varied widely and, in this paper, the term "spore" will be used to designate the particulate bodies which, in aggregate, make up most of the kerogen of tasmanite. It is not meant to infer that they are true spores in the botanical sense.

TABLE 1

Analysis of Tasmanite Ash

Constituent	Range %
Silica	70 - 77
Alumina	11 - 16
Fe_2O_3	5 - 7
CaO	0.4 - 4
MgO	0.7 - 3
SO_3	0.4 - 2
K_2O	2 - 3
Na_2O	0.5 - 2

Descriptions of tasmanite date from 1857 when the first record of the rock appeared in the "Papers and Proceedings of the Royal Society of Van Dieman's Land" - now Tasmania. In the ensuing decade, several references to this "combustible schist" or "white coal" were made in the scientific literature until, in 1864, the name "tasmanite" was given by Church (5). Somewhat later, Newton (13) isolated the spore bodies mentioned above and applied the generic name "Tasmanites" in deference to their origin and specifically "punctatus" because of their punctation or surface markings.

Initially the spores were believed to be algal in origin, but Newton (13) in 1875 rejected this idea and suggested that they were "allied to Lycopdiaceous macrospores". For a long time, these disc-like microfossils were regarded, not without suspicion, as belonging to a plant possibly allied to the Lepidodendroids or Equisetales. However, in 1941, Kräusel (10) showed that the tasmanite discs were indeed fossil leiospheres derived from an alga probably belonging to the Chlorophyceae and this has remained the consensus, the genus retaining the name "Tasmanites". Somewhat later, Wall (17) reaffirmed the identity of Tasmanites and showed its close affinity to the extant spherical green alga Pachysphaera pelagica (Ostenfeld 1899), both of which he placed in the Leiosphaeridae. The paleobotany of both Tasmanites and Leiosphaerida have been discussed by Eisenack (7). It would appear that the relationship between Pachysphaera and Tasmanites is closely parallelled by Bottryococcus braunii which is sometimes found in vast quantities in the Coorong in South Australia and in certain lakes in Siberia. In the case of Bottryococcus, the Permian alga responsible for the torbanites of Scotland and Australia so closely resembles its present day counterpart that palaeobotanists cannot justify a separate genus and have decided to retain the same name for both. Wall's contention that "Pachysphaera is regarded as a living representative of the fossil genus Tasmanites" would apply equally well to Bottryococcus, which contributes both to the extant Coorongite and to the fossil fuel torbanite.

Isolation of Tasmanite Kerogen

The benefication of the organic matter (kerogen) in oil shale by protracted leaching has received extensive study over a long period (4, 12). Usually chemical dissolution and removal of the mineral matter is either weak and ineffectual or is so drastic as to attack the kerogen itself. In the case of tasmanite, however, an initial efficient separation may be achieved by crushing and weak acid leaching followed by systematic screening. As the individual spores are large and of a relatively narrow size range, conventional sieves may be used. Singh (15) gives the extremes as 200-533 μ with a mean diameter of 366 μ.

It is interesting to note that the screen fractions showed the systematic change in properties given in Table 2. The smaller mesh size consists of broken spores, pieces of cuticle, fine silica and clay, whereas the +30 mesh consists essentially in aggregates and adventitious matter.

If gangue be removed as "sink" in an aqueous solution of specific gravity 1.2 and the "float" be screened on a 30, 40, 50, 70, 100 mesh screen system, virtually pure spores may be collected within the -40, +50 mesh size.

TABLE 2

Properties of Tasmanite vs. Particle Size

Screen size	Ash % w/w	Colour of Ash
+30	27	red
-30, +50	41	pink
-50, +70	67	pale pink
-70	88	pinkish grey

Constitution of Tasmanite Kerogen

The organic matter of tasmanite may be divided, from the viewpoint of morphology, into:

1. Entire or nearly entire spores which make up about three quarters of the kerogen.
2. Residual organic matter which, under the microscope, appears as spore fragments, cuticle, vegetal dust and other detritus.

If the spores be removed, the residual organic matter is still oil yielding, although to a lesser degree (about 14 gal/ton), and it is uncertain how much of the non-spore material is made up by contributions from vascular plant remains.

The examination described below was carried out on a sample of "spore case" concentrate which had been prepared, many years previously, by flotation concentration in a ferric chloride solution. The sample, which received no chemical treatment, is referred to hereafter as "the concentrate".

A second quantity of the screened spore concentrate was treated according to the eleven stage purification described by Getzsche, Vicari and Scharer (8). Unfortunately, this prolonged treatment ruptured many spores, but on re-screening a quantity of entire, chemically pure, spores was recovered. Getzsche et al asserted that the purified organic matter was nitrogen and sulphur free and had an elemental analysis corresponding to C = 72.5%, H = 9.2%, O = 18.2%, but one must regard these data of questionable value. Later work by Kurth (11) cast grave doubts on the above analysis and he demonstrated that normal spores had a remarkably uniform composition which is shown in Column IV, Table 3 (even when purified according to Getzsche et al). However, Kurth found that the non-spore organic material was variable in composition and a representative analysis is given in Column III of Table 3.

TABLE 3

Composition of Purified Tasmanite Kerogen (% w/w)

	Range of Spore Material	Non-spore Material	Purified Spore Material	Pure Entire Spores
Carbon	76.9 - 78.8	66.1	78.50	78.10
Hydrogen	9.8 - 10.4	10.2	10.35	10.21
Nitrogen	0.59 - 0.64	1.3	0.64	0.61
Sulphur	4.66 - 5.12	2.0	4.70	5.14
Oxygen (diff)	5.81 - 9.67	20.4	5.81	5.94

Once again one must emphasize that it is imprudent to regard kerogen as a specific substance and, as Cane has pointed out elsewhere (2), it seems extremely improbable that any kerogen has a chemical constitution in the classical sense. Nevertheless, within the accepted definition, these spores, together with much broken material etc., are indeed the kerogen of tasmanite.

Although both the macroscopic and microscopic features of tasmanite might lead one to suspect a chemistry somewhat dissimilar from other shales, this has not been shown to be the case, except for the more important role of sulphur and the nature of the "solubles". Superficial examination of elemental analyses would suggest a "rank" lower than other algal shales, but careful plotting of published data on a Ralston diagram shows no significant trend and, on a S + N free basis, the elemental composition is not abnormal. If, however, one's consideration includes nitrogen and sulphur, it can be seen that the latter element is notably high - organic sulphur exceeds 5% in some samples on a d.a.f. basis. The only other organic rock surpassing this figure is Kimmeridge oil shale [Himus (9)] which, in most aspects, is exceptional.

Tasmanite kerogen which has been concentrated by the flotation/screening technique discussed above is a brown free-flowing powder of specific gravity about 1.09. The ash of the first stage concentrate (flotation/screening) was 24.3%, and, after the prolonged chemical

purification of Getzsche et al (8), this was reduced to 1.1%. The elemental analysis (d. a. f. basis) is shown in Table 3. The concentrate oil yield was 141 gal/ton (U. S.) from which the calculated yield of pure spore material was 186 gal/ton. The oil yield of the spores, purified by the Getzsche method, was 189 gal/ton.

Infra-red examination of the purified de-ashed spores showed absorption maxima corresponding to the normal C-H stretch, C-H bend, carbonyl (ester) and $(CH_2)_n$ rock frequencies characteristic of most kerogens. The benzene/methanol extract spectrum was much the same, except for a strong absorption at 680 cm^{-1}, to which a polysubstituted aromatic structure is tentatively assigned. There were no abnormalities in the spectra of either the kerogen or its pyrolysate except that the latter showed a somewhat more substituted aromatic nature in the 740-820 cm^{-1} region than other shale oils with which the writer has had experience.

Thermal Behaviour

On heating at the rate of 100°C per hour, the concentrate behaved in a manner similar to other algal shales, although thermal instability occurred at a lower temperature. Noticeable decomposition commenced at 255-270° with evolution of water contaminated with colloidal sulphur and carbon dioxide and, at a somewhat higher temperature, the production of a dank smelling, honey-like viscid material from which crystals deposited on cooling. This early product, which amounted to 3.2% of the concentrate, was unlike true tasmanite oil and it is assumed that it represents portions of the resinous soluble matter mentioned below. It is interesting to note that the concentrate purified by Getzsche's method did not show this varnish-like distillate nor the incipient decomposition at 270°C.

Evolution of tasmanite oil, accompanied by the copious production of hydrogen sulphide, started at about 340°C, reached a maximum at about 430°C and was virtually complete at 480°C. Hydrogen sulphide accounts for nearly half the total sulphur. There was some indication, and this has been noted by previous workers (11), that the initial pyrolysis is dissimilar to that occurring in excess of 340°C, at which temperature oil production starts in earnest.

Although no serious attempt was made to measure the energetics of the pyrolysis, calculation of the kinetics of the oil forming reactions showed a rate constant of 0.21×10^{-4} sec^{-1} at 350°C, a result strictly comparable with published figures on other shales. The available data did not permit the calculation of activation energies.

When the de-ashed spores were heated to about 350°, there was complete structural collapse and the retort charge was transformed into a bubbling mass of bitumen-like material. This, of course, is the tarry intermediate, characteristic of the penultimate stage (3) of kerogen pyrolysis. Apparently there is sufficient mineral matter in the case of the concentrate to maintain a degree of solidarity, although a coherent mass of coke was obtained.

Tasmanite oil

Table 4 gives the general properties of tasmanite oil which has been produced by gentle pyrolysis of the concentrate, the temperature being maintained below 450°.

Table 4

Properties of Tasmanite Oil

Specific Gravity @ 15°C	0.854
Refractive Index @ 15°C	1.4684
Tar Acids %	4.5
Tar Bases %	3.2
Sulphur %	2.22
Nitrogen %	0.34
Saturates %	43.9

The oil is a thin brown liquid with a remarkably clinging odour, thought to be connected with the nitrogen bodies rather than sulphur compounds. It is low in wax but high in sulphur, the amount of which, with respect to distillation temperature, goes through a maximum and then decreases. The sulphur bodies are alkyl and aryl thiols, thiophene and more complex substances. As with all materials of this nature, it is difficult to state with certainty how much sulphur in the oil has been formed during pyrolysis from inorganic sulphur and the organic matter, but oils exceeding 2.7% S have been produced from the upper portions of the seam.

The nitrogen compounds (tar bases) are largely alkyl pyridines and quinolines, but another type of nitrogen compound appears present which could possibly be alkaloidal in structure.

This contention is supported by a pronounced physiological reaction when working with the isolated bases. This bio-active material is being examined by another group in this University.

Solubles

The nature of the material extracted by a benzene/methanol mixture is different from that of all other shales so far examined. The extract was a brown resinous varnish-like material (4.1% w/w on the concentrate) unlike the normal waxy or bitumenous extract. An infra-red spectrum showed considerably more aromatic characteristics than usual and it is believed that the extract may consist substantially of portion of the resistant coat discussed by Wall (17). Possibly the extract may, in its present form, be related to abietic acid as early research gave strong indications of retene structures in the dehydrogenated extract.

LITERATURE CITED

(1) Anon., Oil Shale and Cannel Coal Vol. I, Glasgow Conference. Minutes of Meeting 10. 6. 38, Institute of Petroleum, London, 1938.

(2) Cane, R. F., Proc. 7th World Petm. Congress (Mexico), P. D. 14, Vol. III. Elsevier (in press). 1967.

(3) Cane, R. F., Oil Shale and Cannel Coal Vol. II, p. 592. Institute of Petroleum, London, 1951.

(4) Carlson, A. J., Univ. Calif. Publ. Eng. 3, (6), 295-342 (1937.

(5) Church, A. H., Phil Mag. 28, 465-470 (1864).

(6) Down, A. L. and Himus, G. W., Jour. Inst. Pet. 26, 329-335 (1940).

(7) Eisenack, A., Paleontographia 110, 1-19 (1958).

(8) Getzsche, F., Vicari, H. and Scharer, G., Part 3, Helv. Chim. Acta. 14, 67-78 (1931).

(9) Himus, G. W., Oil Shale and Cannel Coal Vol. II, p. 112. Institute of Petroleum, London, 1951.

(10) Krausel, R., Palaeontographia 86, 113-135 (1941).

(11) Kurth, E. E., D. Sc. Thesis (unpublished), University of Tasmania, Hobart, 389 pp., 1934.

(12) McKee, R. H. and Goodwin, R. T., Qtly. Colo. School of Mines 18, (1), 29 (1923).

(13) Newton, E. T., Geol. Mag. 12, 337-343 (1875).

(14) Reid, A. McI., Mineral Resources No. 8, Vols. I and II, p. 14 et seq., Geol. Survey, Dept. of Mines, Tasmania, 1924.

(15) Singh, T. C., Pap. Proc. Roy. Soc. Tas. 66, 32-36 (1931).

(16) Tourtelot, H. A. and Tailleur, I. L., U. S. Geol. Survey, open file Report, 1965 (1966) 17.

(17) Wall, D., Geol. Mag. 99, 353-362 (1962).

Figure 1. Tasmanite Spores

JOINT SYMPOSIUM ON OIL SHALE, TAR SANDS, AND RELATED MATERIAL
PRESENTED BEFORE THE DIVISION OF PETROLEUM CHEMISTRY, INC.
AND THE DIVISION OF WATER, AIR, AND WASTE CHEMISTRY
AMERICAN CHEMICAL SOCIETY
SAN FRANCISCO MEETING, April 2-5, 1968

CHARACTERIZATION OF THE SATURATES AND OLEFINS IN SHALE-OIL GAS OIL

By

H. B. Jensen, J. R. Morandi, and G. L. Cook
Laramie Research Center, Bureau of Mines, U. S. Dept. of Interior, Laramie, Wyoming

INTRODUCTION

One of the most important phases of shale-oil research is the characterization of shale-oil distillate fractions. The naphtha fraction has been described in detail (1), but it comprises only 5 to 10 per cent of shale-oil crudes and extrapolation of the naphtha characterization to heavier distillates is not of much value. Although the middle-distillate fraction comprises about 20 per cent of shale-oil crudes, very little has been reported on the characterization of this material. The gas-oil fraction is the largest distillate fraction of shale oil, amounting to about 30 per cent of the shale oil, and it is characterization of the saturates and of the olefins in this gas oil that this paper will report.

Separation of a Green River shale-oil gas oil (boiling range 300 to 600°C) into compound-type concentrates has been previously described (2). Figure 1 is a flow diagram showing the methods used to separate the gas oil into a nitrogen-compound concentrate (43%), an aromatic concentrate (22%), an olefin concentrate (19%), and a saturate concentrate (16%). Characterization of the nitrogen-compound concentrate in terms of model compounds has been reported (3) and work is presently in progress to characterize the aromatic concentrate.

This paper describes the paraffins and olefins in shale-oil gas oil in terms of hydrocarbon-compound types within rather broad limits. The saturates are described with respect to the normal paraffin chain length, to the degree of branching in the branched paraffin, and to the number of condensed-ring structures. The olefins are described in the same terms as the saturates with the addition of describing the location of the double bond. Some possible precursors of the saturates and olefins in the original kerogen are also discussed.

CHARACTERIZATION OF SATURATE CONCENTRATE

The saturate concentrate, prepared as described earlier (2), was characterized utilizing one further separation step, that of thermal diffusion. The fractions from the thermal-diffusion separation were examined by mass spectroscopy (MS) and nuclear magnetic resonance spectroscopy (NMR).

Thermal-Diffusion Separation

A sample of the saturate concentrate was charged to a liquid-thermal-diffusion column operated under the following temperature conditions: Water outlet, 95°C; water inlet, 45°C; top of column, 110°C; middle of column, 100°C; and the bottom of the column, 70°C. The sample was in the column under these conditions for 100 hours. Table 1 lists the refractive indices of the fractions from this separation. The refractive indices show little difference in the composition of the first eight fractions from the thermal-diffusion column. This consistency of composition of the top eight fractions will also be shown in the characterization by mass and NMR spectroscopy.

Mass Spectral Characterization

High-voltage mass spectra of each of the thermal-diffusion fractions were obtained. These MS data were treated by Lumpkin's method (4) to determine the amounts of paraffins, noncondensed naphthenes, and condensed naphthenes with up to six rings per molecule. Lumpkin's method did not give a breakdown between normal paraffins and branched paraffins, and a method of estimating this breakdown was developed.

The method of estimating the normal paraffin-branched paraffin split, using 70-volt MS, is based upon three premises: (1. Branched paraffins have small parent ions, (2. a standard

TABLE I. - Refractive indices of thermal-diffusion fractions from the saturate concentrate

Fraction	Refractive index, $n_D^{60\ °C}$ [1/]
1	1.4346
2	1.4347
3	1.4348
4	1.4350
5	1.4351
6	1.4353
7	1.4357
8	1.4360
9	1.4395
10	1.4503

1/ Run at 60 °C because samples were solid at 20 °C.

TABLE II. - Composition of thermal-diffusion fractions from the saturate concentrate, volume-percent

Alkane type	Fraction							Total concentrate
	1	2	5	7	8	9	10	
n-Paraffins	58	61	60	52	49	31	13	50
Branched paraffins	42	39	39	45	45	46	28	40
1-Ring naphthenes	--	--	1	3	6	19	30	7
2-Ring condensed naphthenes	--	--	--	--	--	3	14	2
3-Ring condensed naphthenes	--	--	--	--	--	1	8	1
4-Ring condensed naphthenes	--	--	--	--	--	--	4	<1
5-Ring condensed naphthenes	--	--	--	--	--	--	2	
6-Ring condensed naphthenes	--	--	--	--	--	--	1	

TABLE III. - Normal-paraffin distribution in saturate concentrate

Carbon number of n-paraffin	Volume-percent of total n-paraffins
22	1
23	1
24	4
25	15
26	23
27	27
28	18
29	10
30	1

TABLE IV. - Types of olefins in the thermal-diffusion fractions from the olefin concentrate by IR spectroscopy

Thermal-diffusion fraction	Mole-percent identified					
	Trans RCH=CHR'	$RCH=CH_2$	$RR'C=CH_2$	RR'C=CHR''	Cis RCH=CHR'	Total
1	31	21	-	7	8	67
2	31	20	-	5	6	62
3	32	19	-	8	4	63
4	33	18	1	8	5	65
5	31	15	1	7	6	60
6	26	12	1	10	4	53
7	17	8	1	10	3	39
8	13	5	2	9	2	31
9	12	3	2	11	3	31
10	12	3	2	10	2	29
Average	24	12	1	9	4	50

TABLE V. - NMR determination of hydrogen types in thermal-diffusion fractions of olefin concentrate

Thermal-diffusion fraction	Atom-percent total hydrogen		
	Methyl hydrogen[1/]	Methylene and methine hydrogens[2/]	Vinyl hydrogen[3/]
1	7.2	88.7	4.1
2	7.5	88.6	3.9
3	8.5	88.0	3.5
4	11.5	85.1	3.6
5	11.7	85.0	3.3
6	16.9	80.2	2.9
7	27.4	70.3	2.3
8	31.7	66.6	1.7
9	36.3	62.2	1.5
10	34.0	64.9	1.1

1/ 0.70 to 1.17 ppm.
2/ 1.17 to 3.00 ppm.
3/ 5.00 to 6.30 ppm.

total ionization for equal volumes of hydrocarbons (either mixtures or pure samples) can be calculated by Hood's method (5), and (3. the average carbon number for the branched and cyclic saturates is the same as for the normal paraffin in each fraction.

The following steps are necessary to use this method:

1. Determine the sensitivity of the monoisotopic molecular ion for a standard total ionization for each normal paraffin. This is done using available pure normal paraffins.
2. Calculate monoisotopic peak height for the molecular ions for the normal paraffins in the unknown sample.
3. Divide these monoisotopic peak heights by the sensitivity for each carbon number. This gives the relative volume (V_r) of each normal paraffin in the sample.
4. Determine the average carbon number of the sample by dividing the sum of the products of the carbon number times the V_r of each carbon number by the sum of the relative volumes.
5. Calculate the standard total ionization (I_s) for the sample according to Hood's method (5).
6. Add all peak heights in the spectrum from m/e 39 to the end of the spectrum of the unknown sample to get the observed total ionization (I_t) for the sample.
7. The following calculation then gives the volume-per cent normal paraffins in the sample:

$$\frac{I_s \times \Sigma V_r \times 100}{I_t} = \text{volume-per cent normal paraffins}$$

Table II lists the alkane-type composition of selected thermal-diffusion fractions and the total saturate concentrate as obtained by a combination of Lumpkin's calculations and the above calculation for the amount of normal paraffin in a sample.

The method of estimating the normal paraffins was also used to determine the carbon-number distribution of the normal paraffins in the thermal-diffusion fractions. This distribution is calculated as follows:

$$\frac{V_r \times 100}{\Sigma V_r} = \text{per cent of total normal paraffin in each carbon number}$$

Table III is the summation of the normal-paraffin distribution from the thermal-diffusion fractions from the saturate concentrate. Thus, 93 per cent of the total normal paraffins in the saturate concentrate had chain lengths from 25 to 29 carbon atoms.

Nuclear Magnetic Resonance Characterization

The NMR spectra of the 10 thermal-diffusion fractions were used to estimate the relative amounts of the different kinds of hydrogen in each of the thermal-diffusion fractions. Using carbon tetrachloride as the solvent and tetramethylsilane as an internal standard, the 0.70- to 1.05-ppm band was used to determine the methyl hydrogens, and the 1.05- to 2.00-ppm band was used to determine the combined methylene and methine hydrogens. Integration of the NMR spectra of the thermal-diffusion fractions shows that fractions 1 through 8 are similar and contain 88 per cent methylene-plus-methine hydrogens and 12 per cent methyl hydrogens. These data indicate that there is an average of three methyl groups per branched paraffin molecule, or only an average of one branch per molecule.

The bottom two thermal-diffusion fractions show substantial increases in methyl hydrogens. The percentage of methyl hydrogen in thermal-diffusion fraction 9 was 16 per cent, and in thermal-diffusion fraction 10 it was 18 per cent. From these data and those in Table II it can be calculated that the number of methyl groups per average cyclic molecule is 4 for fraction 9 and is 3.5 for fraction 10.

Discussion of the Saturate Concentrate

The overall picture of the saturate concentrate from the shale-oil heavy gas oil is that it contains 50 per cent straight-chain paraffins, 93 per cent of which have chain lengths from 25 to 29 carbon atoms. The branched paraffins comprise 40 per cent of the saturates and have only one branch per molecule. The 10 per cent of the saturates that is cyclic material is predominantly 1-ring cyclic but shows evidence of compounds with up to six condensed rings. This cyclic material is either multisubstituted or the substitutions are branched because the NMR spectra indicate that the average cyclic molecule has four methyl groups per molecule.

CHARACTERIZATION OF OLEFIN CONCENTRATE

One portion of the olefin concentrate, prepared as described earlier (2), was separated into 10 thermal-diffusion fractions and each fraction was examined by IR, NMR, and UV spectroscopy.

TABLE VI. - Number of vinyl hydrogens per average olefin molecule in the thermal-diffusion fractions of the olefin concentrate

Fraction	Number of vinyl hydrogens per average olefin molecule
1	2.2
2	2.1
3	2.0
4	1.9
5	1.8
6	1.6
7	1.3
8	1.0
9	0.7
10	0.5

TABLE VII. - Composition of the thermal-diffusion fractions from the HOC, volume-percent

Alkane type	Fraction										Total HOC
	1	2	3	4	5	6	7	8	9	10	
n-Paraffins	85	82	75	73	71	28	5	--	--	--	42
Branched paraffins	15	18	25	27	18	25	26	9	--	--	16
1-Ring naphthenes	--	--	--	--	10	34	31	20	7	2	10
2-Ring condensed naphthenes	--	--	--	--	1	9	21	21	15	10	9
3-Ring condensed naphthenes	--	--	--	--	--	3	11	23	28	28	9
4-Ring condensed naphthenes	--	--	--	--	--	1	5	15	23	22	7
5-Ring condensed naphthenes	--	--	--	--	--	--	1	8	16	20	4
6-Ring condensed naphthenes[1/]	--	--	--	--	--	--	--	2	8	11	2
7-Ring condensed naphthenes[1/]	--	--	--	--	--	--	--	2	3	5	1
8-Ring condensed naphthenes[1/]	--	--	--	--	--	--	--	--	--	2	<1

1/ By extension of Lumpkin's mass spectrometry method.

TABLE VIII. - Carbon-number distribution[1] of normal alkanes in the thermal-diffusion fractions of the HOC, volume-percent

Carbon No.	Fraction 1	2	3	4	5	6	7	Average[2]
21	1	1	1	1	1	1	-	1
22	2	2	2	1	1	2	2	2
23	3	3	2	2	3	2	4	3
24	5	5	5	5	6	5	11	6
25	20	20	20	20	16	22	20	20
26	24	24	25	23	23	23	24	24
27	22	23	23	23	23	22	25	23
28	15	15	16	17	18	16	12	15
29	6	5	5	6	7	7	2	5
30	2	2	1	2	2	-	-	1
Average carbon number for each fraction[3]	26.3	26.2	26.3	26.3	26.4	26.3	25.9	26.3

1/ Values are in volume-percent of the total n-alkane in each fraction.
2/ Shows the carbon-number distribution for the n-alkanes in the HOC.
3/ Values shown here are for the n-alkanes in each fraction.

TABLE IX. - Comparison of the C/H weight ratios of the thermal-diffusion fractions of the HOC

Fraction	C/H weight ratios Combustion	MS
1	5.72	5.78
2	5.70	5.78
3	5.78	5.78
4	5.75	5.78
5	5.75	5.80
6	6.08	5.92
7	6.13	6.07
8	6.21	6.44
9	6.36	6.73
10	6.84	6.80
Average[1]	6.03	6.09

1/ Value on original HOC = 6.00.

Another portion of olefin concentrate was hydrogenated with Raney nickel at one atmosphere of hydrogen and 85°C. This hydrogenated olefin concentrate was separated into 10 thermal-diffusion fractions which were examined by MS and NMR spectroscopy. Carbon-type composition of each of the thermal-diffusion fractions was determined by a density-refractivity intercept method (6), and carbon-hydrogen ratios were determined on each fraction.

Unhydrogenated Olefin Concentrate

A portion of the olefin concentrate was charged to the thermal-diffusion column with the operating conditions being the same as shown for the thermal-diffusion separation of the saturate concentrate. Each of the 10 thermal-diffusion fractions was examined by IR and NMR spectroscopy.

IR Examination

The IR method of Saier (7) was used to estimate the types of olefinic linkages in each of the thermal-diffusion fractions. The method was developed by Saier for use in the naphtha boiling range so that the present extrapolation to the gas-oil range contains the assumption that the molar absorptivities of the several types of double bonds are constant. This method does not yield information on the concentrations of tetrasubstituted or cyclic olefins; hence, the information presented in Table IV characterizes only the chain portion of the concentrate. About half of this chain unsaturation occurs as trans internal olefin; a fourth as terminal, or alpha olefin without beta substitution; a sixth as the trisubstituted internal olefin; a tenth occurs as the cis internal olefin; and a very small amount occurs as the terminal olefin with beta substitution. These data show that only 50 per cent of the molecules in the olefin concentrate have unsaturation in the chain portion of the molecule.

NMR Examination

The NMR spectra of the 10 thermal-diffusion fractions were used to determine amounts of the different kinds of hydrogen. Using carbon tetrachloride as solvent and tetramethylsilane as an internal standard, the following bands were used to estimate the types of hydrogen: Methyl hydrogen from 0.70 to 1.17 ppm; methylene and methine hydrogen from 1.17 to 3.00 ppm; and vinyl hydrogen from 5.00 to 6.30 ppm. Table V gives the results of these integrations. The percentages of vinyl hydrogen were used with the data on average carbon and hydrogen numbers to calculate the average number of vinyl hydrogens per molecule. (The data on the average carbon and hydrogen numbers will be developed in the section on HOC.) Table VI lists the average number of vinyl hydrogens per molecule in each thermal-diffusion fraction. The data in Tables IV and VI show that doubly bonded carbons in the molecules in the bottom thermal-diffusion fractions are more highly substituted than they are in the top fractions.

UV Examination

The UV spectra of the 10 thermal-diffusion fractions from the olefin concentrate showed that there was not present a significant quantity of aromatics. An attempt was made to calculate the concentration of conjugated diolefins and cyclic diolefins by a matrix method using molar extinction coefficients for available compounds. These reference compounds had molecular weights much lower than the compounds in the heavy-gas-oil olefin concentrate; thus, the results are only approximate. The calculations showed a constant level of about 1 volume- per cent conjugated diolefins in each of the top seven thermal-diffusion fractions. They showed no conjugated cyclic diolefins in the top four fractions, 2 per cent in fraction 5, 4 per cent in fraction 6, and 6 per cent in fraction 7. Fractions 8 to 10 had UV spectra too complicated to interpret with the matrix used.

Hydrogenated Olefin Concentrate

A 100-gram sample of the olefin concentrate was dissolved in 400 ml of isooctane and 85 grams of activated, Raney-nickel catalyst were added to the mixture. The Raney-nickel catalyst was prepared according to the "C" method of Hurd (8). This mixture was heated to reflux temperature and hydrogen gas was bubbled through the refluxing solution for 8 hours. Ninety-nine grams of the hydrogenated olefin concentrate (HOC) were recovered from the hydrogenation reaction.

A sample of the HOC was charged to a thermal-diffusion column with the operating conditions the same as given for the thermal-diffusion separation of the saturate concentrate. MS and NMR spectroscopy were used to characterize the fractions from the thermal-diffusion column. This characterization was made with respect to the relative amounts of normal paraffins, branched paraffins, and naphthenic compounds in each fraction. These data were compared to the data obtained by the density-refractivity intercept method of Kurtz (6) and to carbon-hydrogen ratios obtained analytically.

TABLE X. - Thermal-diffusion separation of the HOC

Fraction	Density $D^{20\ °C}_{4\ °C}$	Refractive index, $n_D^{20\ °C}$
1	0.8230	1.4551
2	0.8095	1.4494
3	0.7995	1.4507
4	0.7982	1.4496
5	0.8088	1.4539
6	0.8173	1.4567
7	0.8363	1.4648
8	0.8674	1.4767
9	0.9171	1.4976
10	0.9570	1.5124
Average[1]	0.8439	1.4667

1/ The original HOC had a density of 0.8442 and a refractive index of 1.4677.

TABLE XI. - Comparison of carbon-type composition of thermal-diffusion fractions from the HOC as determined by Kurtz' method and by MS analysis

Fraction	Carbon-type composition			
	Kurtz' method[1]		MS analysis[2]	
	Paraffin atoms, percent	Naphthene atoms, percent	Paraffin atoms, percent	Naphthene atoms, percent
1	85	15	100	0
2	100	0	100	0
3	100	0	100	0
4	100	0	100	0
5	97	3	97	3
6	91	9	88	12
7	79	21	77	23
8	62	38	57	43
9	40	60	39	61
10	21	79	32	68

1/ See reference (6).
2/ Estimated from MS pattern.

TABLE XII. - NMR determination of hydrogen types in thermal-diffusion fractions of the HOC

Thermal-diffusion fraction	Atom percent total hydrogen		Average number methyl groups per nonlinear molecule[3/]
	Methyl hydrogens[1/]	Methylene and methine hydrogens[2/]	
1	11.9	88.1	3.0
2	12.9	87.1	3.9
3	14.4	85.6	4.5
4	14.5	85.5	4.4
5	16.0	84.0	5.1
6	22.2	77.8	4.7
7	30.8	69.2	5.4
8	38.4	61.6	6.5
9	45.5	54.5	7.4
10	48.0	52.0	7.6

1/ 0.75 to 1.05 ppm.

2/ 1.05 to 5.00 ppm.

3/ Calculated from: (1) Atom percent methyl hydrogen, (2) the composition data shown in table VII, and (3) the average carbon number shown in table VIII.

MS Characterization

The high-ionizing-voltage mass spectral data were treated by Lumpkin's method (4) to determine the amounts of paraffins, noncondensed naphthenes, and condensed naphthenes with up to six condensed naphthene rings per molecule. This method worked well for thermal-diffusion fractions 1 through 7; however, it was evident from MS patterns that the bottom three fractions contained compounds with more than six condensed naphthene rings. The method of Lumpkin was extrapolated by smooth lines to cover seven, eight, and nine condensed naphthene rings. The normal paraffin-branched paraffin split was made as described previously. Table VII shows the results of these calculations for the thermal-diffusion fractions and also shows the summary for the total HOC.

As described in the saturate section, the MS data also provided an opportunity for estimating the carbon-number distribution for the normal paraffins in those fractions which have normal paraffins, and Table VIII shows these results.

The data in Tables VII and VIII were used to calculate carbon-hydrogen ratios for each of the thermal-diffusion fractions. The average ring-number content of each thermal-diffusion fraction was calculated using the data in Table VII. This average ring number was used to calculate the average Z number in the general hydrocarbon formula. The average carbon number listed in Table VIII and the average Z number are used to calculate the empirical formula and C/H value for each fraction. For thermal-diffusion fractions 8, 9, and 10 the average carbon number used was 26. The calculated C/H data are compared to combustion C/H data in Table IX. The agreement in the C/H values for each fraction is evidence that the data presented in Table VII with respect to the condensed structures are reasonable.

Physical Property Characterization of HOC

Kurtz (6) and coworkers have developed a method of correlating density and refractivity intercept with carbon-type composition. (Refractivity intercept is defined as the refractive index minus one-half of the density.) This correlation can be used for all types of viscous hydrocarbon oils and its application to the analysis of the thermal-diffusion fractions of the HOC provides a check on the MS method of hydrocarbon-type analysis. This check is in addition to the check provided by comparing C/H values as obtained by the MS method with C/H values determined by combustion.

Table X lists the density and refractive-index values for each of the 10 thermal-diffusion fractions. These values and the values for the average carbon number from Table VIII were used to obtain the carbon-type composition for each fraction shown under "Kurtz' Method" in Table XI. The composition values shown under MS analysis in Table XI were calculated from the data shown for each thermal-diffusion fraction in Table VII. In this calculation the condensed naphthene rings were assumed to be catacondensed and consist alternatively of five and six-membered rings. In general the MS results and the results using Kurtz' method agree. This supports the assumption that the condensed naphthenic structures in the HOC are of the catacondensed type.

NMR Characterization

The NMR spectra of the 10 HOC thermal-diffusion fractions were used to show the relative amounts of the different kinds of hydrogens in each fraction. Using carbon tetrachloride as solvent and tetramethylsilane as an internal standard, the amount of methyl hydrogen in each fraction was obtained by integrating the 0.70- to 1.05-ppm band and the combined methylene and methine hydrogens by integrating the 1.05- to 2.00-ppm band. Table XII lists the percentage of hydrogen represented by the areas under each of these two bands and the average number of methyl groups per nonlinear molecule in each of the fractions. This average was calculated using:

1. The per cent methyl hydrogen,
2. the composition data shown in Table VI, and
3. the average carbon number as ahown in Table VIII.

It may be only a fortuitous combination of data that shows the number of methyl groups to be three in the nonlinear part of thermal-diffusion fraction 1 (Table XII). Because there are no cyclic molecules in this fraction, these methyl groups are on branched paraffins and three is the minimum number of methyl groups possible per nonlinear, noncyclic molecule.

The data presented in Table XII show that fraction 1 has an average of one branch per nonlinear, noncyclic molecule; fraction 2 has an average of two branches; and fractions 3 and 4 both have 2.5. The data indicate neither the average length of the branch nor the point of branch attachment. In general, the lower the fraction in the column the greater is the average number of methyl groups per nonlinear molecule.

If we assume that the noncyclic branched-paraffin molecules in fraction 5 have the same

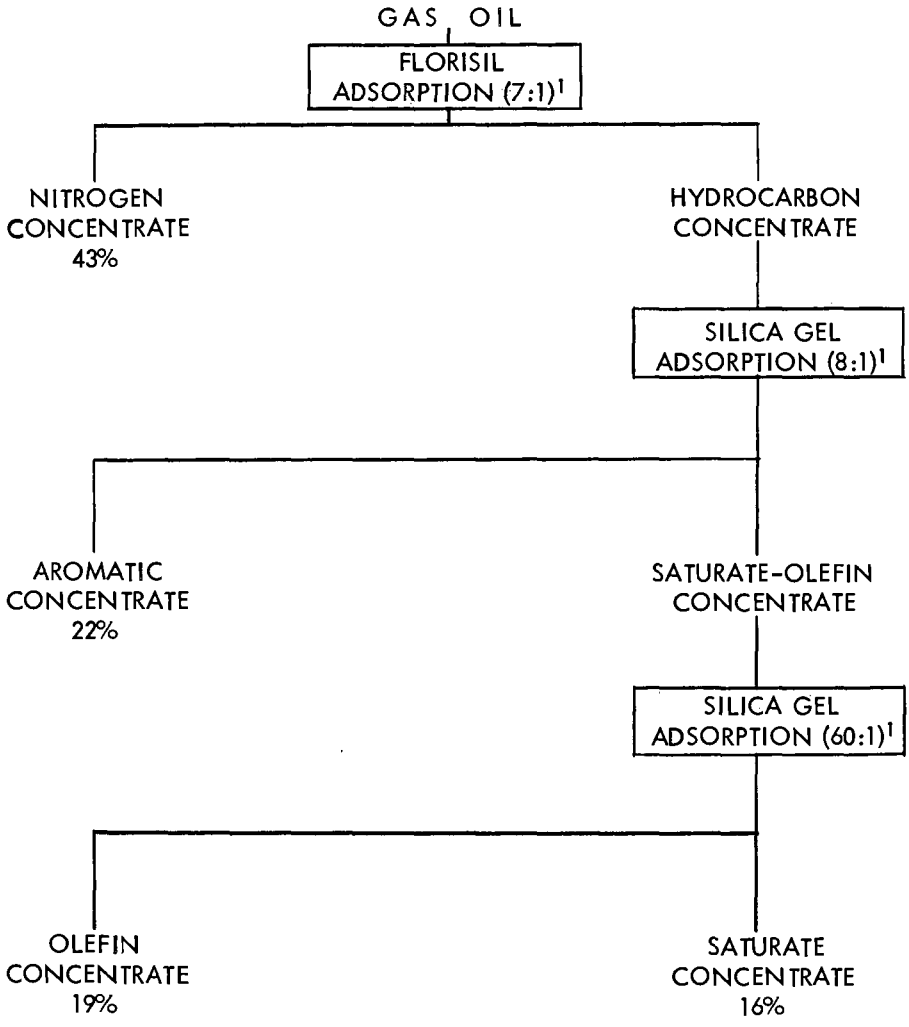

[1] Adsorbent-to-oil ratio.

FIGURE 1. - Separation of gas oil.

average number of methyl groups as were calculated for fraction 4 (4.5 groups per molecule), the calculated, average number of methyl groups per cyclic molecule is six. There is no way of determining the most likely configuration in which these six methyl groups are attached to the single, cycloparaffin ring; but if there are six methyls per average cyclic molecule, the average chain length for the alkyl substituent is three carbon atoms.

A similar calculation was made for thermal-diffusion fraction 10. This fraction had an average of eight methyl groups per molecule and an average of four condensed naphthene rings. If the ring system is catacondensed and the four rings are all six membered, there are no carbons left for chain construction. Although a single compound cannot be used to describe all of the molecules in this fraction, the following type structure is consistent with the NMR, the MS, the C/H-ratio, and the carbon-type data:

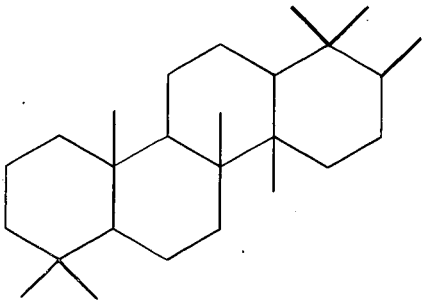

Whatever the case for ring structure, there must be several alkyl attachments in order to explain the large proportions of methyl hydrogens.

The particular type structure presented for the average condensed ring compounds in fraction 10 was chosen because it can be thought of as a possible thermal modification of a triterpane which has been identified in Green River kerogen (9). In general, these types of structures suggest that their precursors in the complex kerogen macrostructure may have been derived from materials related to steroids, triterpanes, or similarly condensed ring materials.

Discussion of the Olefin Concentrate

The data for the olefin concentrate from shale-oil heavy gas oil show that two-fifths of the olefin is straight chain; one-sixth branched olefin; one-tenth each of one-ring, two-ring condensed, and three-ring condensed olefins; and one-sixth of combined four-ring to eight-ring condensed olefins. Ninety per cent of the straight-chain olefins have chain lengths from 24 to 29 carbon atoms, and it is estimated from infrared spectra that about one-third of these normal olefins are alpha olefins, about one-half are trans internal olefins, and one-sixth are cis internal olefins.

The branched noncyclic olefins are not highly branched. For instance, those branched olefins in the top thermal-diffusion fraction (HOC fraction 1) have an average of only one branch per molecule, and the branched olefins in fractions 3 and 4 average 2.5 branches per molecule. The data for the branched olefins are not sufficiently detailed to allow positioning of the olefin bond with respect to the branching.

The cyclic compounds in the olefin concentrate appear to be highly substituted or highly branched. For example, the one-ring compounds that are in HOC thermal-diffusion fraction 5 have six methyl groups per average molecule. The average configuration of the molecule that fits the data for fraction 10 of the HOC indicates that the condensed cyclic olefins are catacondensed with an average of eight methyl groups per molecule.

The vinyl-hydrogen content of the thermal-diffusion fractions of the original concentrate is additional evidence for either cyclization or multisubstitution in the bottom-fraction material. The presence of terminal olefins in the top fraction provides a reasonable explanation of the 2.3 vinyl hydrogens per molecule because each internal normal olefin has two or less vinyl hydrogens and each terminal olefin has three. There is an average of only one-half of a vinyl hydrogen per molecule in fraction 10 which indicates multisubstitution on the olefinic carbons.

The data on neither the original olefin nor the hydrogenated olefin are sufficient to allow positioning of the double bond in the majority of the olefin-concentrate molecules, especially those molecules which are cyclic.

CONCLUSIONS

Spectral and chemical examinations of a saturate concentrate and an olefinic concentrate from a shale-oil heavy gas oil have shown 50 per cent of the saturates and 40 per cent of the olefins are straight chain. The branched paraffins are considerably less branched than are the branched olefins. The branched paraffins are 40 per cent of the saturates and the branched olefins are 15 per cent of the olefins.

The cyclic paraffins and cyclic olefins both show considerable range of ring condensation with up to six condensed saturate rings and evidence of nine condensed rings in the olefins. The cyclic naphthenes are 10 per cent of saturates and the cyclic olefins are 45 per cent of the olefins. The degree of substitution on the cyclics in both concentrates is large.

ACKNOWLEDGMENT

The work upon which this report is based was done under a cooperative agreement between the Bureau of Mines, U. S. Department of the Interior, and the University of Wyoming.

LITERATURE CITED

(1) Dinneen, G. U., Van Meter, R. A., Smith, J. R., Bailey, C. W., Cook, G. L., Allbright, C. S., and Ball, J. S., BuMines Bull. 593, 1961, 74 pp.

(2) Dinneen, G. U., Smith, J. R., Van Meter, R. A., Allbright, C. S., and Anthoney, W. R., Anal. Chem. 27, 185 (February, 1955).

(3) Dinneen, G. U., Cook, G. L., and Jensen, H. B., Anal. Chem. 30, 2026, (December, 1958).

(4) Lumpkin, H. E., Anal. Chem. 28, 1946 (1956).

(5) Hood, Archie, Anal. Chem. 30, 1218 (1958).

(6) Kurtz, S. S., King, R. W., Jr., Stout, W. J., Peterkin, N. E., Anal. Chem. 30, 1224 (1958).

(7) Saier, Eleanor, L., Pozefsky, Abbot, and Coggeshall, Norman, D., Anal. Chem. 26, 1258 (1954).

(8) Hurd, Charles, D., and Rudner, Bernard, J.A.C.S. 73, 5157 (1951).

(9) Hills, I. R., Whitehead, E. V., Anders, D. E., Cummins, J. J., and Robinson, W. E., Chem. Commun. (London), No. 20, 752 (October 19, 1966).

JOINT SYMPOSIUM ON OIL SHALE, TAR SANDS, AND RELATED MATERIAL
PRESENTED BEFORE THE DIVISION OF PETROLEUM CHEMISTRY, INC.
AND THE DIVISION OF WATER, AIR, AND WASTE CHEMISTRY
AMERICAN CHEMICAL SOCIETY
SAN FRANCISCO MEETING, April 2-5, 1968

USE OF CARBONIC ACID TO CONCENTRATE KEROGEN IN OIL SHALE

By

Rex D. Thomas
Bartlesville Petroleum Research Center, Bureau of Mines,
U. S. Dept. of the Interior, Bartlesville, Oklahoma

INTRODUCTION

Research to determine the characteristics of the bonding energy between kerogen and the mineral constituents of oil shale is being conducted at the Bartlesville Petroleum Research Center. A major problem encountered in this research is the separation of unaltered kerogen from the mineral constituents. The major mineral constituents in the oil shale are dolomite, calcite, quartz, and feldspars. Minor amounts of illite, pyrite, and analcite are usually present (5). The term kerogen as used in this paper means all of the organic material.

The ideal method for separating kerogen from the mineral matter in oil shale should fulfill several requirements. First, the kerogen should not be altered chemically during the process. Second, the method should yield enough material for elemental analysis and degradation studies. Finally, the kerogen concentrate should be fully representative of the organic material in the oil shale.

Both physical and chemical methods have been used for concentrating kerogen from the mineral matter (1). Physical methods include gravity techniques and methods based on wettability differences. Chemical methods include digestion in various acids such as acetic (2), hydrochloric and/or hydrofluoric.

This paper describes a method using carbonic acid to concentrate the organic material in oil shale. Carbonic acid is a weak acid formed when carbon dioxide dissolves in water. Carbonic acid was selected because it should be too weak to alter the kerogen, yet does dissolve carbonates such as calcite and dolomite. It ionizes mainly into H^+ and HCO_3^- and dissolves carbonates by converting them to the soluble bicarbonates.

APPARATUS

The apparatus used in this study is shown in Figure 1. The stainless steel cylinder is prepared from 4-inch tubing. The glass liner is a 1-liter beaker with the lip sawed off. The tubing for water and carbon dioxide is 1/8-inch plastic and enters the system through fittings that are drilled out so the tubing goes all the way through. A piece of fine (Whatman #42) filter paper is attached to the face of the fritted glass filter. This is removed after each run and a new piece applied. The only metal that the solution contacts is the stainless steel valves.

EXPERIMENTAL PROCEDURE

Two samples of oil shale from the Rifle, Colorado, area were selected for use in this study. The Fischer Assay Analysis of these samples by the Laramie Petroleum Research Center is shown in the following table.

TABLE 1.--Fischer Assay Analysis of Colorado Oil Shale Samples

	Weight-percent				Gallons per ton	
Sample Number	Oil	Water	Spent Shale	Gas Loss	Oil	Water
1	6.8	1.3	90.0	2.0	18.0	3.0
2	15.25	1.6	79.5	3.7	40.8	7.7

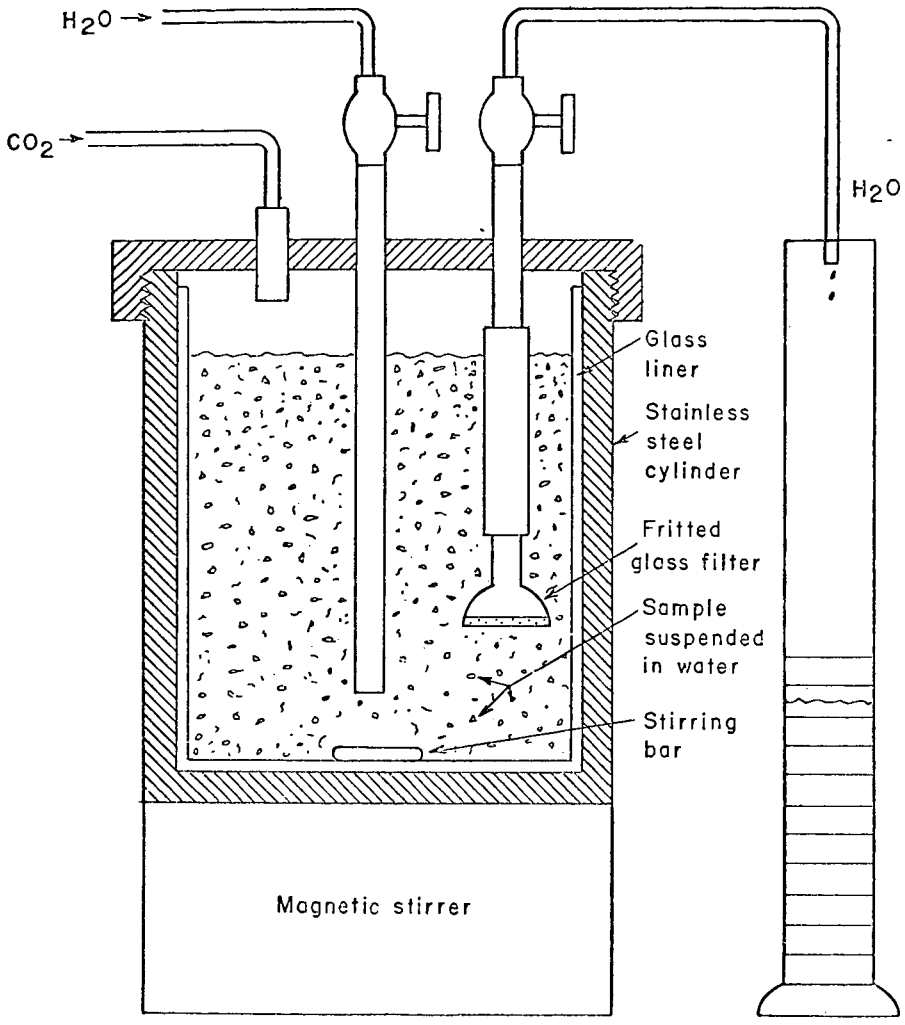

FIGURE 1.–Apparatus for Digestion of Oil Shale in Water Saturated With Carbon Dioxide.

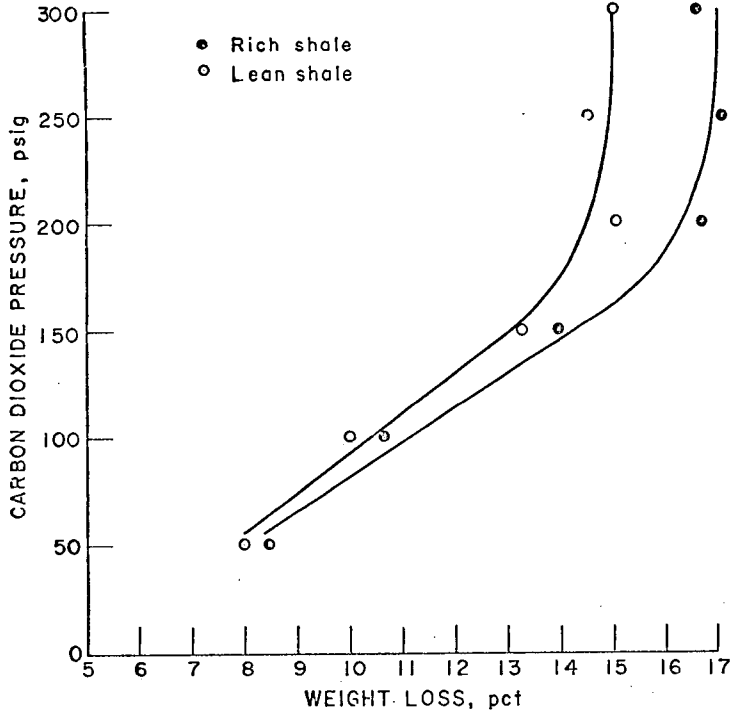

FIGURE 2.-Effect of Carbon Dioxide Pressure on the Soluble Material in Oil Shale.

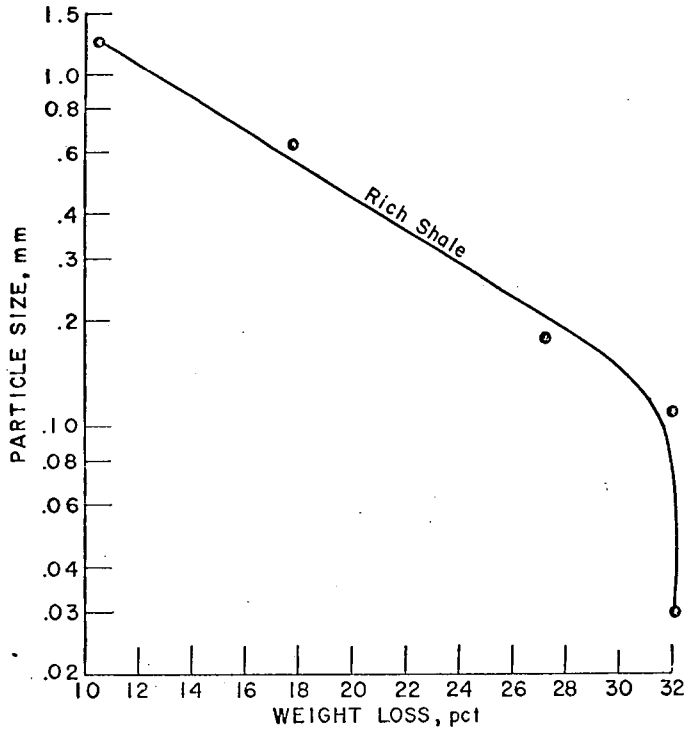

FIGURE 3.-Effect of Particle Size on the Carbonic Acid Soluble Material in Oil Shale.

Sample Number 1 is a lean, light yellowish brown oil shale. Sample Number 2 is a rich, dark brown oil shale. About 200 grams of each oil shale was crushed in a jaw crusher and ground with mortar and pestle till all the sample passed through a 200-mesh screen. The samples were vacuum dried (80°C) for 3 days to remove all the free water and stored in air-tight containers.

Samples of oil shale were weighted into the glass liner of the apparatus in Figure 1. Distilled water was added and the sample stirred in contact with air until water wet. The glass liner was placed in the stainless steel cylinder and assembly of the apparatus was completed. Carbon dioxide pressure was applied discharging the solution from the system through the filter. The system was flushed with carbon dioxide before more distilled water was pumped in under pressure. A batch technique was used so the system was stirred under pressure from 2 hours to overnight before solution was discharged through the filter. Calcium and magnesium were determined in the effluent water by titrating with EDTA (ethylenediaminetetraacetic acid). When no further calcium or magnesium were detected in the effluent, extraction was complete. Wet chemical analysis using hydrochloric acid was carried out on the oil shale after treatment by carbonic acid. The analysis confirmed that some iron and aluminum and all the calcium and magnesium had been removed.

Both oil shales were treated with hydrochloric acid for comparison with the carbonic acid treatment. A batch technique was used with overnight standing at low heat (70°C).

The total carbon and hydrogen in all samples was determined by combustion analysis. Mineral carbon (carbonates) was determined by treating the sample with acid to evolve carbon dioxide. Organic carbon was determined by difference.

RESULTS AND DISCUSSION

The effect of carbon dioxide pressure on the removal of soluble minerals in oil shale was determined first. Samples of both shales were suspended in 800 milliliters of distilled water, placed under carbon dioxide pressure, and stirred for 8 hours. Each sample weighed 2 grams. An aliquot of 300 milliliters was discharged through the filter under pressure. This was evaporated to dryness at low heat (95°C) and weighed to determine total solids. This data was used to calculate weight loss. This procedure was repeated for various pressures from 50 to 300 psig. The weight loss increased with increasing pressure up to 200 psig where it leveled off as shown in Figure 2. The pH of water saturated with CO_2 levels off at 3.3 in this region (3). Optimum pressure is, therefore, 200 psig, and this pressure was used for successive experiments.

A slight discrepancy is observed in the results in that the higher weight loss occurred in the oil shale with the lower carbonate content. Obviously, other minerals are being dissolved that are more soluble than the carbonates, under these conditions. Chemical analysis revealed the presence of gypsum ($CaSO_4$) which is more soluble under these conditions (4).

The effect of particle size on the removal of soluble minerals in oil shale was determined next. A sample of each oil shale was crushed and sieved. The weight loss in carbonic acid was determined for each particle size. For the rich shale weight loss increased with decreasing particle size from 1.25 mm (10 mesh) to 0.10 mm (150 mesh) where it leveled off as shown in Figure 3. Optimum particle size is therefore 150 mesh or finer. Samples used in all other experiments were finer than 200 mesh. For the lean oil shale, particle size did not affect weight loss over the indicated range. The effect of particle size on the rich shale is probably caused by the occlusion of carbonates by kerogen. The lean shale is low in kerogen, and therefore very little occlusion can occur.

At optimum conditions, carbonic acid removed about 90% as much material as was removed with hydrochloric acid. The results of both treatments are shown in Table 2.

TABLE 2.--Weight Loss of Shales Under Optimum Conditions

Sample	Weight Loss, Percent	
	HCl	H_2CO_3
Rich oil shale	36.2	32.1
Lean oil shale	57.6	53.4

These data show that a substantial portion of the mineral matter was removed from oil shales by the carbonic acid. Analysis of the samples treated with carbonic acid revealed that all the calcium and magnesium had been removed. It was noted also that no carbon dioxide evolved when the sample was subsequently treated with hydrochloric acid. Therefore, carbonic acid is as effective as hydrochloric acid in removing calcite, dolomite. and other carbonates and

other calcium and magnesium minerals. Chemical analysis revealed that excess weight loss in hydrochloric acid was caused by the dissolving of more aluminum and iron compounds.

The organic carbon and hydrogen contents of all samples, determined by combustion analysis, are shown in Table 3.

TABLE 3.--Combustion Analysis of Treated Oil Shales

Sample Description	Organic Carbon, Percent	Hydrogen, Percent	C/H
Lean Oil Shale	6.40	1.10	5.91
Treated with HCl	14.44 (6.12)[a/]	2.44 (1.04)	5.92
Treated with H_2CO_3	13.44 (6.26)	2.26 (1.05)	5.94
Rich Oil Shale	17.8	2.47	7.21
Treated with HCl	27.4 (17.5)	3.82 (2.44)	7.17
Treated with H_2CO_3	25.6 (17.4)	3.57 (2.42)	7.22

a/ Numbers in parentheses are based on the original oil shale.

The organic carbon content of the original oil shales is subject to an error of 0.4% carbon, while the treated samples are accurate to within 0.1% carbon. The organic carbon content of the original oil shale is subject to a larger error because it is determined by difference. The inorganic carbon content is high (24% CO_2 for lean shale and 11% CO_2 for rich shale) compared to the organic carbon content in the original samples. The inorganic carbon content is also subject to a larger experimental error. The results show that within experimental error organic carbon content and the carbon-to-hydrogen ratio are not affected by treatment with either acid. Both of these facts indicate that the kerogen is unaltered by treatment with either acid. However, the color of the sample of oil shale treated with hydrochloric acid was darker than the sample treated with carbonic acid, which indicates that hydrochloric acid may have reacted with the kerogen.

Treatment with carbonic acid is a very good first step in separating the organic material from the mineral matrix of oil shale. Further concentration can be obtained by physical means. Centrifuging the sample treated with carbonic acid in a saturated aqueous solution of calcium chloride yields a concentrate containing 85% to 90% of the organic material with an ash content of less than 30%. Centrifuging the original sample yielded only 15% of the kerogen and an ash content of 50%.

CONCLUSIONS

All the mineral carbonates such as calcite and dolomite can be removed from an oil shale by treatment with carbonic acid. Optimum conditions for removal are a carbon dioxide pressure of 200 psig and oil shale particles smaller than 0.10 mm (150 mesh). The organic carbon content of the oil shale is not affected by carbonic acid. The lack of color change in the product also indicates the organic material is unaltered by carbonic acid. Analyses can be performed on this concentrate without interference from inorganic carbon.

ACKNOWLEDGMENTS

This paper is based on research conducted at the Bureau of Mines, Bartlesville Petroleum Research Center, Bartlesville, Oklahoma, in cooperation with the Bureau of Mines, Laramie Petroleum Research Center, Laramie, Wyoming.

LITERATURE CITED

(1) Forsman, James P., Chapter 5 in "Organic Geochemistry". Monograph No. 16, Earth Science Series, Pergamon Press, Oxford, England, 1963, pp 148-179.

(2) Hubbard, Arnold B., Smith, H. N., Heady, H. H., and Robinson, W. E. "Method of Concentrating Kerogen in Colorado Oil Shale by Treatment With Acetic Acid and Gravity Separation". BuMines Rept. of Inv. 4872, 1952, 8 pp.

(3) Quinn, Elton, L., and Jones, Charles L. "Carbon Dioxide". American Chemical Society Monograph No. 72, Reinhold Publishing Corporation, New York, N.Y., 1936, pp 113-124.

(4) Linke, William F. "Seidell's Solubilities of Inorganic and Metal Organic Compounds". 4th Ed., vol. 1, A.C.S., Washington, D. C., 1958, p. 544.

(5) Stanfield, K. E., Frost, I. C., McAuley, W. S., and Smith, H. N., BuMines Rept. of Inv. 4825, 1951, 27 pp.

JOINT SYMPOSIUM ON OIL SHALE, TAR SANDS, AND RELATED MATERIAL
PRESENTED BEFORE THE DIVISION OF PETROLEUM CHEMISTRY, INC.
AND THE DIVISION OF WATER, AIR, AND WASTE CHEMISTRY
AMERICAN CHEMICAL SOCIETY
SAN FRANCISCO MEETING, April 2-5, 1968

THE FORMATION OF PRISTANE, PHYTANE AND RELATED ISOPRENOID HYDROCARBONS BY THE THERMAL DEGRADATION OF CHLOROPHYLL

By

Geoffrey S. Bayliss
Esso Production Research Company, Houston, Texas

INTRODUCTION

In recent years an increasing number of isoprenoid related hydrocarbons have been isolated from crude oils and oil-shale bitumens. The first identification of 2,6,10,14-tetramethylhexadecane (1) was closely followed by the characterization of the C_{14}, C_{15}, C_{16}, C_{18}, C_{19}, C_{20} and C_{21} isoprenoid hydrocarbons in an East Texas crude oil (2,3). Recently the C_{17} isoprenoid 2,6,10-trimethyltetradecane, which completes the homologues series from C_{14} to C_{21}, has been reported (4). A feature common to this series is the 2,6,10-trimethylundecane structure which would suggest a stepwise cleavage by the loss of a methyl group from the next highest member. To date, no compounds have been reported in petroleum which typify a dual terminal cleavage as would be indicated by the compound 6,10,14-trimethylhexadecane; this, however, may be a reflection of the difficulties inherent in isolating individual components from such complex mixtures. The identification of isoprenoid hydrocarbons in crude petroleum has aroused considerable interest about their origin and possible geochemical significance. Undoubtedly, the symmetry and the unequivocal relationship of these materials to natural biosynthetic processes provide substantial evidence in favor of the biogenic origin of petroleum. Similarly, while it is generally accepted that the most likely precursor of pristane and phytane is the phytol component of chlorophyll, more recently squalane has been suggested as an attractive alternative. There still remains, however, much speculation about the mechanisms whereby isoprenoid hydrocarbons can be formed from these sources under geologic conditions. Most of the proposed reaction sequences require an early liberation of phytol from the chlorophyll molecule by mile acid, alkaline or enzymatic hydrolysis. According to Bendoraitis, pristane and phytane are formed from phytol in an appropriate sequence of reactions entailing reduction, oxidation, dehydration, and decarboxylation. Bogomolov (5), has pointed out the unfavorable decarboxylation step in this sequence and has proposed an alternative mechanism in which phytol is oxidized to a β-hydroxy acid which is more readily decarboxylated than is the phytanic acid. Another mechanism, proposed by Curphey (6) postulates phytol as the source of a number of petroleum hydrocarbons generated by reactions involving epoxidation and thermal cracking. Notably, none of these processes explain the formation of lower isoprenoid compounds found in petroleum. Furthermore, it seems ambiguous that free phytol has not been reported as a predominant component of recent sediments although Blumer (7) has suggested this absence as being due to the conversion of phytol to phytadiene products on catalytic dehydration of the alcohol by adsorption on clay mineral surfaces. On the other hand, it has been suggested (8) that the absence of pristane and phytane in organic rich deposits from Mud Lake, Florida, postulated as a Post Pleistocene-Recent analog of the Green River oil shale, indicates the phytyl grouping is still bound as an integral part of the chlorophyll molecule.

In view of the lack of knowledge about the preservation of organic matter in sediments, the undisputable evidence that hydrocarbons have been formed at relatively late periods in the geologic age of the sediment and the generally accepted concepts of geothermal maturation of organic matter, a further postulate would be that the bulk of the isoprenoid hydrocarbons found in crude petroleums and oil shale bitumens are formed by the geothermal cleavage of the phytol components of chlorophylls preserved in situ in the organic kerogen of the sediment. This study was an attempt to establish whether or not isoprenoid hydrocarbons, notably pristane and phytane, could be generated by the thermal degradation of chlorophyll.

EXPERIMENTAL

Extraction and Separation of Chlorophylls

Fresh-water green algae, collected during May, was homogenized and extracted with methanol. The crude product was extracted into n-hexane and the chlorophyll isolated by partition chromatography on alumina. UV spectra of the product, Figure 1, was in agreement with published data (9) with a calculated C_a:C_b 1.7. Alfalfa chlorophyll was extracted from a commercially available product (Matheson, Coleman and Bell; C_a:C_b 2.5 $\pm$ 1) and was purified in an identical manner as for the algal chlorophyll. Both products were used in this study without further purification.

Hydrogenolysis

Hydrogenolysis has been used extensively as a means of thermally degrading oil-shale kerogens (10) and of solubilizing coals into crude liquid products (11). Consequently, this method was applied in degrading the materials reported on in this paper.

The isolated chlorophylls dissolved in tetralin were hydrogenolyzed in a 1 Liter Magnadrive Autoclave at 800°F for fifteen minutes in a hydrogen atmosphere. The solvent was removed from the reaction mixture by low temperature vacuum distillation. Because of solvent breakdown at the conditions of hydrogenolysis, no attempt was made to analyze products with a molecular composition less than C_{10}. For the oil shale study, shale from the Mahogany Ledge Zone, Green River Formation, was micronized and solvent extracted with a mixture of methanol, acetone and benzene in an ultrasonic tank (12). The shale had an original organic content of 14.7% of which 1.6% comprised solvent extractable bitumens. The extracted shale was hydrogenolyzed in a manner identical to that outlined for the chlorophylls.

Chromatography

The crude hydrogenolysis extracts were deasphaltened by n-pentane precipitation and the products separated into saturate, aromatic, and NSO fractions by partition chromatography on activated alumina (Alcoa F-20 Chromatographic grade alumina, 100-200 mesh; activated at 40°C for six hours). The saturate fraction was rechromatographed on activated silica gel (Davidson Chemicals, grade 923, 100-200 mesh; 40°C for one hour).

Instruments

The gas chromatograph used was an Aerograph Model 200 with a 20' 1/16" o.d., 3% Apiezon on 100-120 mesh Aeropak 30 column. The unit was temperature programmed to increase from 165° to 290°C at a rate of 4° per minute.

Mass spectrometric analyses were carried out on a Consolidated Electrodynamic Corporation Model 21-103C Mass Spectrometer fitted with a Mascot digitizer printout.

Ultraviolet spectra were recorded on a Beckmann Model DK-1 Recording Spectrophotometer.

Hydrogenolyses were run in a Standard 1-Liter Magnadrive Autoclave (Autoclave Engineers Incorporated) fitted with a Honeywell Pyro-Vane temperature control unit.

Reference Compounds

Reference isoprenoid hydrocarbons were isolated by the preparative gas chromatographic separation of a 300°C crude oil distillation cut. Each isoprenoid hydrocarbon was characterized by mass spectrometry with the spectra being in close agreement with published data (3).

RESULTS DISCUSSION

The complete thermal degradation of an alfalfa and of an algal chlorophyll extract was accomplished by high pressure, high temperature solvent hydrogenolysis. Under similar conditions greater than 90% of the organic kerogen of a Green River Oil Shale was solubilized. The hydrogenolysis products were isolated as dark brown--black tars which could be separated by absorption chromatography into asphaltene, saturate, aromatic and NSO fractions. The percentage compound-type composition of the reaction products is shown in Table I. The excellent reproducibility of the process is shown by the values quoted for three separate oil-shale hydrogenolyses. For the purpose of this study only the saturate fractions obtained from silica gel chromatography were analyzed. To achieve brevity in this report, the hydrogenolysis saturate products from the alfalfa chlorophyll, the algal chlorophyll, the oil shale kerogen 1, and the oil shale solvent extractable bitumen will be referred to as the alfalfa, algal, oil shale and bitumen saturates. Analysis of the saturate products was carried out by gas chromatography and high voltage mass spectrometry. Comparison of the gas chromatograms illustrated in Figures 2, 3, 4

TABLE I

HYDROGENOLYSIS AND CHROMATOGRAPHY DATA

	Alfalfa Chlorophyll	Algal Chlorophyll	Oil-Shale Bitumen	Oil-Shale Kerogen 1	Oil-Shale Kerogen 2	Oil-Shale Kerogen 3
Weight Hydrogenolysed	2.561	0.278		6.58	6.58	6.58
Weight Recovered	2.548	0.269		6.21	6.27	6.23
Alumina Chromatography						
Weight % Asphaltenes	2.4	1.0	21.3	30.3	32.3	35.1
Weight % Saturates	29.4	26.9	11.2	17.9	14.9	14.8
Weight % Aromatics and and Eluted Non-hydrocarbons	49.3	30.0	50.0	36.2	38.0	39.1
Weight % Nonrecovered	18.9	42.1	17.5	16.6	14.8	11.0
Silica Gel Chromatography						
Weight % Saturates	7.6	3.7	7.9	5.2	6.3	6.5

FIGURE 1

ULTRAVIOLET SPECTRA OF CHLOROPHYLL EXTRACTS

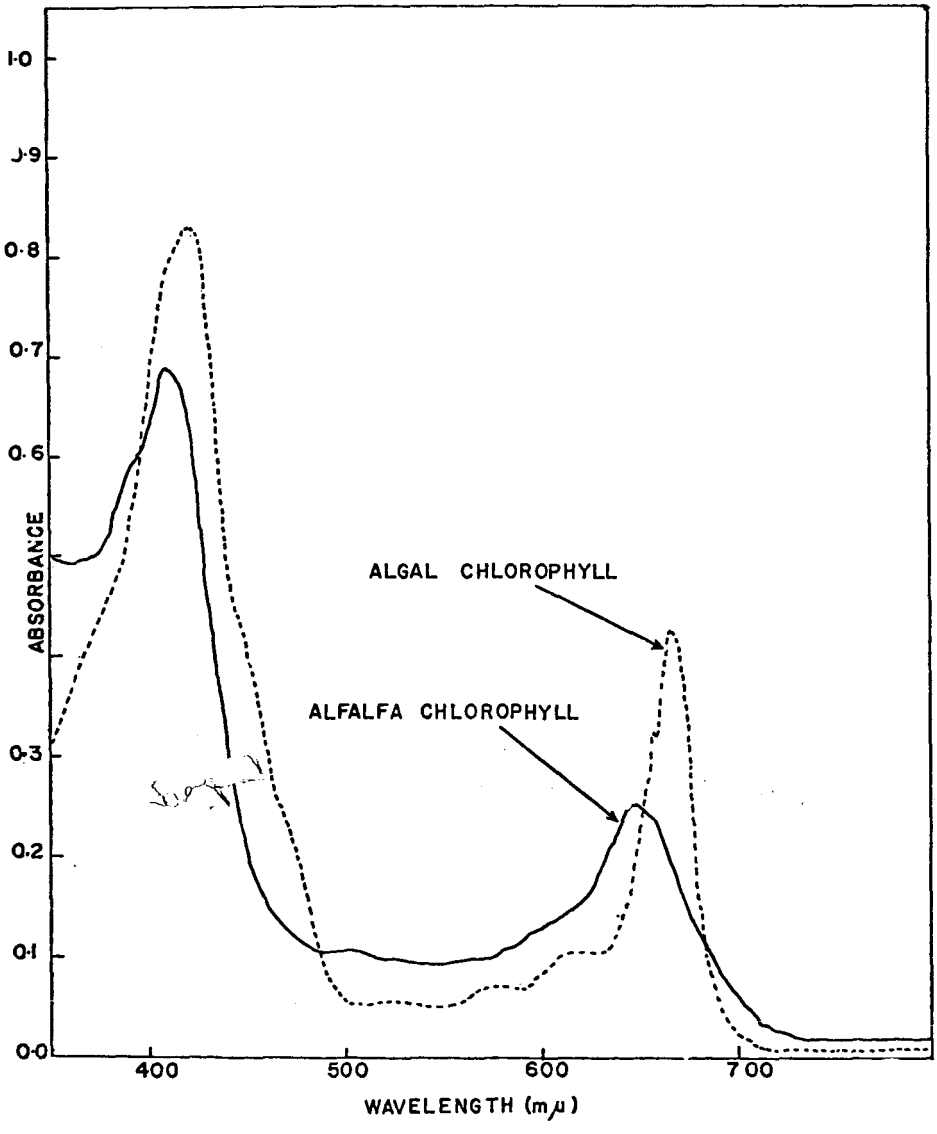

and 5, shows varying degrees of complexity, with the differences being mainly in relative peak intensities rather than in compound types. The bitumen saturates contained pristane and phytane (1:3) as the major isoprenoid hydrocarbons along with another notable response at a retention time coincident with that for the normal C_{17} hydrocarbon. Analysis of the oil shale saturates showed several differences, particularly the predominant amount of pristane formed from the kerogen by this process. The overall complexity of the oil shale saturate products was as expected and in fact suitable attenuation of the detector response for the bitumen analysis gave a chromatogram similar for the two fractions. In a comparable analysis of the alfalfa saturates, the most notable features were that the complexity of the compound types increased and that there was about three times as much pristane as phytane. An appreciable quantity of the C_{15} isoprenoid was also present although the C_{18} and the C_{16} isoprenoid hydrocarbons were only present in trace amounts. In contrast, analysis of the algal saturates showed there was about three times as much phytane as pristane. Lower isoprenoid hydrocarbons were undetectable in this extract. A compound at RT 9 minutes was present in both chlorophyll saturates but this has not yet been identified.

These saturate fractions were further characterized by mass spectrometry. Partial mass spectra data for each of the samples is represented in a plot of the relative peak intensity (m/e 71 = 100) for the C_nH_{2n-1}, C_nH_{2n}, C_nH_{2n+1}, and the C_nH_{2n+2} series of molecular and fragment ions. The values are reported by the diagrammatic presentation for the series, n = 10 through 20, in Figures 6, 7, 8, 9, 10, 11, 12 and 13.

In the case of the bitumen saturates the predominant isoprenoid character is shown by the large m/e 183, m/e 253 and m/e 267 responses in the C_nH_{2n+1} series. Presence of the normal C_{17} hydrocarbon is also confirmed by the intensity of the m/e 240 molecular ion in the C_nH_{2n+2} series. Comparison of this spectra with the partial mass spectra of the oil shale saturates shows a close agreement between the two sets of data. The high concentration of isoprenoid compounds is again reflected in the m/e 183 fragment ion, but in this instance the comparative unimportance of the normal C_{17} hydrocarbon is shown by the absence of peaking in the C_nH_{2n+2} series. Notably, the C_nH_{2n} and the C_nH_{2n-1} species are identical with a predominant fragmentation being recorded at m/e 181 and 195.

Similar evaluation of the partial mass spectra for the algal and alfalfa saturates shows fragment ions at m/e 183 and m/e 239; whereas the C_nH_{2n+2} series is characterized by the molecular ion peaks for values of n = 13, n = 15, and n = 17. It is of note that the relative intensities for these ions is greater than that expected for the parent ions of isoprenoid hydrocarbons, being intermediate between that for the parent ion of a branched hydrocarbon and that for the n-paraffin of similar molecular weight. The most outstanding difference shown in the formation of hydrocarbon products from the thermal degradation of the chlorophylls is illustrated in the partial mass spectra of the relative intensities of the C_nH_{2n-1} and the C_nH_{2n} series. In the C_nH_{2n} series for the alfalfa saturates, a large relative response is shown for the molecular ion m/e 238 which would be consistent with that expected for a C_{17} mono-olefin. Other olefinic molecular ions were also indicated by peaking at n = 13 and n = 15 although these responses were much less intense. In contrast, the partial mass spectra of the algal saturates showed a predominant response for an olefinic molecular ion, m/e 210, which would indicate a C_{15} mono-olefinic hydrocarbon. Again, other olefinic species were indicated n = 13, n - 17 and n = 19.

Such differences in the isoprenoid hydrocarbons formed by the thermal degradation of the chlorophylls suggest a fundamental difference in the molecular structure of the phytyl component. The location of the olefinic bond and the possible stereochemical characteristics of the molecule are two possibilities. These features would undoubtedly influence the point at which preferential cleavage of the hydrocarbon chain could occur. Several schemes are outlined (Figure 14) to explain the predominant amounts of pristane and of phytane in the hydrogenolysis products.

In scheme I, the preferred cleavage is postulated to occur between the C_{19}-C_{20} bond in a non-olefinic saturate hydrocarbon chain. This is applicable to the oil-shale kerogen products since the absence of olefinic compounds, shown by the relative low response in the C_nH_{2n} series, indicates the phytyl isoprenoid precursor in the kerogen may have been hydrogenated under geologic conditions. Subsequent cleavage during hydrogenolysis gives pristane as the major hydrocarbon product.

To explain the results for the bitumen and the chlorophyll saturates, a process such as illustrated in scheme II would be necessary. Scheme II (a) would explain the relatively greater abundance of phytane in these products, whereas scheme II (b) would account for the predominance of pristane. The cleavage at the points indicated is based on the preferred electron impact fragmentation of myrecene (13). Such mechanisms may reflect possible isomerization processes participating in the early diagenesis of organic matter in sediments.

One other explanation for the preferred formation of pristane and phytane from the alfalfa and the algal chlorophylls is that hydrogenation of the olefinic bond may occur before cleavage.

FIGURE 2

GAS CHROMATOGRAM OF ALFALFA CHLOROPHYLL HYDROGENOLYSIS PRODUCTS

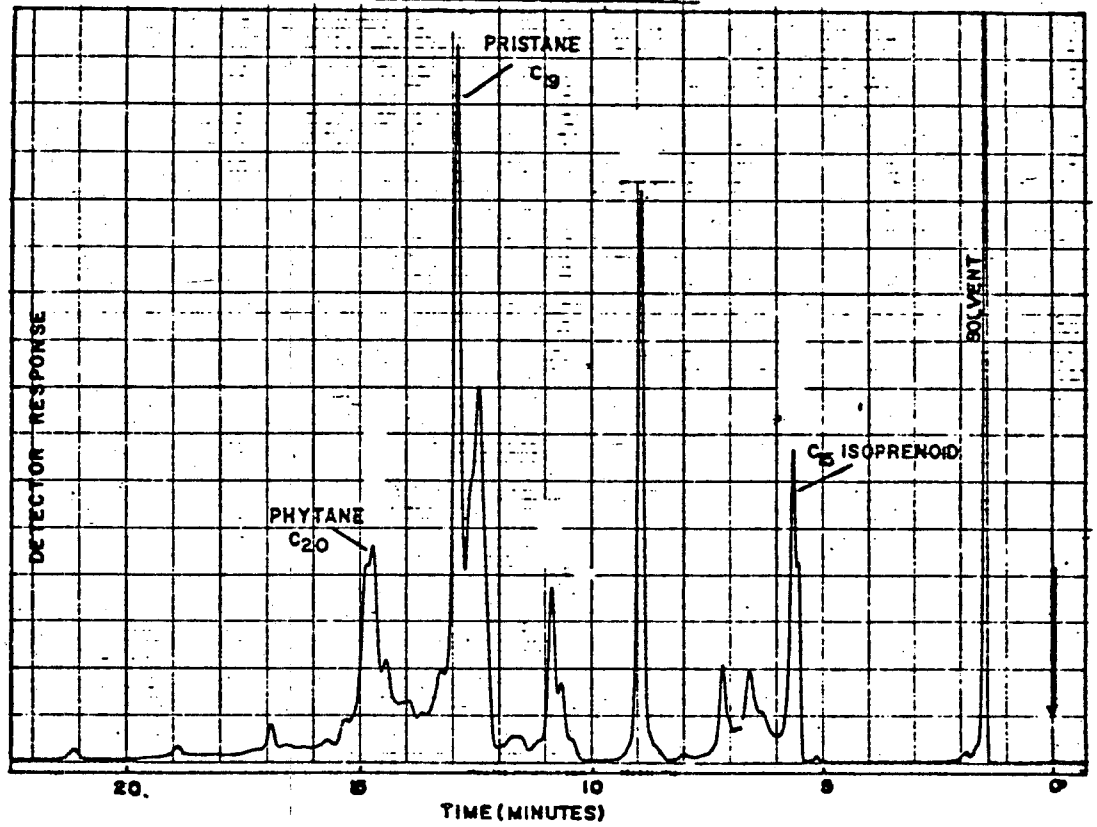

FIGURE 3

GAS CHROMATOGRAM OF ALGAL CHLOROPHYLL HYDROGENOLYSIS PRODUCTS

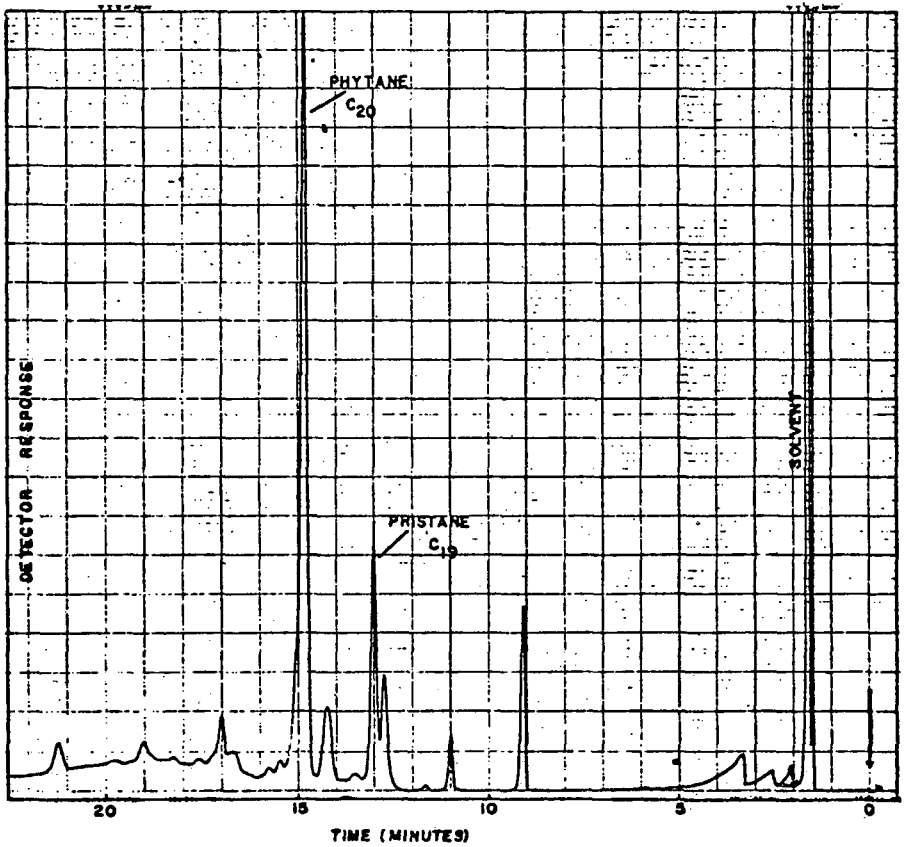

FIGURE 4

GAS CHROMATOGRAM OF OIL-SHALE BITUMEN

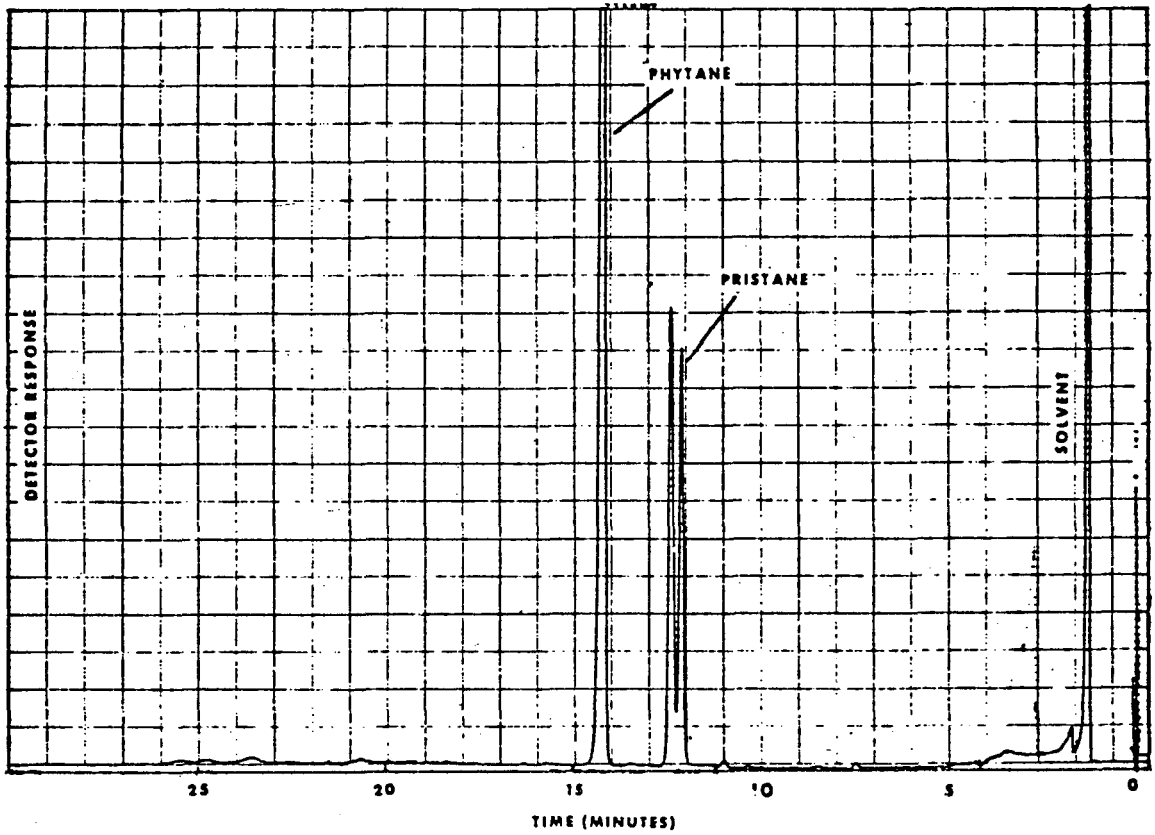

F124

FIGURE 5

GAS CHROMATOGRAM OF OIL-SHALE HYDROGENOLYSIS PRODUCTS

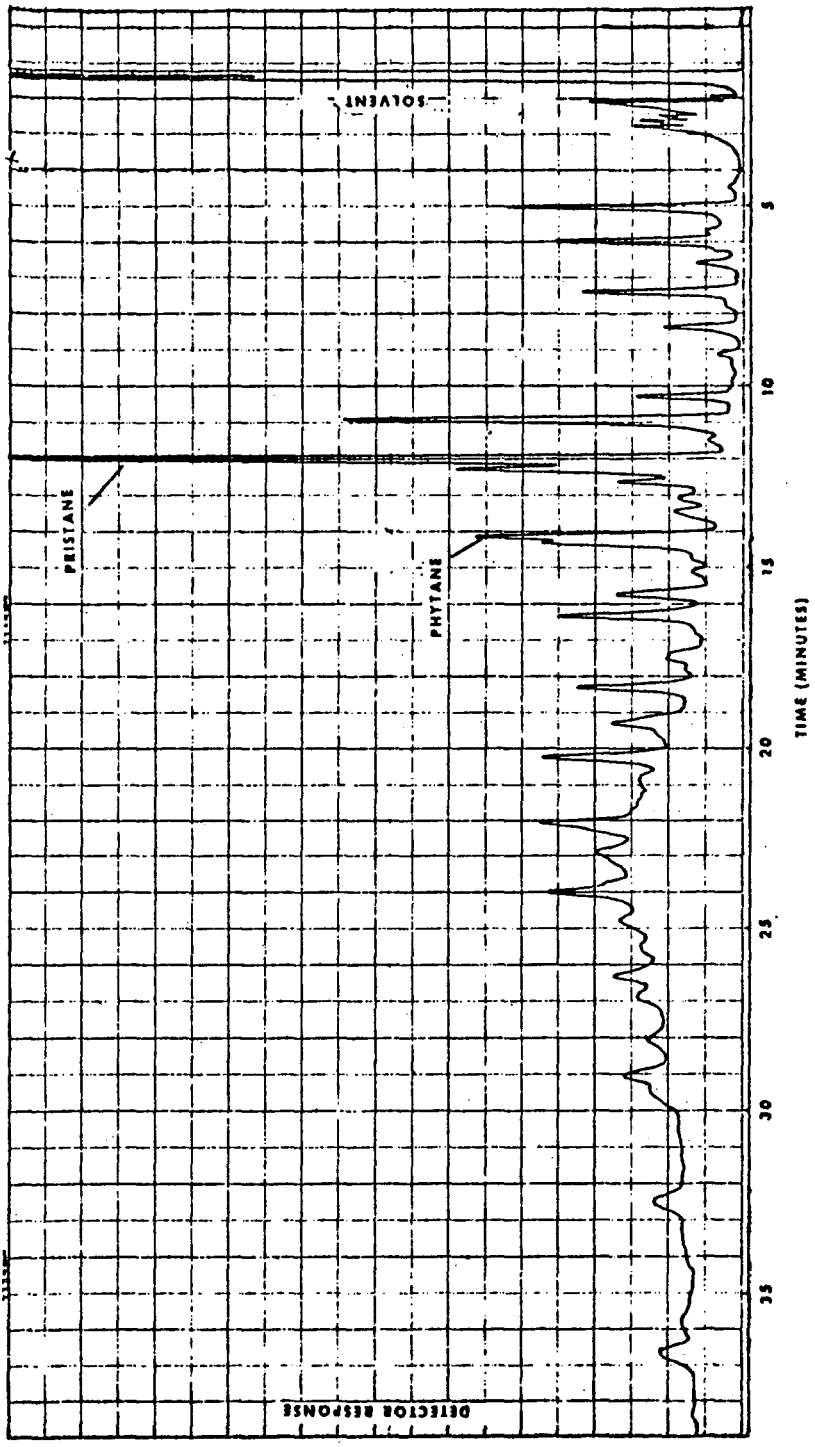

FIGURE 6

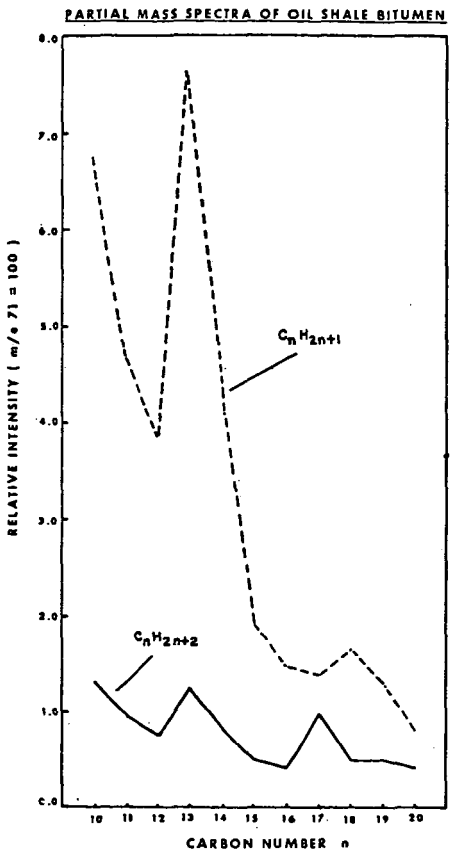

FIGURE 7

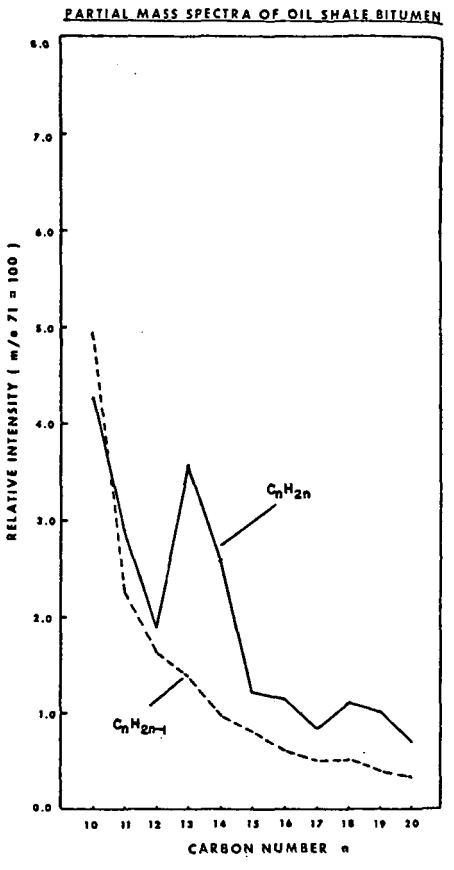

FIGURE 8

PARTIAL MASS SPECTRA OF OIL-SHALE HYDROGENOLYSIS PRODUCTS

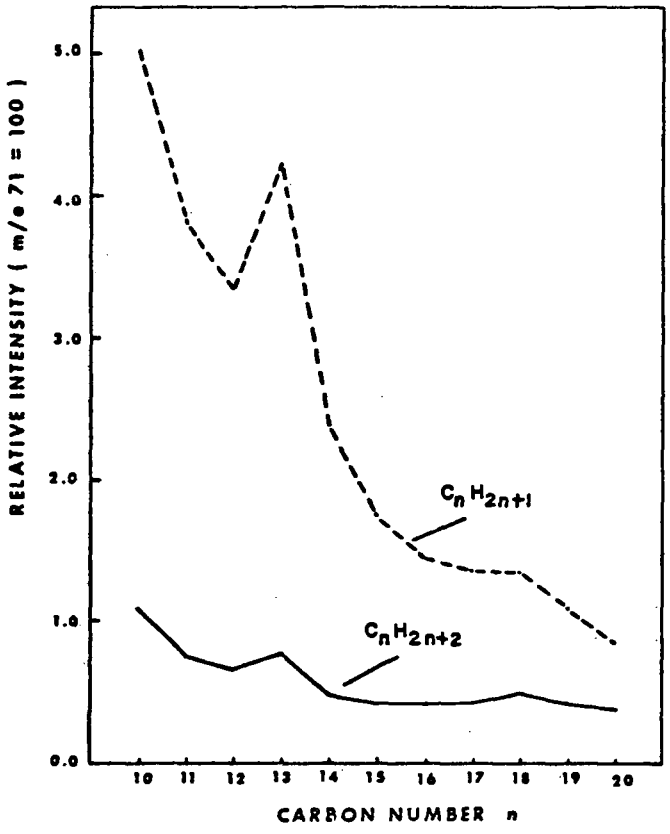

FIGURE 9

PARTIAL MASS SPECTRA OF OIL-SHALE HYDROGENOLYSIS PRODUCTS

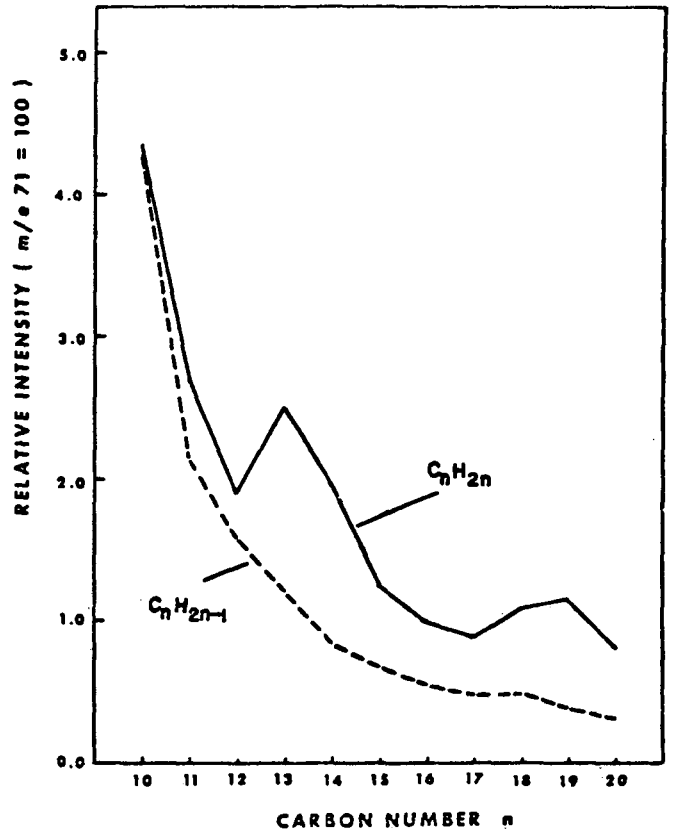

FIGURE 10

PARTIAL MASS SPECTRA OF ALFALFA CHLOROPHYLL HYDROGENOLYSIS PRODUCTS

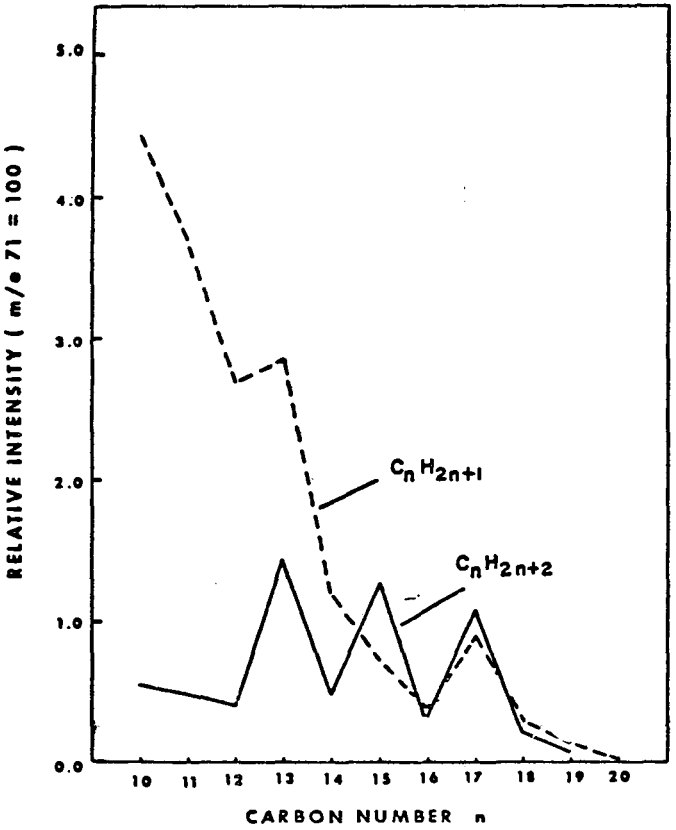

FIGURE 11

PARTIAL MASS SPECTRA OF ALFALFA CHLOROPHYLL HYDROGENOLYSIS PRODUCTS

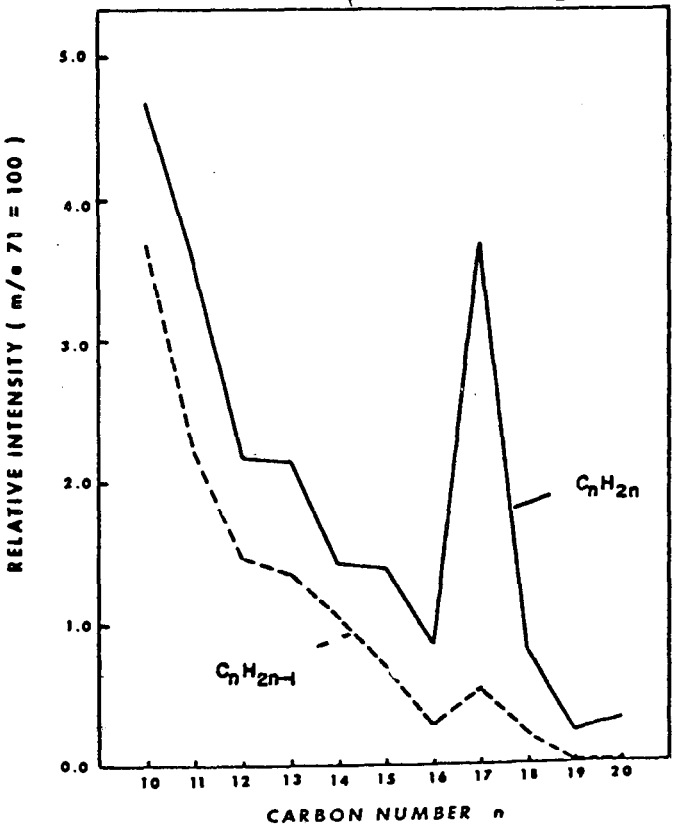

FIGURE 12

PARTIAL MASS SPECTRA OF ALGAL CHLOROPHYLL HYDROGENOLYSIS PRODUCTS

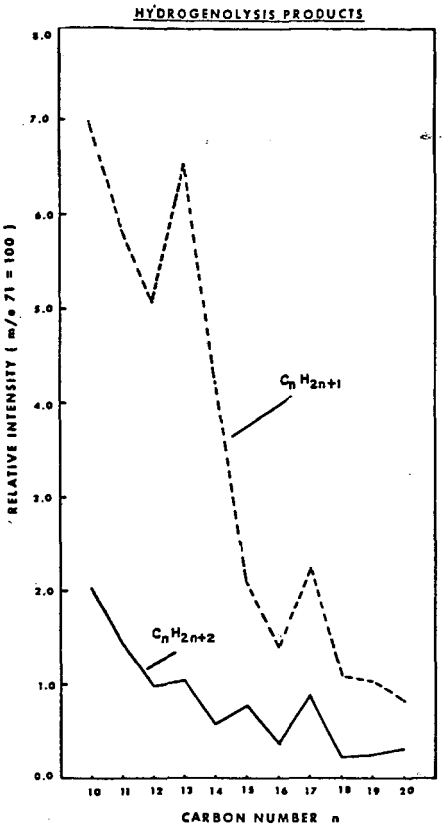

FIGURE 13

PARTIAL MASS SPECTRA OF ALGAL CHLOROPHYLL HYDROGENOLYSIS PRODUCTS

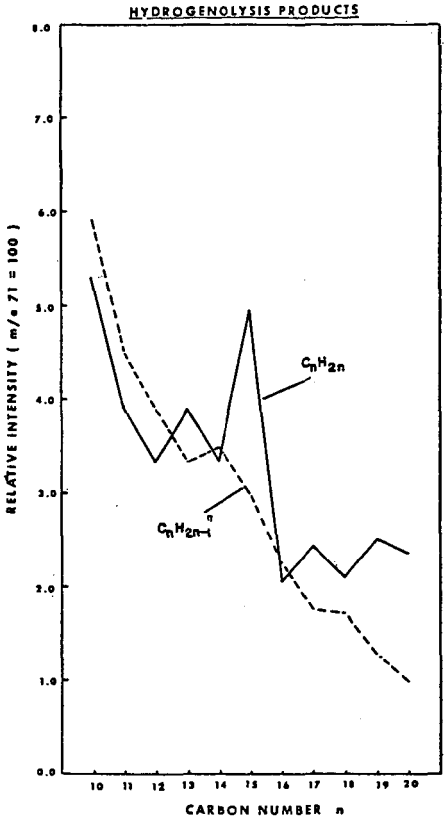

FIGURE 1 4

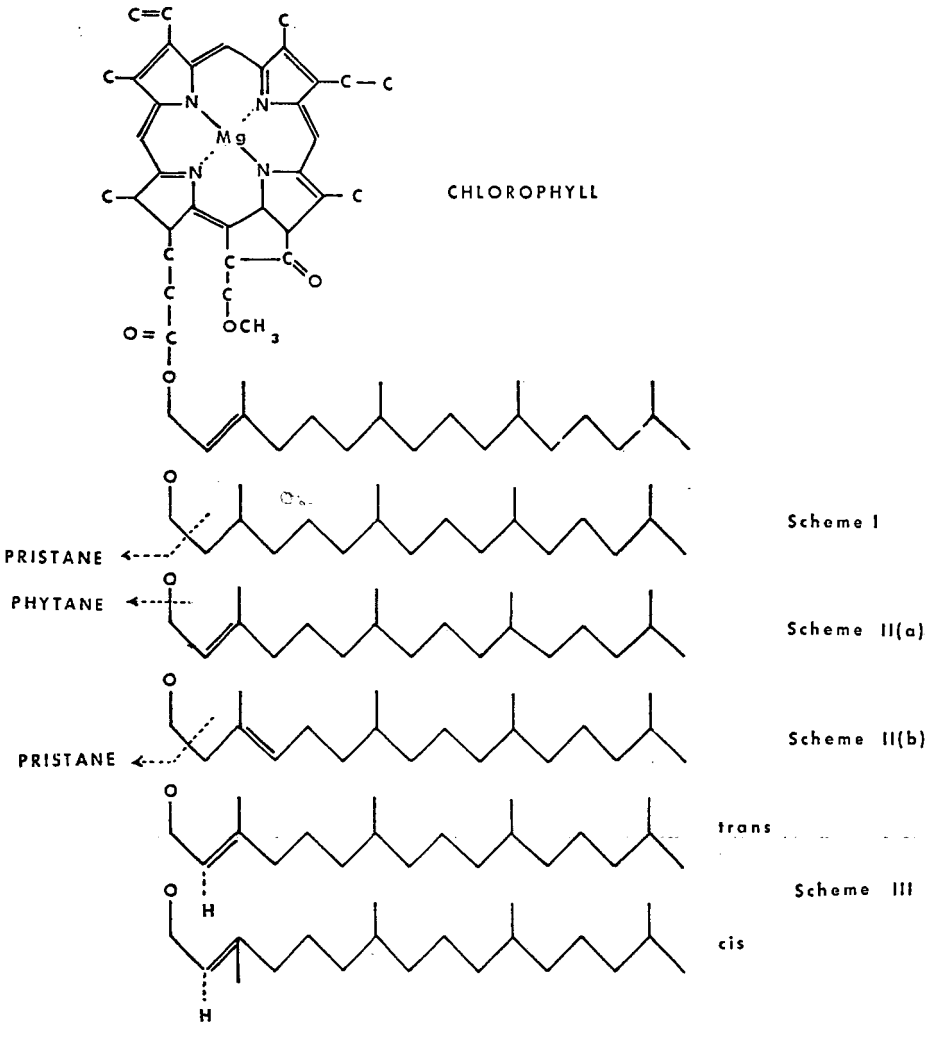
CHLOROPHYLL
PRISTANE
PHYTANE
PRISTANE
Scheme I
Scheme II(a)
Scheme II(b)
trans
Scheme III
cis

The cis and trans isomers shown in scheme III could account for such a difference since the relative rates of hydrogenation of these isomers under the hydrogenolysis conditions will be dependent upon the stereochemical hindrance from the rest of the molecule. Subsequent thermal cleavage would take place by scheme I. This would suggest that the olefinic bond in alfalfa chlorophyll is more susceptible to hydrogenation.

Clearly, the complex nature of the reaction sequences shown for the thermal degradation of these relatively simple molecules emphasizes the general lack of knowledge about the geochemical processes resulting in the formation of petroleum. It is hoped that continued research will result in a better understanding of some of these mechanisms.

ACKNOWLEDGMENTS

The author wishes to thank Esso Production Research Company for permission to publish this material. The author is also indebted to J. N. Mercer for obtaining the mass spectra and to H. E. Lumpkin for helpful discussions in interpreting the spectral data.

LITERATURE CITED

(1) Dean, R. A., and Whitehead, E. V., Tetrahedron Letters 21, 768, (1961).
(2) Bendoraitis, J. G., Brown, B. L., and Hepner, L. S., Anal. Chem. 34, 49, (1962).
(3) Bendoraitis, J. G., Brown, B. L., and Hepner, L. S., 6th World Petroleum Congress (1963).
(4) McCarthy, E. D., and Calvin, M., A. C. S. Meeting, September (1966).
(5) Bogomolov, A. I., Trudy Vsesoyuznogo Nauchno-Issledovatel'skogo Geologorazvedochnogo Instituta 227, 10, (1964).
(6) Curphey, E. G., Petroleum (London), 15, 297 (1952).
(7) Blumer, M., Science 149, 722, (1965).
(8) Belsky, T., McCarthy, E. D., and Van Hoeven, W., Personal Communication.
(9) Smith, J. H. C., and Benitez, A. (1955) Chlorophylls: Analysis in Plant Materials. In "Modern Methods of Plant Analysis". (K. Paech and M. V. Tracey eds.) Vol. IV, Springer, Berlin, pp. 142.
(10) Hubbard, A. B., and Fester, J. I., M. S. Bureau of Mines, Report of Investigations, 5458, (1959).
(11) Pelipetz, M. G., Weller, S., and Clark, E. L., Fuel 29, 208, (1950).
(12) McIver, R. D., Geochim et Cosmochim. Acta. 26, 343, (1962).
(13) Ryhage, R., and Von Sydow, E., Acta Chem. Scand. 17, 2025, (1963).

JOINT SYMPOSIUM ON OIL SHALE, TAR SANDS, AND RELATED MATERIAL
PRESENTED BEFORE THE DIVISION OF PETROLEUM CHEMISTRY, INC.
AND THE DIVISION OF WATER, AIR, AND WASTE CHEMISTRY
AMERICAN CHEMICAL SOCIETY
SAN FRANCISCO MEETING, April 2-5, 1968

ANALYSIS OF THE MINERAL ENTRAPPED FATTY ACIDS ISOLATED FROM THE GREEN RIVER SHALE (EOCENE)

By

A. L. Burlingame and B. R. Simoneit
Department of Chemistry and Space Sciences Laboratory
University of California, Berkeley, California 94720

INTRODUCTION

The Green River Shale, of Eocene age, has been the object of extensive organic geochemical studies. Most of the investigations have been concerned with the extractables and have resulted in the characterization of various classes of compounds. The hydrocarbon fraction, which has been most thoroughly investigated, includes normals, isoprenoids, iso and anteiso alkanes, steranes and triterpanes, and aromatics (1-5). Various reports have dealt with the organic acid fraction. The presence of a homologous series of normal fatty acids (6, 7), iso and anteiso acids (8), isoprenoid acids ranging from C_9 to C_{21}, with the exception of C_{18} (9-12), dicarboxylic acids ranging from C_{12} to C_{18} (12), C_{11} and C_{14} methylketoacids (13), and several series of aromatic acids (14) have been established.

We wish to report on the analysis of the organic acids liberated after demineralization of the exhaustively extracted shale. The families of compounds found were essentially the same as those reported present in the solvent soluble fraction of the shale.

EXPERIMENTAL

A sample of Green River Shale from Parachute Creek, 8 miles NW of Grand Valley, Colorado (long. W 108°7'; lat. N 39°37'; el. 7300') was pulverized to pass 200 mesh. The powdered rock was exhaustively extracted using ultrasonication, as well as Soxhlet extraction with 3:1 benzene/methanol. This was followed by two room temperature digestions (2 days each) with 1:1 concentrated hydrofluoric acid/hydrochloric acid. To remove sulfides and free sulfur, the residue was further treated with zinc dust and 6M hydrochloric acid (Forsman and Hunt). By repetitive ultrasonic extractions with 4:1 benzene/methanol 0.17% (by weight of original rock) of solubilized organics were isolated and subsequently separated into 0.04% neutrals and 0.13% acids (the kerogen residue amounted to 48%). The acid fraction was esterified with BF_3/methanol, passed over silica gel and clathrated with urea yielding 1:3 normals/branched-cyclics (see flowsheet Fig. 1). The total, normal and branched-cyclic fractions were chromatographed on a 5' x 1/8" column, packed with 3% SE-30 on chromosorb and programmed from 100-270°C at 10°/min. with a flow rate of 50 ml/min. The GLC components were identified by their retention times, coinjection of standards, low resolution mass spectra and then correlated to the high resolution mass spectra of the total mixtures run on a C. E. C. 21-110B mass spectrometer with direct inlet at ion source temperatures from 150-270°C. Figure 2 illustrates a GLC run on the three fractions. In the normal fraction there is an even/odd predominance as established by characterization of the peaks. The labeled peaks were checked by coinjection of authentic standards. This same distribution is also found in the summation of the high resolution mass spectra at varying ion source temperatures of each fraction. Figure 3 is an example of a summed high resolution mass spectrum of the totals fraction. The masses are plotted in methylene units (15). On the abscissa, each major division marker corresponds to the saturated ion, e.g. C_nH_{2n+1}, with the number of carbon/hydrogen atoms given below. There are 14 units between each major division, and the number of hydrogen atoms of an unsaturated or cyclic ion is obtained simply by determining the difference from the position of the next higher saturated ion. The even/odd predominance of the monocarboxylic acids is also evident in the high resolution mass spectra of the normals and totals fraction, and can be easily discerned in the C/H O and C/H O_2 plots of Figure 3.

Table 1

Organic Acids from the Demineralized, Exhaustively Extracted Green River Shale

	Range	Max. Conc.
Normal Acids	C_1-C_{32} *	C_{16} and C_{24}
	C_8-C_{30} ≠	
Branched Acids	C_8-C_{22} *	C_{20}
	C_8-C_{15} ≠	
Dicarboxylic Acids	C_3-C_{18} *≠	C_6
Methylketoacids	C_4-C_{16} *	C_{11}
Aromatic Acids (phenyl)	C_7-C_{15} *	C_9
Aromatic Acids (naphthyl)	C_{10}-C_{14} *	C_{11}
Triterpenoid Acids	C_{28}-C_{34} *	C_{30}

* determined by mass spectrometry

≠ determined from gas chromatograms

Figure 1

Experimental Flowsheet

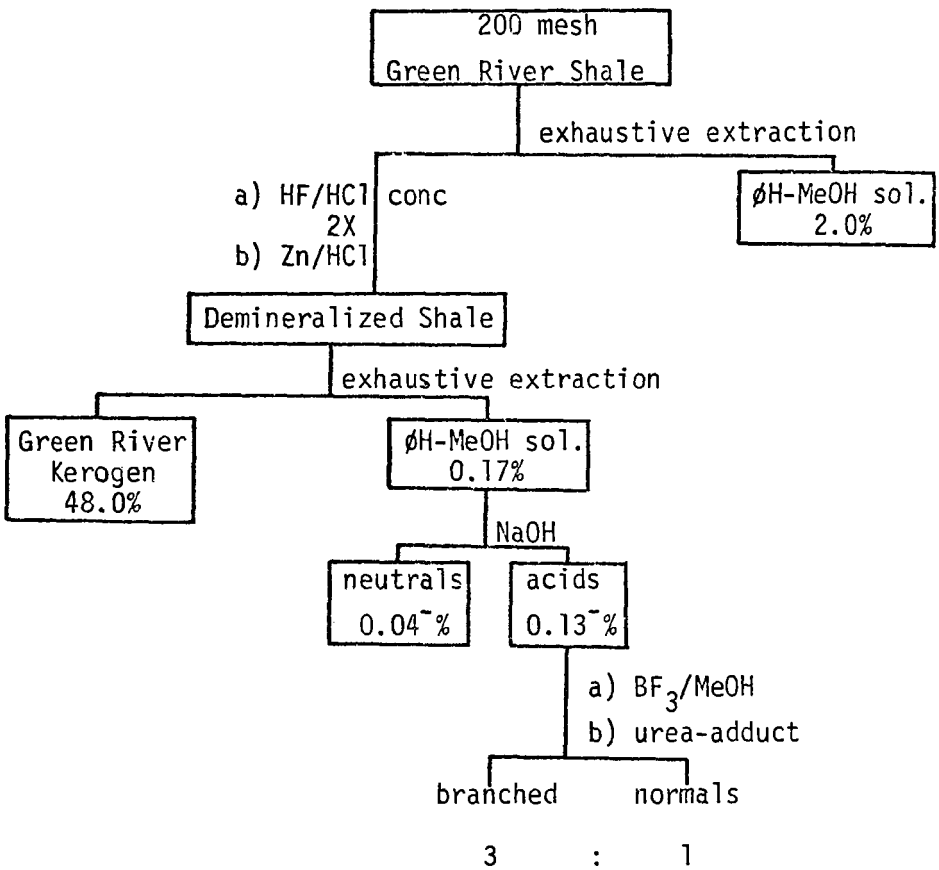

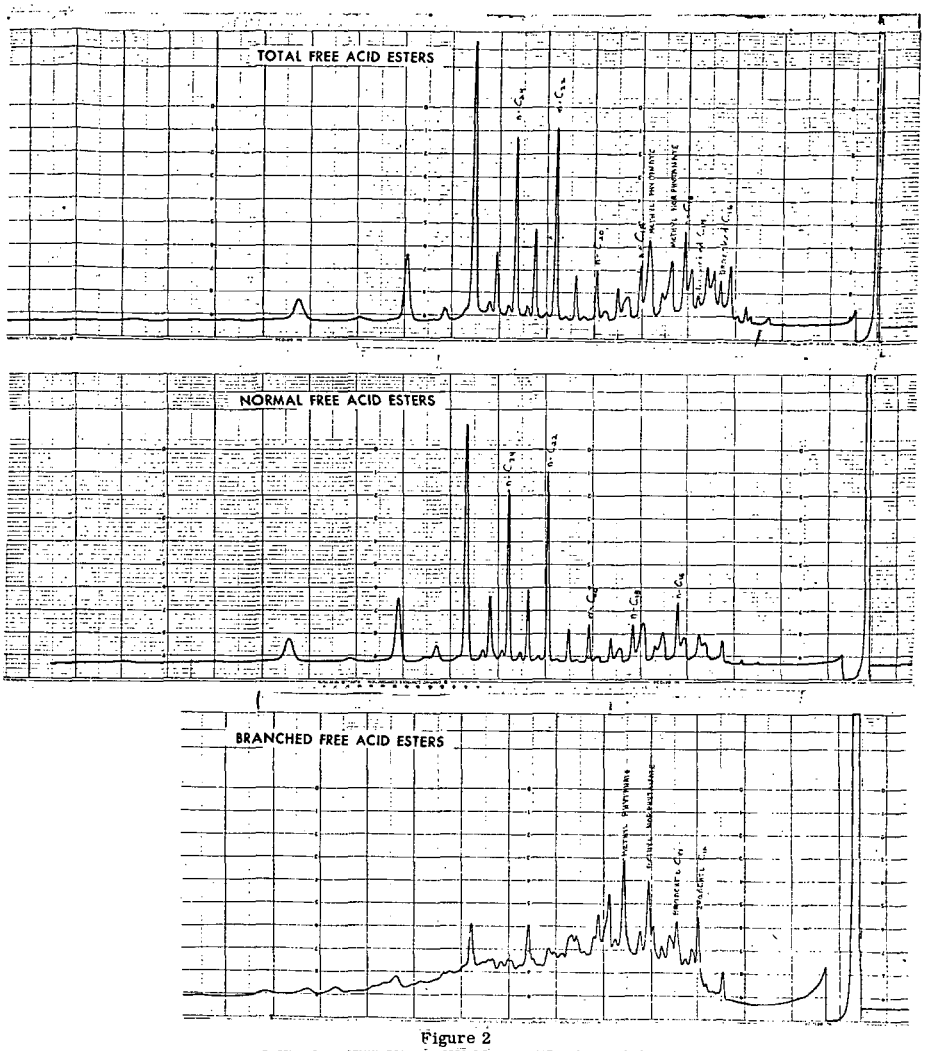

Figure 2

FATTY ACID METHYL ESTERS AFTER DEMINERALIZATION OF GREEN RIVER SHALE; TEMPERATURE PROGRAMMING FROM 100 TO 250°C ON 5' x 1/8", 2% SE—30 COLUMN

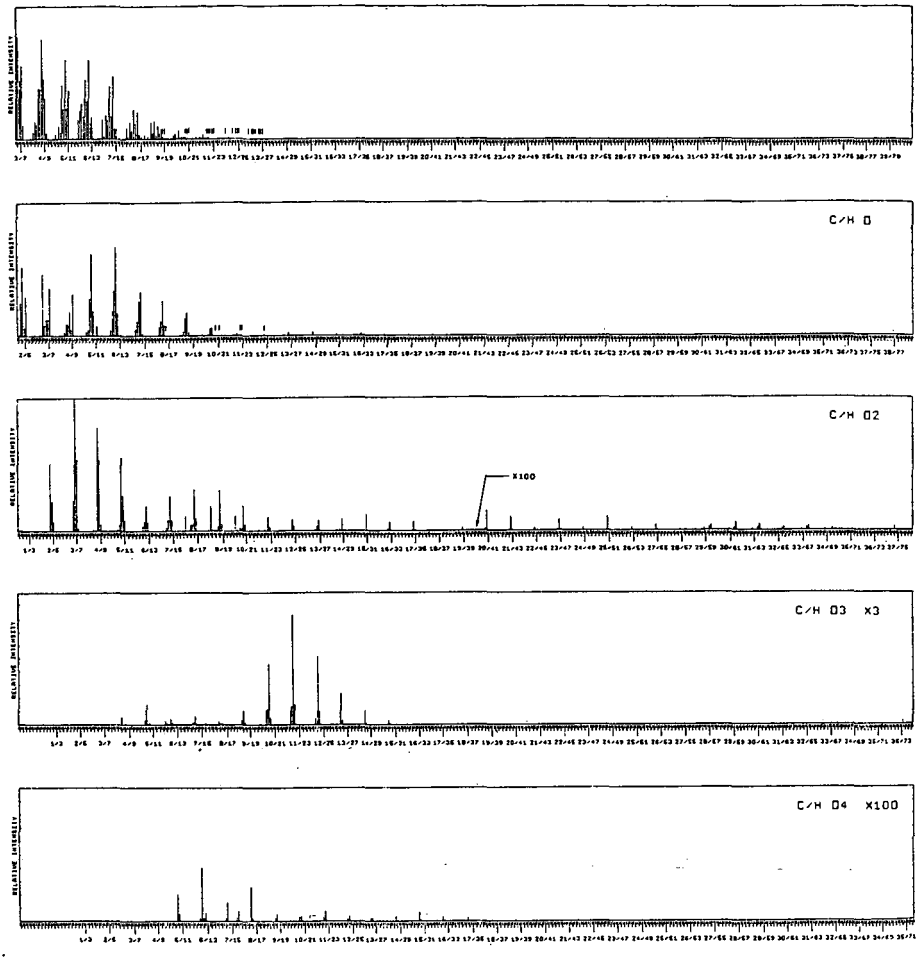

FIGURE 3 HIGH RESOLUTION MASS SPECTRUM OF THE TOTAL FRACTION OF ACID ESTERS ISOLATED AFTER DEMINERALIZATION OF THE GREEN RIVER SHALE (ION SOURCE TEMP. 150–170° C).

Figure 4 Low resolution mass spectrum of Dimethyl undecane-1,11-dioate isolated from Green River Shale.

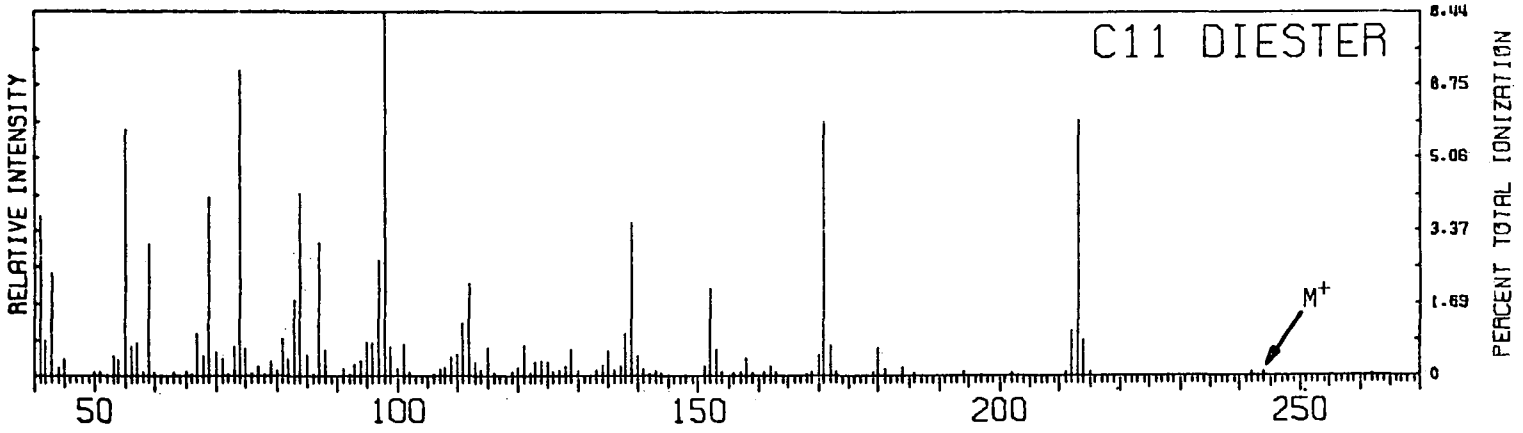

F187

RESULTS

The findings of this study are listed in Table 1 and described below in the same order as in the introduction. The homologous series of normal fatty acids found in the GLC ranged from C_8-C_{30} with maxima at C_{16} and C_{24}; the same was found in the high resolution mass spectra, only the range was C_1-C_{32} due to greater sensitivity. The branched acids detected ranged from C_8-C_{22}; the cutoff on the GLC was C_{15} and the major constituents were phytanic and norphytanic acids. These two aforementioned series were the major portion of the acid extract. The following series are described in order of decreasing concentration. Dicarboxylic acids ranging from C_3-C_{18} with a maximum at C_6 (adipic acid) were found both in the GLC collection and high resolution mass spectra. Even though the molecular ions of this series are small, they were detectable and further substantiated by the presence of the strong peaks due to losses of $CH_3O\cdot$ and $CH_2{=}C{=}O$ (Figure 4) (16). As, for example, in Figure 3 the C_{11} diester of Figure 4 has its molecular ion $C_{13}H_{24}O_4$ in the C/H O_4 plot; the loss of $CH_3O\cdot$ results in the peak at $C_{12}H_{21}O_3$ in the C/H O_3 plot and the following loss of ketene yields the peak at $C_{10}H_{19}O_2$ in the C/H O_2 plot. Methylketoacids were found with compositions of C_4-C_{16} with the distribution maximum at C_{11} in the high resolution mass spectra. In the GLC they were buried among the major constituents. Their molecular ions were of reasonable intensity and the compound identities were further substantiated by the strong losses of $CH_3O\cdot$ and C_3H_5O (13, 17). To illustrate with an example, again referring to Figure 3, the molecular ion $C_{11}H_{20}O_3$ is in the C/H O_3 plot, loss of $CH_3O\cdot$ results in the peak at $C_{10}H_{17}O_2$ in the C/H O_2 plot and M-C_3H_5O in the peak $C_8H_{15}O_2$ also in the C/H O_2 plot. The keto-acids exhibit a further characteristic strong peak due to M-$CH_3O\cdot$ - C_3H_5O, which corresponds to $C_7H_{12}O$ for this example and is found in the C/H O plot.

The two major series of aromatic acids, namely methyl substituted benzoic and methyl substituted naphthoic acids (14) were also found. The identification of these compounds is based on the elemental compositions of the molecular ions and their respective strong M-$CH_3O\cdot$ peaks in the high resolution mass spectra of the total and branched-cyclic fractions. The major peaks due to the aromatic acids present in the C/H O_2 and C/H O plots of Figure 3 were deleted, since the compositions of the ions fall at the same nominal mass as the molecular ions of the saturated acids and the aromatic tic mark over the peak would be misleading (there are some aromatic ions in the C/H plot of Figure 3). The aromatic acids consisting of a substituted phenyl ranged from C_7 (benzoic acid) to C_{15} with the distribution maximum at C_9; the bicyclic aromatic acids ranged from C_{10} (indanoic acid) to C_{14}, the major constituent being C_{11} (naphthoic acid). At higher ion source temperatures in the mass spectrometer, a group of triterpenoid acid esters volatilized and the following molecular ions were observed in the high resolution mass spectra of the totals and branched-cyclic fraction: 428 ($C_{28}H_{46}O_2$), 442 ($C_{30}H_{50}O_2$), 456 ($C_{31}H_{52}O_2$, 470 ($C_{32}H_{54}O_2$), 484 ($C_{33}H_{56}O_2$), 498 ($C_{34}H_{58}O_2$), 512 ($C_{35}H_{60}O_2$) and 458 ($C_{31}H_{54}O_2$). The distribution maximum was at $C_{31}H_{52}O_2$ and the M-$CH_3\cdot$ peaks were also observed. Referring to Figure 3, the molecular ion $C_{31}H_{52}O_2$ is found in the C/H O_2 plot and its corresponding M-$CH_3\cdot$ peak at $C_{30}H_{49}O_2$ in the same plot.

CONCLUSIONS

From these findings it can be concluded that these acids were indigenous to the shale and occur either trapped in the mineral-kerogen matrix, as metal salts, bound to the kerogen by easily hydrolyzed links, or possibly a combination of all three. It was shown by Eglinton et al. (11) that hydrofluoric acid digestion of Green River Shale does not interconvert normal acids to branched acids, lending further support to the fact that these acids did not migrate into the shale after deposition and compaction. Furthermore, these authors have found in subsequent experiments of chromic acid oxidation of kerogen residue after demineralization and exhaustive extraction (18) the same types or organic acids with a few minor differences. This leads to the conclusion that these organic acid groupings are bonded to the kerogen matrix via easily oxidized functionalities, or may be occluded in the polymer interstices in the form of alkanes, ketones or some other oxidizable structure, yielding the acids when liberated by the digestion and subsequent oxidation. For example, the triterpenoid acids found may have been trapped as triterpanes rather than being bonded to the kerogen.

This method of high resolution mass spectral runs using increasing ion source temperatures on whole extracts is extremely useful, especially in experiments where the fraction is too small to run on a GLC-mass spectrometer combination. Further selective experiments to determine absolutely what happens during the kerogen oxidation are in progress at this laboratory.

ACKNOWLEDGMENT

Support of this work through grants from the National Aeronautics and Space Administration (NsG 101 and NGR 05-003-134) is gratefully acknowledged. The authors wish to thank Miss E. Sloan for assistance with the GLC runs.

LITERATURE CITED

(1) Robinson, W. E., Cummins, J. J., Dinneen, G. U., Geochim. Cosmochim. Acta 29, 249 (1965).
(2) Cummins, J. J., Robinson, W. E., Chem. Eng. Data 9, 304 (1964).
(3) Eglinton, G., Scott, P., Belsky, T., Burlingame, A. L., Calvin, M., Science 145, 263 (1964).
(4) Burlingame, A. L., Haug, P., Belsky, T., Calvin, M., Proc. Nat. Acad. Sci. 54, 1406 (1965).
(5) Hills, I., Whitehead, E., Anders, D., Cummins, J., Robinson, W., Chem. Comm. 752 (Nov. 20, 1966).
(6) Abelson, P. H., Parker, P. L., Carnegie Inst. Wash. Year Book 61, 181 (1962).
(7) Lawlor, D. L., Robinson, W. E., Div. Petroleum Chemistry, A. C. S., Detroit Meeting, 5-9 (1965).
(8) Leo, R. F., Parker, P. L., Science 152, 649 (1966).
(9) Eglinton, G., Douglas, A. G., Maxwell, J. R., Ramsay, J. N., Stallberg-Stenhagen, S., Science 153, 1133 (1966).
(10) Ramsay, J. N., Organic Geochemistry of Fatty Acids, M. S. Thesis, University of Glasgow, 1966.
(11) Douglas, A. G., Douraghi-Zadeh, K., Eglinton, G., Maxwell, J. R., Ramsay, J. N., in Advances in Organic Geochemistry (G. D. Hobson, D. Spears, eds.), Pergamon Press, 1966.
(12) Haug, P., Schnoes, H. K., Burlingame, A. L., Science (in press).
(13) Haug, P., Schnoes, H. K., Burlingame, A. L., Chem. Comm. (in press).
(14) Haug, P., Schnoes, H. K., Burlingame, A. L., Geochim. Cosmochim. Acta (in press).
(15) Burlingame, A. L., Smith, D. H., Tetrahedron (submitted).
(16) Ryhage, R., Stenhagen, E., Arkiv Kemi 23, 167 (1964).
(17) Ryhage, R., Stenhagen, E., Arkiv Kemi 15, 545 (1960).
(18) Burlingame, A. L., Simoneit, B. R., Nature (in preparation).

JOINT SYMPOSIUM ON OIL SHALE, TAR SANDS, AND RELATED MATERIAL
PRESENTED BEFORE THE DIVISION OF PETROLEUM CHEMISTRY, INC.
AND THE DIVISION OF WATER, AIR, AND WASTE CHEMISTRY
AMERICAN CHEMICAL SOCIETY
SAN FRANCISCO MEETING, April 2-5, 1968

HIGH RESOLUTION MASS SPECTRAL EXAMINATION OF THE RESIN FRACTION OF PETROLEUM ASPHALTICS

By

John P. Dickie and Teh Fu Yen
Mellon Institute, Carnegie-Mellon University,
4400 Fifth Avenue, Pittsburgh, Pennsylvania 15213

INTRODUCTION

During the past years, several papers have been written which have discussed the properties of the asphaltic fraction of petroleum (5,7,10,11). These studies were carried out on broad fractions and have resulted in a proposal for an average macrostructure of the molecule (4), which is consistent with a variety of data. The asphaltic structure has been pictured as a two-dimensional fabric of condensed aromatic rings, short aliphatic chains, and some naphthenic ring structure (12). The asphaltic molecules contain, in addition to carbon and hydrogen, varying amounts of nitrogen, oxygen, sulfur and metal (particularly vanadium and nickel). Most of the hetero elements are bound into ring structures since the molecules are extremely resistant to oxidation, and detectable functional groups appear to be absent (7). The individual sheets are held into unit cells by associative forces, and in concentrated solution these unit cells can associate further to form larger micelles (5). However, the structures of the individual sheets of the unit cell remain largely speculative and unexplained.

Mass spectral examination has been previously used to visualize the aromatic sheet portion of the asphaltic molecules (4). In these studies on the asphaltene fraction it was postulated that under 70eV impact voltage and at inlet temperatures exceeding 300°C, the aliphatic bonds might be broken, and the volatile fragment would be only the aromatic disk. If the bonds were not broken, and the structure were that of an aromatic sheet attached to a naphthenic net, the material might be expected to be so involatile as not to be seen by the mass spectrograph. In previous work the mass spectrum of the resin fraction (pentane soluble, propane insoluble) was observed to be very similar to that of the corresponding asphaltene (pentane-insoluble) fraction. This was taken as an additional indication of the similarity between the resin and asphaltene fractions. Since what was being seen in the mass spectrum was the aromatic portion of the resin molecule, which differed little from that of the corresponding asphaltene fraction, the difference between the resin and asphaltene molecules from the same crude oil would be only in the amount of the aromatic portion of the material. Also, it had been previously noted that the resin can be easily converted into asphaltenes by high temperature treatment (6), and at 300°C it would be expected that some conversion of the unsaturated naphthenic portion to the aromatic material might have occurred. This would, of course, make the resin fraction appear even more like an asphaltene. The present work is a continuation of the earlier studies (4), but with an improved inlet technique which permitted the resin fraction to be volatilized at lower temperatures and, thus, with less likelihood of being thermally altered. For this reason the mass spectra of these materials were of particular interest in providing information about the composition of the individual molecular sheets. The results of these exact mass measurements on the petroleum resin fractions represent the first attempt to describe exactly the unit sheet of the asphaltic molecule.

EXPERIMENTAL RESULTS

Mass spectra of a Boscan and a Baxterville resin were obtained using an AEI MS-9 spectrometer, equipped with a solid probe inlet system. Conditions for the measurement of this sample were: temperature, 250-270°C; impact voltage, 70eV. For high resolution measurements, slits were narrowed so as to give a resolution of one part in 15,000 (10% valley definition).

The inlet temperature is lower than that which was previously used. It was found possible to get material into the spectrometer at these lower temperatures and obtain a more reproducible

and a longer lasting pattern by depositing the resin onto crushed fire brick from benzene solution by allowing the benzene to evaporate, and packing the coated material onto the inlet probe. Of course, in order to get high resolution mass measurements, a stable, reproducible, relatively intense spectrum is required. At 70eV impact voltage, parent peaks as well as fragments from slightly higher mass ranges are to be expected.

The exact mass of selected peaks in this spectrum were measured by the peak-matching technique using perfluoro-t-butylamine as the standard. Approximately 60 peaks within each envelope were measured with an estimated accuracy of ±20 ppm. Although the instrument is capable of mass measurements with an accuracy of 5 to 6 ppm, it was realized that such precision could not be achieved in view of the relatively low peak intensity. The error was estimated by remeasuring a given peak over a period of time and noting the variation in the measured value.

The possible molecular compositions for each peak were calculated using a computer program which required specification of the atom concentrations of carbon, hydrogen, nitrogen, oxygen and sulfur, and the mass range. The atomic concentration of the elements was selected to give a broad range of possibilities, probably much outside practical limits; e.g., this material has an average carbon composition of ca. 85%, which would indicate that at mass 400 there would be approximately 30 atoms of carbon per molecule. A range of carbon between 15 and 45 atoms per molecule was allowed for this calculation. In a similar fashion, the atom concentration of hydrogen was bracketed at 10 to 92, and nitrogen, oxygen and sulfur, between 0 and 5 atoms per molecule. It should be noted that, on the average, the concentration of sulfur in these materials is less than 6%, which would indicate less than 1 atom of sulfur per molecule (at mass 400); thus, at a limit of 5 atoms, it would seem that all reasonable possibilities would be covered. After the computer printed out the elemental composition possibilities, two additional tests were applied: 1. A calculation to determine whether each peak was parent or a singly-charged fragment by use of the formula (2) $R = (2C - H + N + 2)/2$. 2. A calculation of the hydrogen-to-carbon atom ratio. If R is a whole number, the peak is a parent; if it is fractional, the peak is a fragment. (Sulfur and oxygen do not effect the calculation since they are divalent.) Here R is defined as the total number of rings and/or double bonds which are present in a particular molecule. Since the resins have an average H/C atom ratio of 1.28, any formulations having values outside of the approximate range 1 to 1.6 were discarded as being unlikely. However, some pure hydrocarbon formulations were not discarded although they had low H/C values; also the limits were extended when the number of possibilities was small.

The possible formulas remaining after these operations are tabulated in Tables I and II along with the measured exact mass, the difference between this measured mass and the formula mass, the H/C atom ratio for the particular material, and the R-value. Table I lists parent peaks and fragment peaks of the Baxterville resin; Table II contains a similar tabulation for the Boscan resin.

Figure 1 shows a low (10eV) and high (70eV) impact voltage spectrum of the Boscan resin. All peaks were mass measured from the 70eV spectrum since the intensity of the low voltage spectrum did not allow exact mass measurement. The doubly-charged envelope can be seen at mass range 110 m/e to 220 m/e in the 70eV spectrum, showing that the fragment peaks which were measured at masses 250 m/e through 400 m/e are singly-charged species. Also, it should be noted that in the low voltage spectrum the most intense peaks appear, in general, at odd mass numbers.

DISCUSSION

Work on the micro structure of the asphaltic materials involves the same two lines of attack that were used and are being used on the macro structure. These are to: 1. Carry out information gathering experiments, the results of which will be used to postulate possibilities for the structures. 2. Devise experiments which will confirm or deny these postulations. The exact mass measurement of some peaks in the resin fractions of the asphaltic material really fall into both categories.

Some average structures for asphaltic materials have been written (3,12) which utilize the results of NMR, elemental analyses, infrared measurements, etc. Therefore, an exact mass measurement can confirm the presence of postulated structures. In fact, the aromatic portion of the postulated structures could be rationalized as the type of formulation indicated by the mass spectra.

Equally important, however, is the exact mass measurement of given peaks which allows us to eliminate some possible structures and to determine that at a given molecular weight there is a limited number of structure possibilities. Many molecular compositions which were theoretically possible on the basis of molecular weight have been eliminated: 1. Because of their

variance from the allowed H/C atom ratio. 2. Because of the content of an excessive amount of hetero elements. In a material with an average of less than one atom of oxygen, nitrogen and sulfur per molecule, it would be unusual to find a portion which contained, in addition to four nitrogens, a variety of sulfur and oxygen groups. Therefore, the criterion used for elimination of peaks with excess hetero elements was that any peak containing more than six hetero elements was discarded. An exception was made for peaks which contained not more than three of one element, e.g., $N_3O_2S_2$ or $N_2O_2S_3$ were saved, but $N_3O_3S_2$ was discarded. If four of the hetero elements (e.g., three N and one S) were part of the metal ligand, it would seem likely that one or two hetero atoms could be found elsewhere in the molecule. Although none of these peaks can be unequivocally identified as porphyrin, such substances are seen in concentrated fractions (1). Table III lists all of the elemental combinations possible after consideration of only mass measurement and H/C ratio. The disposition of each possibility is indicated.

Several observations from the data are possible. Peaks which were chosen for measurement in the mass spectra were, of course, the ones that stood out most from the background. It is interesting that there is not a 14 mass difference in large peaks through the entire mass scale. This confirms the postulation that there are very few long paraffinic chains. If the breaking of a paraffinic chain were one of the features of the degradation of an asphaltic molecule, one would expect to find a series of peaks differing by the mass equivalent of a CH_2 group as was found for pure alkyl substituted polynuclear aromatics or naphthenics. Peaks which differ by 32 mass units in a series are also not seen, which indicates that there is little loss of polymeric sulfur. In mass spectra run in these laboratories on asphaltic materials to which polymeric sulfur has been added, the spectra always show peaks differing by 32 mass units. These observations confirm previous postulations that hetero elements are, in general, bound in the ring structure.

Mass spectra run on model compounds both in these laboratories on alkyl polynuclear aromatics and work reported by Grubb and Meyerson (8) on alkyl substituted benzenes have shown that in substituted conjugated aromatic systems most fragment peaks are formed by either α or β elimination with the latter predominant. In the case of methyl substituted aromatics, the predominant fragment peak is $(A\text{-}CH_2)^+$. The fragment peaks (Tables I and II) do, in fact, contain many structure possibilities which are only one mass unit removed from a peak in the parent listing. As substitution increases ($A\text{-}CH_2\text{-}R$, -R', -R") a combination of α and β cleavage results in the same predominant fragment $(A\text{-}CH_2)^+$. Fragments formed in this fashion should have little aliphatic substitution and, therefore, a high R-value. Perhaps, several more of the peaks might have been eliminated (e.g., mass number 269.1335 in Table I, the $C_{14}H_{21}O_5$ compound containing only four rings per molecule is much more unlikely than either of the other two possibilities). Further, at mass number 277.1938 both of the first two possibilities might be eliminated leaving the hydrocarbon as the most likely constituents. Also, it is probable that the fragments are largely devoid of side chains, and it is observed that the hetero element distribution varies little between the parent and fragment peaks (Tables IV and V). These are further indications that the hetero elements are most probably in the rings. Tables IV and V ignore the atom concentrations of C and H, which vary greatly, and consolidate the different combinations of hetero elements in the resins for ease of comparison of parent with fragment composition.

The similarity between the R-values and the hetero element composition for the parent and fragment peaks could well be an indication of the polymeric nature of these materials. The parents would be unpolymerized monomers similar to the components of the polymerized higher molecular weights species.

As previously noted, the low voltage spectrum in the range of peaks that were mass measured shows the most intense peaks to have odd mass numbers, indicating an odd number of nitrogens present. The presence of an odd number of nitrogens was not used as a criterion for eliminating parent peaks in the tables; however, it is consistent with the independent observation from EPR examination that some of the ligands to vanadium present in the asphaltic materials may be composed of three nitrogens and another hetero element (probably oxygen or sulfur) rather than four nitrogens as found in the case of porphyrin (9).

If a more accurate mass measurement could be made, many more of these peaks could be eliminated; therefore, this work is at a very preliminary stage, and a study of introduction techniques which will introduce more material into the instrument and allow more accurate measurements is being undertaken.

ACKNOWLEDGMENT

The authors wish to acknowledge the assistance of the following persons from Research services at Mellon Institute: Mr. Stephen J. Ondrey, for his preparation of the samples and his calculations, and Mr. James R. Boal, for the mass spectral work.

This work was sponsored by Gulf Research and Development Company as part of the research program of the Multiple Fellowship on Petroleum.

LITERATURE CITED

(1) Baker, E. W., Yen, T. F., Dickie, J. P., Rhodes, R. E., and Clark, L. F., J. Am. Chem. Soc. 89, 3631 (1967).
(2) Beynon, J. H., "Mass Spectrometry and Its Applications to Organic Chemistry", Elsevier Publishing Company, New York, 1960, p. 313.
(3) Bonavert, G. and Auffray, R., Revue de L'Institut Francais du Petrole XX, 1854 (1965).
(4) Dickie, J. P., and Yen, T. F., Preprints, A. C. S., Div. of Petroleum Chemistry 12, No. 2, B-117 (1967).
(5) Dickie, J. P., and Yen, T. F., Preprints, A. C. S., Div. of Petroleum Chemistry 11, No. 3, 39 (1966).
(6) Erdman, J. G., and Dickie, J. P., Preprints, A. C. S., Div. of Petroleum Chemistry 9, No. 2, 1369 (1964).
(7) Erdman, J. G., and Ramsey, V. G., Geochim. et Cosmochim. Acta 25, 175 (1961).
(8) McLafferty, F. W., "Mass Spectrometry of Organic Ions", Academic Press, New York, 1963.
(9) Yen, T. F., Tynan, E. C., Vaughan, G. B., and Boucher, L. J., Preprints, A. C. S., Div. of Fuel Chemistry 11, No. 4, 264 (1967).
(10) Yen, T. F., and Dickie, J. P., Preprints, A. C. S., Div. of Petroleum Chemistry 11, No. 3, 49 (1966).
(11) Yen, T. F., Erdman, J. G., and Pollack, S. S., Anal. Chem. 33, 1587 (1961).
(12) Yen, T. F., and Erdman, J. G., Preprints, A. C. S., Div. of Petroleum Chemistry 7, No. 3, 99 (1962).

Editor's Note: The Tables and Figure are missing from this paper because of the very extensive listings and difficulty of reproduction. Anyone interested should write directly to the authors for information.